

LIGHT-EMITTING DEVICES WITH POLYNORBORNENES CONTAINING BLUE
ELECTROLUMINESCENT AND CHARGE-TRANSPORT FUNCTIONAL UNITS

by

THOMAS JAMES BOYD

B.S. in Chemistry, Ithaca College
(1994)

Submitted to the Department of Chemistry
in Partial Fulfillment of the Requirements
for the Degree of

DOCTOR OF PHILOSOPHY

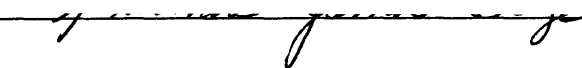
at the

MASSACHUSETTS INSTITUTE OF TECHNOLOGY

June 1999

© Massachusetts Institute of Technology, 1999

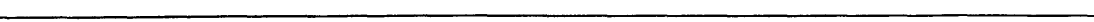
Signature of Author



Department of Chemistry

March 11, 1999

Certified by



Richard R. Schrock

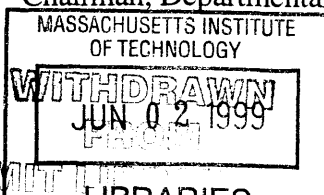
Thesis Supervisor

Accepted by



Dietmar Seyferth

Chairman, Departmental Committee on Graduate Students



Science

MIT LIBRARY

This doctoral thesis has been examined by a Committee of the Department of Chemistry as follows:

Professor Alan Davison _____
Chairman

Professor Richard R. Schrock _____
Thesis Supervisor

Professor Christopher C. Cummins _____

To Kathryn

LIGHT-EMITTING DEVICES WITH POLYNORBORNENES CONTAINING BLUE ELECTROLUMINESCENT AND CHARGE-TRANSPORT FUNCTIONAL UNITS

by

THOMAS JAMES BOYD

Submitted to the Department of Chemistry, March 1999,
in Partial Fulfillment of the Requirements
for the Degree of Doctor of Philosophy in Chemistry

ABSTRACT

Chapter 1

The preparation of a series of monomers and polymers of use in Light-Emitting Devices (LEDs) is described. Two derivatives of the highly blue luminescent and electrochemically stable diphenylanthracene (DPA) with varying bulkiness are incorporated onto norbornene monomers. Electron-transporting monomers based on *t*-butylphenyl-*para*-biphenyl-oxadiazole (PBD) are prepared. The synthesis of hole-transport monomers containing either a tertiary aryl amine or a *para*-triphenyl (PTP) group is described. Oligomers (25mers or 50mers) of homo- and copolymers are made via Ring Opening Metathesis Polymerization (ROMP), using the well-defined molybdenum initiator Mo(N-2,6-*i*-Pr₂-C₆H₃)(CHCMe₂Ph)(*Or*-Bu)₂. The observed high yields (>90%) and low polydispersities are typical of polymers made with this "living" polymerization system. Two new methods for modification of the polynorbornene backbone are introduced. The epoxidation reaction using *meta*-chloroperoxybenzoic acid gives rapid conversion of the carbon double bonds along the backbone. This reaction is mild in scope and does not harm sensitive groups, such as diphenylanthracene. The sulfonation reaction is more aggressive, but is still mild enough for many of the polymers described here. The sulfonated polynorbornenes are greater than 80% sulfonated and have vastly different solubilities than the original polymers.

Chapter 2

The performance of LEDs constructed with spin-coated polynorbornenes is described. To optimize charge balance, two kinds of device structures are employed. The first, a single-layer device containing only spin-coated polynorbornene, is shown to emit blue light at 450 nm, the wavelength of emission expected for DPA. Copolymers with PBD and DPA make devices with much higher output and efficiency. However, all of the single-layer devices suffer from frequent shorting and breakdown. Two-layer devices are constructed with a spin-coated polynorbornene top layer and a sequentially adsorbed poly(phenylene vinylene) (PPV) bottom layer. This bottom layer acts as a hole-transporting layer (lowering threshold voltages), and also improves the stability of the devices. A two-layer device with 5 bilayers of PPV/poly(styrene sulfonic acid) and 20 bilayers of PPV/poly(methylacrylic acid) (300 Å total thickness), in conjunction with 600 Å of a spin-coated copolymer of DPA and PBD (1:1 monomer ratio), provides the best performance: up to 675 nW of blue light and 31 nW/mA efficiency.

Chapter 3

The performance of LEDs constructed with sequentially adsorbed polynorbornenes is described. Employing the sulfonated forms of polynorbornenes allows for the building up of films layer by layer with a suitable polycation, such as poly(allylamine HCl) (PAH). This deposition is performed from aqueous solution, is automated, and provides uniform and defect-free films. The thickness of a PAH/polynorbornene bilayer can be controlled by adding NaCl. Unsalted bilayers are typically 8-13 Å thick, so it is readily possible to fine-tune the overall film thickness and architecture. Single- and dual-layer devices are constructed using sequentially adsorbed polynorbornenes. Increases in light and efficiency comparable to the PPV hole-transport layer (described in CHAPTER 2) are observed for sulfonated polynorbornenes containing PTP. The sulfonated polymers containing DPA form excimers (i.e., excited-state dimers) in water and in films. Several strategies are employed to control excimer formation, including: 1) diluting the solution, 2) "diluting" the polymer by adding a non-DPA comonomer, and 3) increasing the bulkiness of the groups around the anthracene core of DPA. This last strategy provides the best materials for devices made by sequential adsorption. Up to 21 nW and 0.3 mA/nW are observed from a single-layer device with DPA'.

Thesis Supervisor: Dr. Richard R. Schrock
Title: Frederick G. Keyes Professor of Chemistry

TABLE OF CONTENTS

	<u>page</u>
Title Page	1
Signature Page	2
Dedication	3
Abstract	4
Table of Contents	6
List of Figures	9
List of Tables	11
List of Schemes	12
List of Abbreviations Used in Text	13
GENERAL INTRODUCTION	15
CHAPTER 1: Synthesis and Polymerization of Electroluminescent Norbornenes and Chemical Modification of Polynorbornenes	21
Introduction	22
Results and Discussion	23
Blue-Light-Emitting Monomers Based on Diphenylanthracene (DPA).	23
Monomers for Hole and Electron Transport.	28
Sulfonation of the Polynorbornene Backbone.	31
Epoxidation of the Polynorbornene Backbone.	35
Conclusions	37
Experimental Section	38
CHAPTER 2: Light-Emitting Devices Constructed by Spin-Coating Polynorbornene and by Sequential Adsorption of Poly(Phenylene Vinylene)	51
Introduction	52
Results and Discussion	54
Devices with One Layer of Polynorbornene (Type A Devices).	54
Devices with Two-Layers, Polynorbornene with Multilayered Heterostructure (Type B Devices).	60
Role of Charge-Transport in Type A and B Device Performance.	64
Conclusions	66

	<u>page</u>
Experimental Section	66
CHAPTER 3: Light-Emitting Devices Constructed by Sequential Adsorption of Sulfonated Polynorbornene and the Effect of Excimer Formation on Emission and Device Output	68
Introduction	69
Results and Discussion	70
Layer-by-Layer Deposition of Ultra-Thin Films by Sequential Adsorption.	70
Excimer Formation with DPA-Containing Polymers.	73
Single-Layer Light-Emitting Devices.	79
Dual-Layer Light-Emitting Devices.	83
Conclusions	85
Experimental Section	85
APPENDIX A: Enhancement of Device Efficiency Employing Sulfonated Polynorbornene with the Oxadiazole Structural Unit for Electron Transport	89
Introduction	90
Results and Discussion	91
Electron-Transport/Hole-Block Nature of PBD.	91
Preparation of PBD Layers.	92
Devices with Spin-Coated PBD on PPV Heterostructures.	93
Devices with Sequentially Adsorbed PBD on PPV/PAA.	94
Devices with Sequentially Adsorbed PBD on PPP(+)/PPP(-).	95
Conclusions	97
Experimental Section	97
APPENDIX B: Binaphtholate Complexes of Molybdenum that Catalyze Ring Opening Metathesis Polymerization (ROMP) to Form Stereoregular Polynorbornadienes	97
Introduction	98
Results and Discussion	100
General Procedure for Preparation of 3,3' Substituted Binaphtholate Ligands.	100

	<u>page</u>
General Procedure for Initiator Synthesis	100
Synthesis of Highly-Cis, Highly-Isotactic Polynorbornadienes.	103
Conclusions	104
Experimental Section	104
REFERENCES	110
ACKNOWLEDGMENTS	117

List of Figures

	<u>page</u>
<u>Introduction</u>	
Figure INTRO.1 Light-emitting device (LED) with discrete layers for emission, electron transport, and hole transport.	18
Figure INTRO.2 Norbornene monomers for blue light emission (1-2), electron transport (3-4), and hole transport (5-6).	19
 <u>Chapter 2</u>	
Figure 2.1. Deposition of polyelectrolytes by sequential adsorption.	52
Figure 2.2. Spin-coating characteristics of 125 .	54
Figure 2.3. Calibration curves for spin-coating polymers (a) 125 and (b) [150%350%] 50 .	55
Figure 2.4. Schematic of light-emitting devices.	56
Figure 2.5. Configuration of Type A polymer EL devices.	57
Figure 2.6. Performance of device A-[150%350%]50 .	58
Figure 2.7. Optical spectra of 125 .	59
Figure 2.8. Configuration of Type B polymer EL devices.	60
Figure 2.9. Optical spectra of polymers [150%350%] 50 and 350 .	62
Figure 2.10. Degradation of device B-[150%350%]50 .	63
Figure 2.11. Variation in threshold voltage. Devices B-[150%550%]50 , B-[150%350%]50 , and A-[150%350%]50 .	64
Figure 2.12. Performance of device B-[150%350%]50 .	65
 <u>Chapter 3</u>	
Figure 3.1 Sequential adsorption of sulf-125 and poly(allylamine HCl).	72
Figure 3.2 Sequential adsorption of poly(allylamine HCl) (PAH) with 1) poly(methylacrylic acid) (PMA), 5 bilayers; 2) sulf-(12%698%)50 , 30 bilayers; 3) sulf-(12%498%)50 , 35 bilayers.	73
Figure 3.3 Solution photoluminescence of sulf-125 in DMSO and water at a concentration of 1×10^{-3} M.	74
Figure 3.4 Solution photoluminescence of sulf-125 in water.	75
Figure 3.5 Photoluminescence of films of sulf-(1_x%4100-x%)50 .	76
Figure 3.6 Photoluminescence of spin-coated and sequentially adsorbed films.	77

	<u>page</u>
Figure 3.7	Solution photoluminescence of 2×10^{-3} M sulf-(1_x% 4_{100-x}%)50 and sulf-(2_x% 4_{100-x}%)50 in water. 78
Figure 3.8	Photoluminescence of films of sulf-(1_x% 4_{100-x}%)50 and sulf-(2_x% 4_{100-x}%)50 . 79
Figure 3.9	Configuration of polymer EL devices. 80
Figure 3.10	Performance of device ITO/PAH-PMA(5 bilayers)/PAH- sulf-1₂₅ (35 bilayers)/Al. 81
 <u>Appendix A</u>	
Figure A.1	Electron-transporting/hole-blocking mechanism for <i>t</i> -butylphenyl- <i>para</i> -biphenyloxadiazole (PBD) with poly(phenylene vinylene) (PPV). 91
Figure A.2	Sequential adsorption of sulf-4₂₅ and poly(allylamine HCl) on 5 bilayers of PPP(+)/PPP(-). 92
Figure A.3	Performance of device ITO/PPV-SPS (5 bilayers)/PPV-PMA(20 bilayers)/PBD (570 Å)/Al. 93
Figure A.4	Sequentially adsorbed two-layer device with PBD and PPV. 95

List of Tables

	<u>page</u>
<u>Chapter 1</u>	
Table 1.1. Substituted Polynorbornenes	24
Table 1.2. Summary of Sulfonated Polynorbornenes	33
<u>Chapter 2</u>	
Table 2.1. Performance of Type A Devices	57
Table 2.2. Performance of Type B Devices	61
<u>Chapter 3</u>	
Table 3.1. Deposition of Sulfonated Polynorbornenes	71
Table 3.2. Performance of Single-Layer Devices with NBDPA (1) and NBDPA' (2)	82
Table 3.3. Performance of Dual-Layer Devices with NBDPA (1) and NBDPA' (2)	84
<u>Appendix A</u>	
Table A.1. Dual-Layer Device Performance: PPV/PMA//PPV/SPS with Spin-Coated NBPBD'	94
Table A.2. Dual-Layer Device Performance: PPV/PAA with PAH/NBPBD	95
Table A.3. Dual-Layer Device Performance: PPP(+)/PPP(-) with PAH/NBPBD	96
<u>Appendix B</u>	
Table B.1. Characterization of Poly(bisCF ₃ NBD) and Poly(DCMNBD)	103

List of Schemes

	<u>page</u>
<u>Chapter 1</u>	
Scheme 1.1. Synthesis of NBDPA (1).	24
Scheme 1.2. Synthesis of NBDPA' (2).	27
Scheme 1.3. Synthesis of NBPBD (4).	29
Scheme 1.4. Synthesis of NBPTP (6).	30
Scheme 1.5. Sulfonation of Polynorbornene with SO ₃ •dioxane.	32
 <u>Appendix B</u>	
Scheme B.1. Four Regular Geometries of 2,3-Disubstituted Polynorbornadienes.	98
Scheme B.2. Synthesis of Binaphtholate Ligands: Substitution at 3,3'.	101
Scheme B.3. Synthesis of Initiators for ROMP.	102

Abbreviations Used in Text

Ar	aryl
bisCF ₃ NBD	bis(trifluoromethyl)norbornadiene
br	broad
d	doublet
DCMNBD	2,3-dicarbomethoxynorbornadiene
DME	1,2-dimethoxyethane
DPA	diphenylanthracene
<i>t</i> -Bu	tertiary butyl
EL	electroluminescence
eq	equation
Et	ethyl
Et ₂ O	diethyl ether
GPC	gel permeation chromatography
h	hours
Hz	Hertz
IR	infrared
ITO	Indium Tin Oxide
J	coupling constant in Hertz
LED	light-emitting device
m	multiplet
mA	milliAmperes
Me	methyl
min	minutes
M_n	number average molecular weight
[Mo]	Mo(N-2,6-C ₆ H ₃ - <i>i</i> -Pr ₂)(CHMe ₂ Ph)(O- <i>t</i> -Bu) ₂
M_w	weight average molecular weight
NMR	nuclear magnetic resonance
OTf	O ₃ SCF ₃ , triflate, trifluoromethanesulfonate
OTs	tosylate
PAH	poly(allylamine HCl)
PBD	<i>t</i> -butylphenyl- <i>para</i> -biphenyloxadiazole
PDI	polydispersity index (M_w/M_n)
Ph	phenyl
PMA	poly(methylacrylic acid)

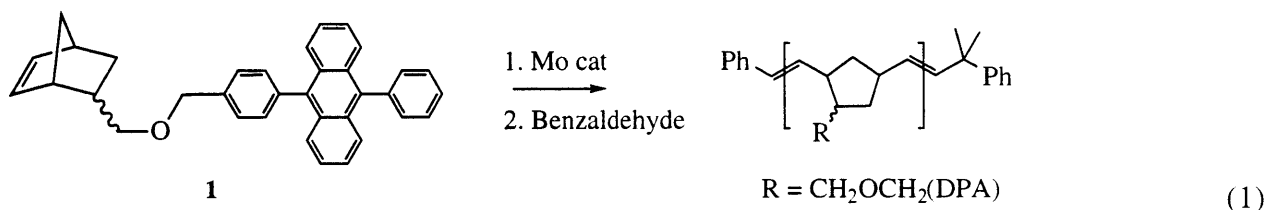
ppm	parts per million
PPP	poly(<i>para</i> -phenylene)
PPV	poly(<i>para</i> -phenylene vinylene)
<i>i</i> -Pr	isopropyl
PTP	<i>para</i> -triphenylene
py	pyridine
q	quartet
ROMP	ring-opening metathesis polymerization
RT	room temperature
s	singlet
SPS	poly(styrene sulfonic acid)
t	triplet
THF	tetrahydrofuran
tol	toluene
UV/Vis	ultraviolet/visible
V	volts
δ	chemical shift downfield from tetramethylsilane
$\lambda_{\text{max,abs}}$	wavelength of maximum optical absorption
$\lambda_{\text{max,em}}$	wavelength of maximum optical emission
ν	frequency

GENERAL INTRODUCTION

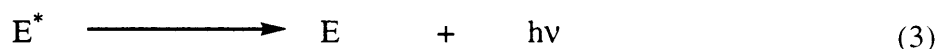
Research and discovery of new materials and structures for building light-emitting devices (LEDs) is driven mainly by the increasing need for thin, bright, and efficient displays in cellular phones, laptop computers, and similar applications.¹⁻³ Polymer-based LEDs, especially, have generated substantial interest since stable, high-efficiency devices were constructed from poly(phenylene vinylene) (PPV).^{4,5} Polymeric materials are more attractive for this application than solid-state inorganic materials or organic small molecules, because they can be readily processed into films. This is especially important for the construction of large surface area devices. A considerable body of work has been published on the electroluminescence (EL) of conjugated polymer systems, such as PPV, poly(*p*-phenylene) (PPP), and poly(thiophene).⁵⁻¹⁸ The literature has also included reports of relatively rare blue-light-emitting polymers based on phenylene vinylene (PV) systems, with PV either as a side chain or part of the polymer backbone,^{8,14,19,20}. Among these is a blue-light electroluminescent polynorbornene that contains a pendant PV trimer.¹⁹ In general, polymers that contain pendant chromophores have not been studied nearly as widely as polymers with chromophores as part of the backbone. The high threshold voltages (15-25 V) and low light emission levels in the few pendant chromophore systems investigated render them less attractive options compared to the more commonly reported conjugated polymers.^{2,8,19,21}

This thesis will focus first on the incorporation of electrochemically stable diphenylanthracene (DPA), a blue-light-emitting molecule widely used in chemiluminescence,²²⁻²⁷ into norbornene-based monomers. Polymerization of these monomers via ring opening metathesis polymerization (ROMP) was accomplished using a commercially available, well-defined initiator, Mo(N-2,6-*i*-Pr₂C₆H₃)(CHMe₂Ph)(O-*t*-Bu)₂ ([Mo]).^{19,28-30} [Mo] reacts with a wide variety of functionalized, readily prepared norbornenes or norbornadienes to give polymers in a controlled (living) manner,³¹⁻³³ the polymerization being terminated in a Wittig-like reaction by adding benzaldehyde. Norbornene monomers that contain a variety of pendant groups^{29,34-37} have been synthesized from readily available *exo/endo*-4-substituted-norbornenes (e.g., *exo/endo*-4-hydroxymethylnorbornene). Polymers prepared by ROMP of *exo/endo*-4-substituted-norbornenes

are amorphous since the polymer contains both exo and endo substituents, cis and trans double bonds, and head to tail, tail to tail, and head to head monomer relationships in the polymer backbone. Diphenylanthracene (DPA), either as a vacuum-deposited film or in a polymer matrix, has not been pursued previously as an emitter in LEDs, mainly due to DPA's poor film-forming qualities.³⁸ In amorphous films made by ROMP of **1** (eq 1), diphenylanthracene should not be able to migrate readily to form crystalline regimes.



In order to achieve optimum performance from devices, it is necessary to control the transport of holes and electrons in the polymer film.^{2,6,39-43} The diagram below (Figure Intro.1) shows an idealized device structure, containing several layers with differing functions. The electron-transport layer is composed of a material which readily accepts electrons, but not holes (i.e. positive charge carriers). The hole-transport layer readily accepts holes, but not electrons. Upon applying an electric field across this film, holes and electrons are forced to recombine in the center layer. This sandwiched center layer contains an emitting species, E, which forms the excited state, E*, upon recombination of holes and electrons in the form of E^{•+} and E^{•-} (eq 2). E* subsequently decays by photon emission (eq 3). The three-layer structure helps to balance the flow of holes and electrons through the film and confines E* away from the surface of the electrodes, where it could be readily quenched.



A series of monomers were studied that contains blue-light emitting, hole-transporting, and electron-transporting groups (Figure Intro.2). Polymers made via ROMP were prepared from

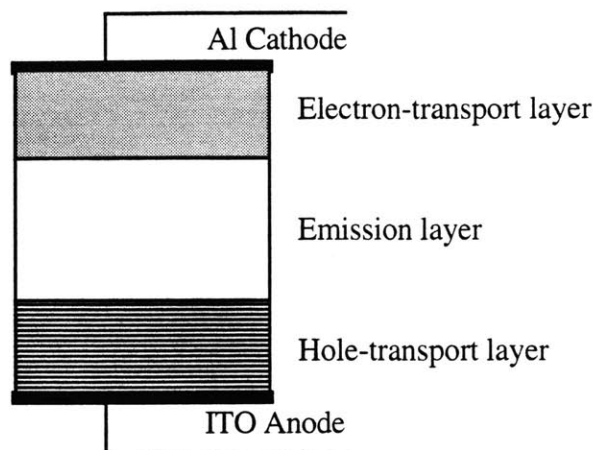


Figure Intro.1. Light-emitting device (LED) with discrete layers for emission, electron transport, and hole transport. (ITO = Indium Tin Oxide, a conductive, transparent material.)

these monomers. Copolymers incorporating both carrier transport and DPA structural units were also investigated. The synthesis of these materials is described in CHAPTER 1.

CHAPTERS 2 and 3 of this thesis investigate two options for creating discrete regions of emission and charge transport in a polymer film. Both options incorporate the novel sequential adsorption technique recently developed by Professor Dr. Michael Rubner and coworkers at the Massachusetts Institute of Technology. This technique allows deposition of alternating layers of polycation and polyanion, each held in place by ionic interaction with the preceding layer.^{9,10,44,45} The process overcomes one of the greatest difficulties in forming separate film regions for charge transport and emission (Figure Intro.1): etching the bottom layer upon deposition of the top layer. In CHAPTER 2 a hole-transporting film constructed by sequential adsorption of water-soluble PPV is described. Subsequent spin-coating of electroluminescent polynorbornenes from chlorobenzene does not etch this layer. CHAPTER 3 describes multilayered polynorbornene films constructed entirely by the sequential adsorption technique.

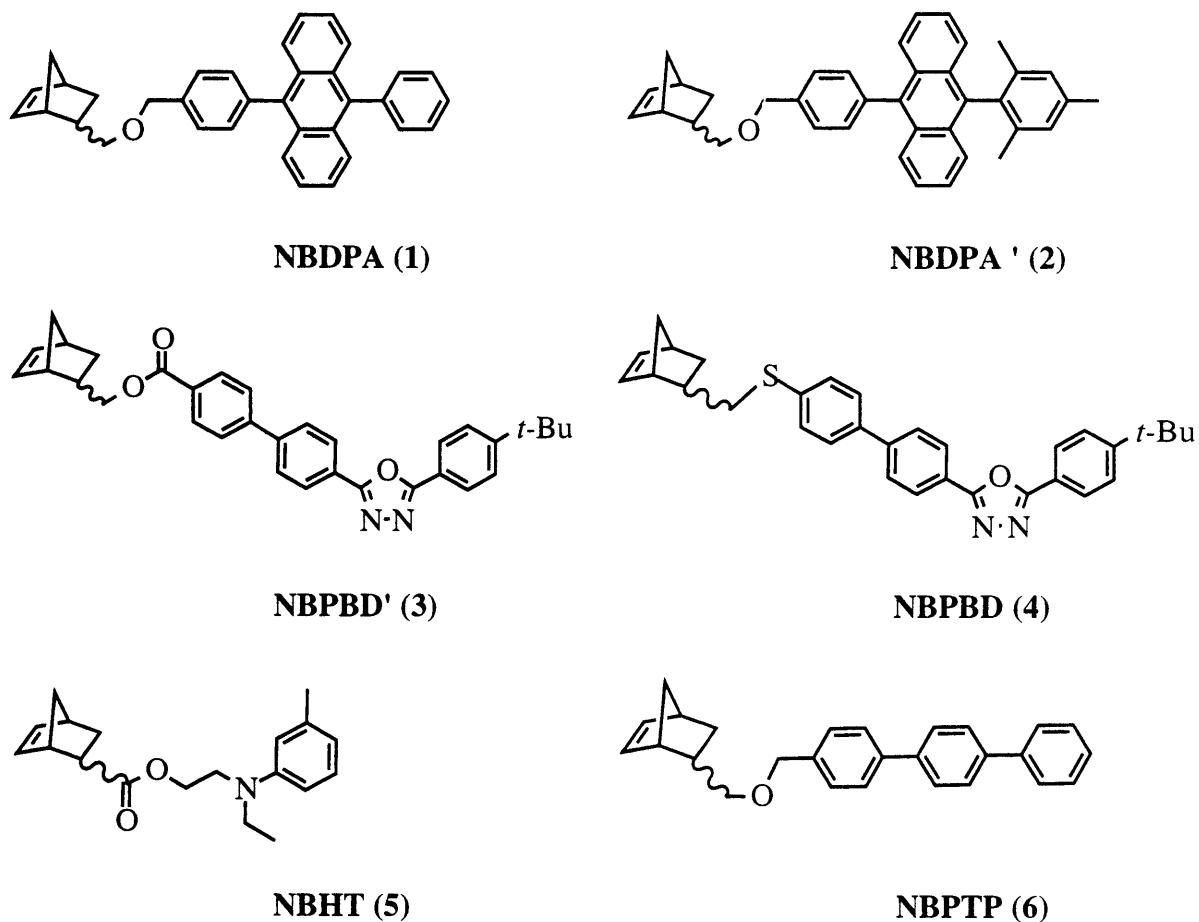


Figure Intro.2. Norbornene monomers for blue light emission (**1-2**), electron transport (**3-4**), and hole transport (**5-6**).

The descriptive labeling and numbering scheme in Figure Intro.2 will be used in CHAPTERS 1-3 and APPENDIX A. The following convention will be employed for polymers.

Unmodified homopolymers:	E_n
Unmodified copolymers:	$[E_x \% E'_{100-x \%}]_n$
Modified homopolymers:	sulf-E_n or epox-E_n
Modified copolymers:	sulf-$[E_x \% E'_{100-x \%}]_n$

Where **E**, **E'** = electroactive monomers shown in Figure Intro.2; **n** = total # of repeat units (both monomers); **x** = percent of **E** in the copolymer; **100 - x** = percent of **E'** in the copolymer; **sulf-** = sulfonated form of the polymer; and **epox-** = epoxidized form of the polymer.

CHAPTER 1

Synthesis and Polymerization of Electroluminescent Norbornenes and Chemical Modification of Polynorbornenes

Some of the material covered in this chapter has appeared in print:

Boyd, T. J.; Geerts, Y.; Lee, J.-K.; Fogg, D. E.; Lavoie, G. G.; Schrock, R. R.;
Rubner, M. F. *Macromolecules* **1997**, *30*, 3553.

Introduction

The very active field of Light Emitting Devices (LEDs) still has much need for research into the design and synthesis of new materials.^{2,3} Therefore, the goals of this project are to prepare potentially useful monomers and polymers and evaluate their efficacy in devices. This chapter will explore the synthesis of a library of norbornene-based monomers and polymers for LED application. For emission, the focus will be on a series of monomers containing diphenylanthracene (DPA), a highly blue photoluminescent, yet electrochemically stable, species.^{22,24,46-49} For electron-transport, the group *t*-butylphenyl-*para*-biphenyloxadiazole (PBD) will be investigated, since it is widely used as an electron carrier or to block holes.^{6,18,50,51} Both DPA and PBD crystallize readily; as a result they are unsuitable for stable films in LEDs. However, PBD or DPA bound to polymerized norbornene should be unable to separate and crystallize. Hole-transport (electron-blocking) monomers based on *N,N*-diethyl-2-methylaniline and *para*-triphenylene (PTP) will also be discussed.^{52,53} The building of LEDs with the homopolymers and copolymers formed with these new monomers will be discussed in CHAPTER 2 and CHAPTER 3.

CHAPTER 1 also describes epoxidation and sulfonation techniques that are applicable to substituted polynorbornenes. These general methods can be used on *any* polynorbornene with relatively robust side groups. Chemical oxidation to form terminal epoxides provides a widely-used route to preparing graft copolymers or highly crosslinked materials, and is frequently reported in the current polymer literature.⁵⁴⁻⁵⁶ Polymers modified by sulfonation have a variety of potential uses, including solid/liquid separation in water treatment,⁵⁷⁻⁵⁹ ion-exchange resins,^{55,60} reverse osmosis membranes,^{58,61,62} and biomedical applications.⁶³⁻⁶⁵ Technology for sulfonation of polymeric materials such as polystyrene is well developed.⁵⁶ Surprisingly, reports on modification of polynorbornene formed by ring-opening metathesis polymerization (ROMP) are sparse. The literature contains examples of sulfonation,^{66,67} hydrogenation,^{68,69} and carbonamide⁷⁰ derivatives. Of these, only hydrogenation has been reported for substituted norbornenes, despite the fact that recent years have witnessed increasing interest in these materials

due to the availability of living polymerization techniques using well-defined metal alkylidene catalysts. Application of the sulfonated forms of electroluminescent polynorbornenes in order to build films by sequential adsorption of polyelectrolytes will be explored in CHAPTER 3.

Results and Discussion

Blue-Light-Emitting Monomers Based on Diphenylanthracene (DPA).

The blue-light-emitting monomer, **1**, was prepared in an overall yield of 42% following the route shown in Scheme 1.1. This approach is a variation of that developed by Dr. Yves Geerts and is a general method for attaching aromatic systems to a norbornene. Originally, 9-bromoanthracene, **8**, was prepared in 85% yield and required column chromatography to purify. However, when more care was taken to use fresh bromine and to monitor closely the reaction by NMR, the yield for this step increased to 98%, rendering chromatographic purification unnecessary. In the initial synthesis, a pinacol borate was isolated by column chromatography and subsequently reacted with **8** to form **1**. However, the instability of the pinacol borate was such that typical yields for these two steps were around 7%. Since by proton NMR there was high conversion to the diethyl borate, **7**, it was determined that the intermediate need not be isolated. Immediate reaction with **8** gave far higher yields than previously observed for the two-step sequence (50% versus 7%), and made it feasible to prepare gram quantities of the monomer, **1**.

The absorption and emission properties of **1** were similar to 9,10-diphenylanthracene itself.⁴⁶ $\lambda_{\text{max,abs}} = 398 \text{ nm}$ (DPA: $\lambda_{\text{max,abs}} = 388 \text{ nm}$); $\lambda_{\text{max,em}} = 442 \text{ nm}$ ($\lambda_{\text{ex}} = 360 \text{ nm}$) (DPA: $\lambda_{\text{max,em}} = 422 \text{ nm}$ ($\lambda_{\text{ex}} = 265 \text{ nm}$)). Polymerization of 25 equiv of **1** with $\text{Mo}(\text{N-2,6-}i\text{-Pr}_2\text{C}_6\text{H}_3)(\text{CHMe}_2\text{Ph})(\text{O-}t\text{-Bu})_2$ ([Mo]) in toluene, followed by quenching with benzaldehyde, provided a high yield of homopolymer **125** (Table 1.1). As expected, the polydispersity of **125** was low, consistent with the living nature of this ROMP reaction. Unlike crystalline DPA, **125** formed transparent amorphous films when spin-coated from chlorobenzene. Polymers containing 25 or 50 equivalents of monomer were chosen in this project since they can be precipitated readily in certain solvents, yet dissolve readily in others to give solutions suitable for preparing films.

Scheme 1.1. Synthesis of NBDPA (1).

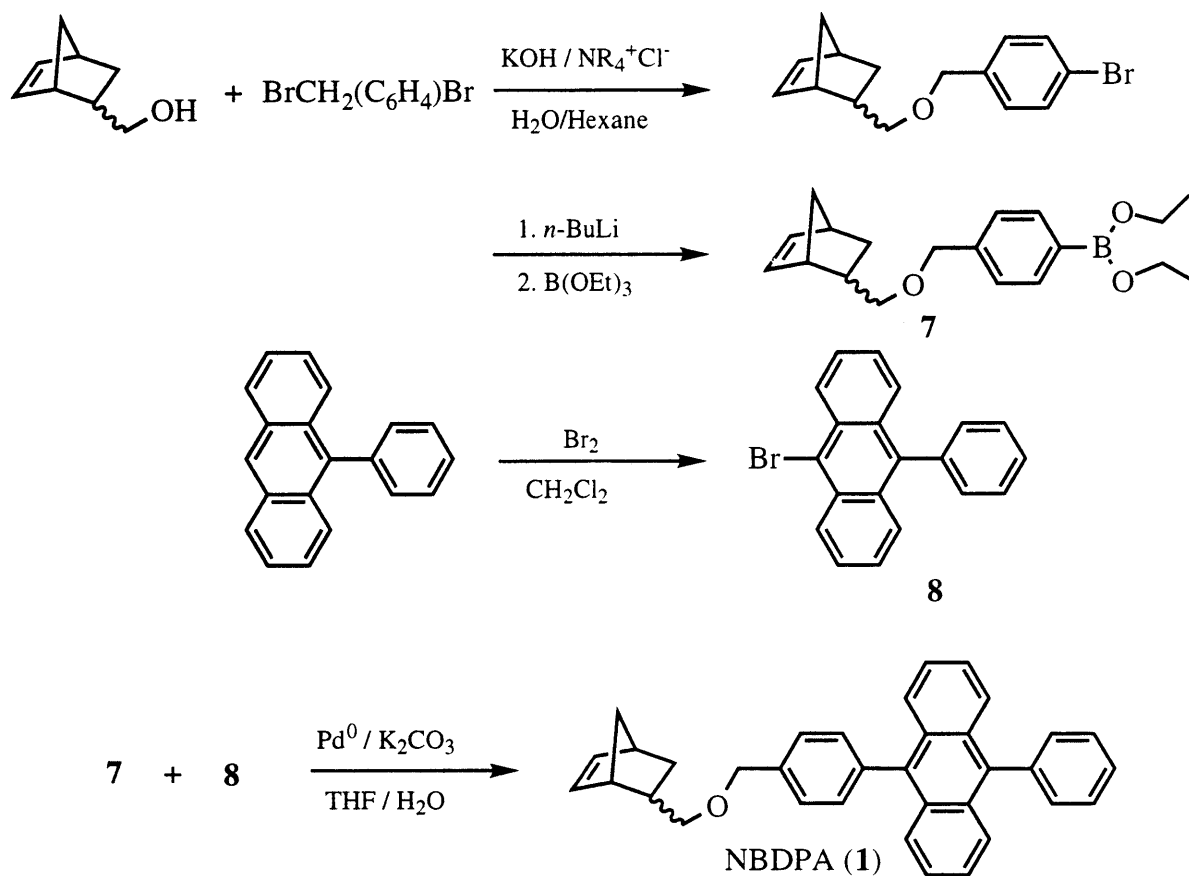
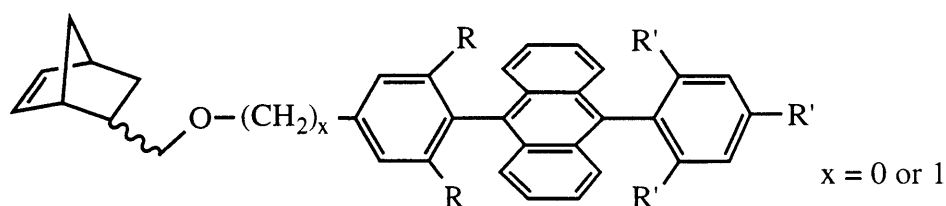


Table 1.1. Substituted Polynorbornenes

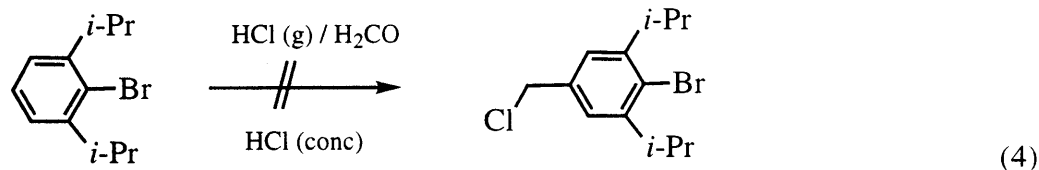
Polymer ^a	Yield (%)	Mol. Wt. (calc.)	M_n^b	M_w/M_n
1 ₂₅	95	12 800	19 400	1.04 ± 0.11
2 ₂₅	94	12 900	8000	1.07 ± 0.02
3 ₅₀	97	24 700	53 800	1.05 ± 0.08
4 ₂₅	99	12 400	8 700	1.19 ± 0.04
6 ₅₀	99	18 600	21 600	1.81 ± 0.04

^aPolymers consisted of 25 or 50 repeat units. ^bAll molecular weights were determined by GPC in CH₂Cl₂ using a light scattering detector coupled to a differential refractometer.

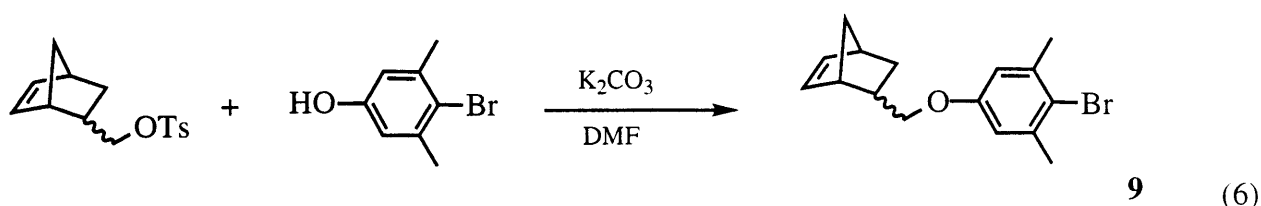
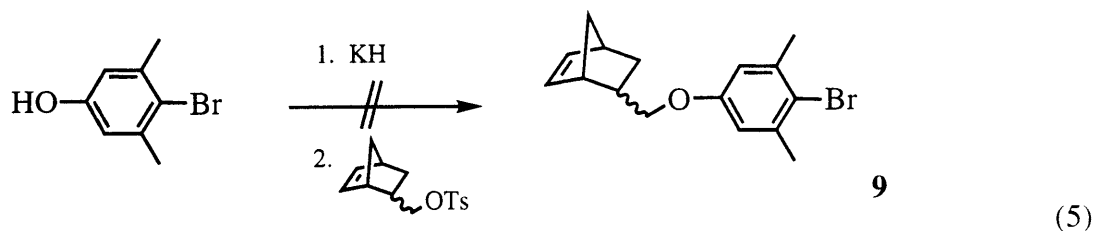
In certain cases, polymers containing **1** formed self-quenching excimers (discussed fully in CHAPTER 3). For this reason, a bulkier form of DPA became a synthetic target. The emission from DPA derivatives arises from the anthracene core; the phenyl groups are important primarily to block the reactive 9 and 10 sites on anthracene, as well as to increase the photoluminescence quantum yield.^{46,47} It was hypothesized that adding substituents directed above and below the anthracene plane to one or both of these phenyl rings should greatly increase the sterics without modifying the emission properties.



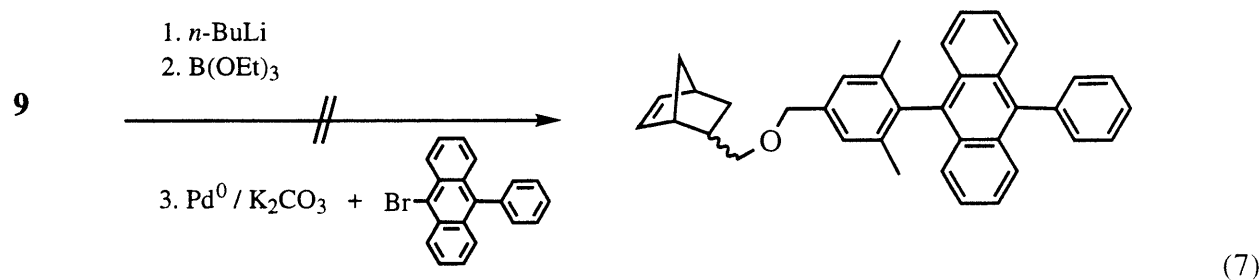
The norbornenyl side of the anthracene was the first synthetic focus. Chloromethylation of 1-bromo-2,6-diisopropylbenzene was attempted using standard conditions (eq 4). Halogens are known to activate chloromethylation in the *para* position, although alkyl groups are deactivating.^{71,72} In this case, only starting material was recovered, so the alkyl groups were too deactivating.



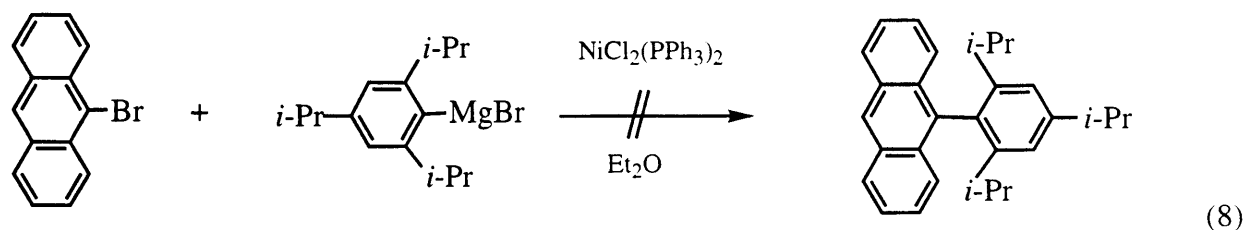
The next target was to use the commercially available 4-bromo-3,5-dimethylphenol to form **9**, a species that in the target monomer could flank the anthracene unit with two methyl groups. Equations 5 and 6 show two attempts to prepare **9** with norbornene tosylate. The relatively standard S_N2 reaction conditions in eq 6 proved effective in giving **9** in 60 % yield after heating to 90-100 °C for several days.



Subsequent use of **9** to perform the Suzuki coupling in eq 7 proved unsuccessful; perhaps the steric bulk of **9** combined with the already bulky 9-bromo-10-phenylanthracene was too great to fit around the Pd⁰ catalyst. If so, further attempts at substitution on the norbornenyl side of anthracene will also be difficult.

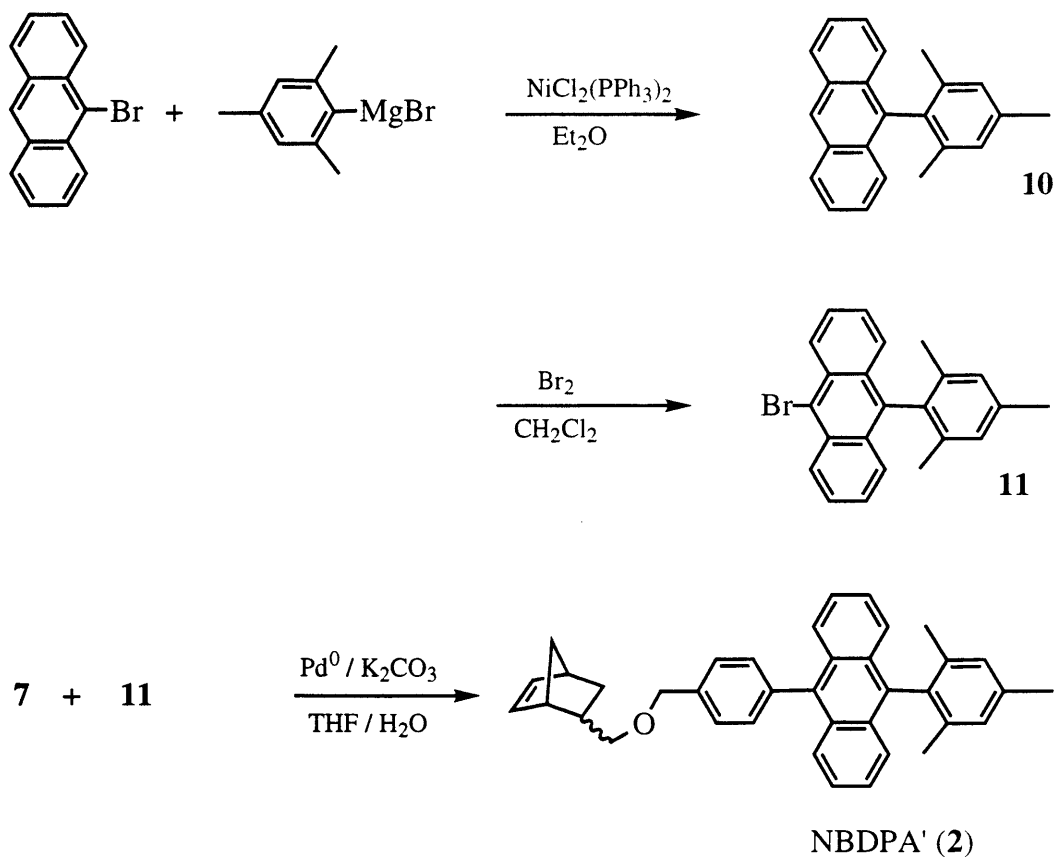


Modification of the phenyl ring on the side of anthracene opposite the norbornenyl group was explored next. The Grignard coupling of 9-bromoanthracene with 2,4,6-triisopropylphenylmagnesium bromide was attempted (eq 8), but yielded a mixture of starting material and several products, the separation of which by column chromatography was not possible.⁷³ Perhaps here, too, the combination of reagents was too bulky for the coupling to proceed smoothly.



Switching to the less bulky mesitylmagnesium bromide successfully provided the desired coupling product, **10**, in 58% yield (see Scheme 1.2). Bromination of **10** with fresh Br₂ was carried out in 30 min at room temperature, yielding **11** in virtually quantitative yield. The norbornenylphenyl diethyl borate, **7**, was prepared *in situ* as described above. The coupling of **7** with **11** was achieved in 58% yield to give the new NBDPA' monomer, **2**. The overall yield for the 5 steps was 32%. The ability to run the reactions on a gram scale and the relative lack of

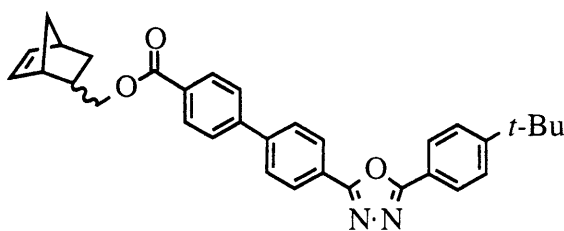
Scheme 1.2. Synthesis of NBDPA' (**2**).



column chromatography purification (once after each aryl coupling step) made this a readily achievable reaction sequence. The final product had the anthracene protected on one side by methyl groups above and below the ring plane. (The proton NMR spectra of **10**, **11**, and **2** show an upfield shift for these methyl group resonances as expected for their position relative to the anthracene ring current.) The homopolymer **225** was readily prepared using [Mo] in high yield and with low polydispersity (Table 1.1). The absorption and emission properties of **2** were similar to **1** and 9,10-diphenylanthracene itself: $\lambda_{\text{max,abs}} = 399 \text{ nm}$ (**1**: $\lambda_{\text{max,abs}} = 398 \text{ nm}$); $\lambda_{\text{max,em}} = 443 \text{ nm}$ ($\lambda_{\text{ex}} = 360 \text{ nm}$) (**1**: $\lambda_{\text{max,em}} = 442 \text{ nm}$ ($\lambda_{\text{ex}} = 360 \text{ nm}$)).

Monomers for Hole and Electron Transport.

The electron-transport monomer, **3**, was synthesized in an overall yield of 65% using a procedure developed by Dr. Deryn Fogg.⁷⁴ Absorption and emission wavelengths were shifted somewhat from *t*-butylphenyl-*para*-biphenyloxadiazole itself:⁴⁶ $\lambda_{\text{max,ab}} = 325 \text{ nm}$ (PBD: $\lambda_{\text{max,ab}} = 302 \text{ nm}$); $\lambda_{\text{max,em}} = 425 \text{ nm}$ ($\lambda_{\text{ex}} = 360 \text{ nm}$) (PBD: $\lambda_{\text{max,em}} = 360 \text{ nm}$ ($\lambda_{\text{ex}} = 313 \text{ nm}$)).

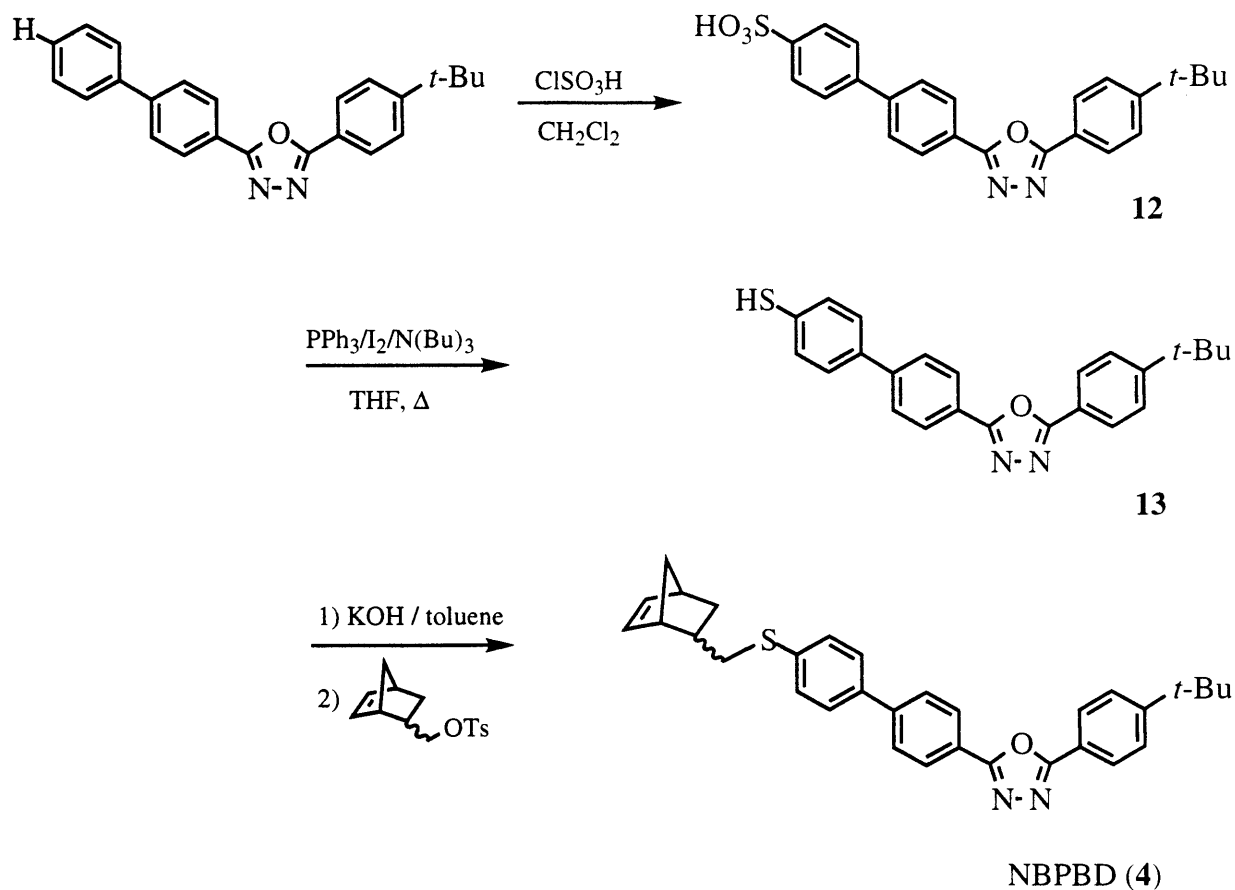


NBPBD' (3)

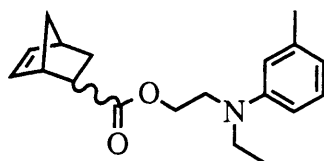
A second monomer was designed with the PBD structural unit attached to norbornenyl via a thioether linkage. Scheme 1.3 shows the preparation of NBPBD (**4**). The synthesis was accomplished in 30% overall yield in 4 steps; **4** can be readily prepared on the gram scale. The first step involved sulfonation of *t*-butylphenyl-*para*-biphenyloxadiazole, which occurred quantitatively on a 10 g scale to give **12**. The reduction of **12** to the thiol, **13**, proceeded cleanly. However, decomposition of **13** to a deep yellow material occurred within hours upon exposure to

light. A significant loss of yield occurred during this step if **13** was purified by column chromatography before proceeding to the final reaction. The overall yield was significantly improved by eliminating this purification step. The primary byproduct to form **13** was triphenylphosphine oxide, the presence of which should not affect the nucleophilic substitution reaction in the final step. The final product, NBPBD, was stable to light which lessened the losses during purification. Absorption and emission wavelengths for **4** were shifted somewhat from *t*-butylphenyl-*para*-biphenyloxadiazole itself:⁴⁶ $\lambda_{\max,ab} = 339$ nm (PBD: $\lambda_{\max,ab} = 302$ nm); $\lambda_{\max,em} = 395$ nm { $\lambda_{ex} = 360$ nm} (PBD: $\lambda_{\max,em} = 360$ nm { $\lambda_{ex} = 313$ nm}).

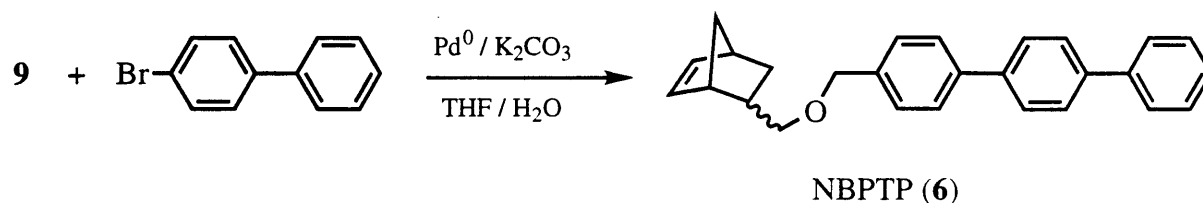
Scheme 1.3. Synthesis of NBPBD (**4**).



The hole-transporting monomer, NBHT (**5**), was prepared in 69% yield using a procedure developed by Dr. Jin-Kyu Lee.^{53,74} Synthesis of the hole-transport material, NBPTP (**6**), is shown in Scheme 1.4. NBPTP was prepared in three steps with a 43% yield, following a procedure very similar to that for **1** (only the final step is shown in Scheme 1.4).

NBHT (**5**)

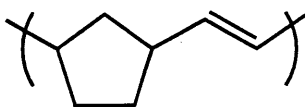
Homopolymers of **3**, **4** and **6** were prepared (Table 1.1) with [Mo]. As expected, high yields and low polydispersities were obtained. A series of copolymers was made by slowly adding a mixture of either monomer **1** or **2** with monomer **3**, **4**, **5**, or **6** to a solution of [Mo]. The presence of two different propagating alkylidene complexes and two different monomers ensures that four different propagation steps can take place. (The number of possibilities is actually twice that since two rotameric forms^{75,76} of each propagating alkylidene can be present.). The structural differences and steric bulk of **1-6** projected well away from the norbornene double bond, so their rates of propagation were expected to be similar. However, to ensure that the monomer distribution was uniform, the two-monomer mixture was slowly added to a solution of [Mo]. The overall monomer ratio in each copolymer was verified by proton NMR peak integrations and by the high yields (90 % or greater based on total monomer feed).

Scheme 1.4. Synthesis of NBPTP (**6**).

The properties of these homopolymers and copolymers when spin-coated in LEDs will be discussed in detail in CHAPTER 2. The next section describes how polynorbornenes can be transformed into water-soluble polyanions, suitable for making films for LEDs by sequential adsorption. CHAPTER 3 will discuss the attributes of devices made with the polyanionic forms of these polymers.

Sulfonation of the Polynorbornene Backbone.

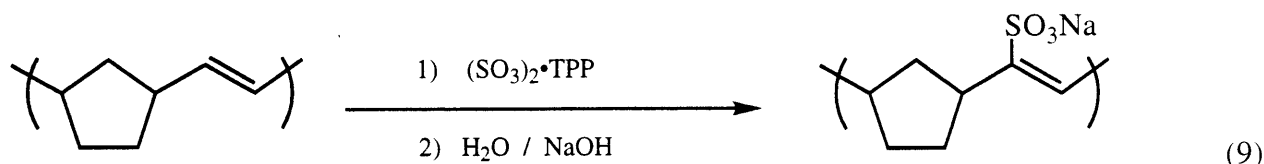
A wide variety of sulfonation reagents exists that can be used to sulfonate ethers, esters, alcohols, and carbon-carbon double bonds, both aromatic and non aromatic.⁷⁷⁻⁸⁰ These reagents vary in both their selectivity and in their reactivity. Many commercially-available sulfonation reagents are sold as base adducts of SO_3 , such as $\text{SO}_3\cdot\text{pyridine}$, or $\text{SO}_3\cdot N,N\text{-dimethylacetamide}$. These solids are easily handled and are effective at sulfonating terminal double bonds. The parent polynorbornene, **14₁₀₀**, was treated with $\text{SO}_3\cdot\text{pyridine}$, the most reactive of the commercially-available adducts, but no reaction occurred. Apparently, the strength of the adduct makes it unsuitable for use as a sulfonation reagent. This is not surprising based on the limited reactivity of $\text{SO}_3\cdot\text{pyridine}$ with internal olefins reported in the literature.⁷⁷ At the other end of the reactivity spectrum exist SO_3 and H_2SO_4 . Although both are suitable for producing highly sulfonated polymers in some cases (such as with polystyrene), they readily react with most aromatic groups. As a result, they are unacceptable for the purpose of deriving a *general* technique for polynorbornene sulfonation.



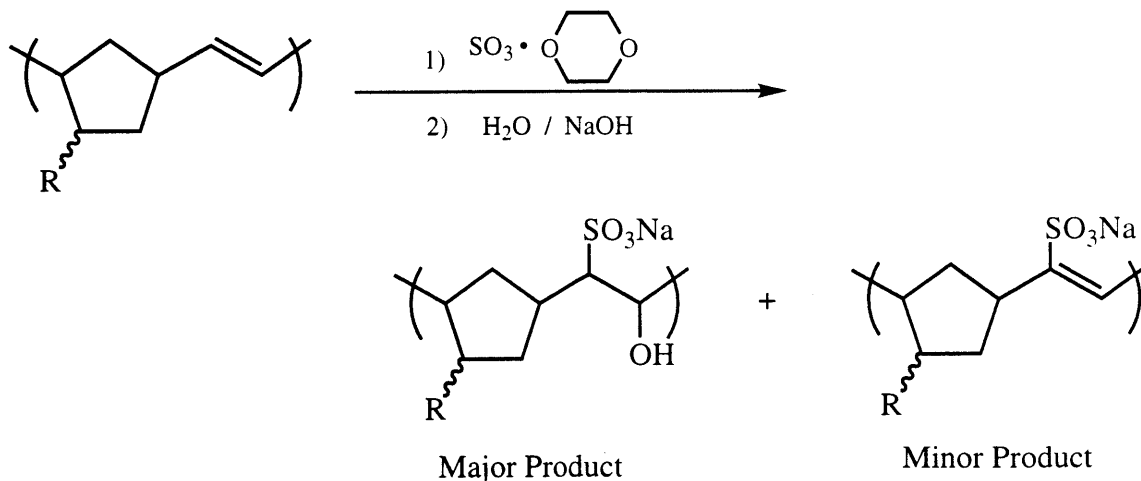
14₁₀₀

In the only set of papers published on polynorbornene sulfonation, a reagent of intermediate reactivity, $\text{SO}_3\cdot\text{triethylphosphate}$ (TPP), was employed.^{66,67} The reaction completely conserved the double bond in the polymer (eq 9). However, $\text{SO}_3\cdot\text{TPP}$ was not considered for this

application because it is known to react with aromatic rings and other sensitive groups. These are exactly the type of functionalities in monomers **1-6** that make them interesting for LED application. Sulfur trioxide•dioxane was found to be a more appropriate reagent; it has the reactivity necessary to effectively sulfonate the double bond, but is generally inert towards aromatic rings and ethers. Unlike $\text{SO}_3\cdot\text{TPP}$, $\text{SO}_3\cdot\text{dioxane}$ can produce two variants upon quenching of the reaction mixture (Scheme 1.5). One of these contains a saturated C-C bond and the other regenerates the C-C double bond.⁷⁸⁻⁸⁰



Scheme 1.5. Sulfonation of Polynorbornene with $\text{SO}_3\cdot\text{dioxane}$.



The $\text{SO}_3\cdot\text{dioxane}$ reagent was made by adding 10 equiv of SO_3 to 15 equiv of dioxane in dry CH_2Cl_2 at $0\text{ }^\circ\text{C}$ (SO_3 reacts with water to make H_2SO_4 , which can form aryl sulfonates). A polymer solution was then added over the course of 30 seconds and the mixture was allowed to warm to room temperature. After stirring at room temperature for three hours, the reaction was

quenched by addition of aqueous NaOH. All solvent was removed *in vacuo* and the residue was extracted with DMSO overnight. The insoluble material (both NaOH and the reaction byproduct, NaSO₄, are insoluble in DMSO) was removed by centrifugation and the DMSO supernatant was removed *in vacuo*, leaving the sulfonated polymer.

When applied to **14**₁₀₀, this process yielded **sulf-14**₁₀₀, which is highly sulfonated and has solubility properties vastly different from the starting polymer. The percent sulfonation of **sulf-14**₁₀₀ was determined by proton NMR to be at least 79% by measuring the disappearance of the olefinic protons at 5.3 ppm relative to the aliphatic protons, which are unaffected. Since a mixture of sulfonation products is expected (Scheme 1.5), some of the remaining olefinic peak arises from the sulfonated minor product. It is therefore quite likely that sulfonation is greater than 79%, although this has not been quantified. The IR spectrum of **sulf-14**₁₀₀ shows characteristic peaks at 1199 and 1043 cm⁻¹, which are indicative of SO₂ stretches, and also the disappearance of the strong cis (740 cm⁻¹) and trans (966 cm⁻¹) olefin CH bends .

Since the SO₃•dioxane reagent was successful in the test case, the reaction was next applied

Table 1.2. Summary of Sulfonated Polynorbornenes

polymer	Sulfonation (%) ^a
sulf-14 ₁₀₀	79
sulf-1 ₂₅	85
sulf-2 ₂₅	90
sulf-4 ₂₅	92
sulf-6 ₅₀	89

^a Amount of sulfonation determined by integration in proton NMR of olefinic resonances, assuming that all olefin present is unreacted (this is a lower limit, see Scheme 1.5).

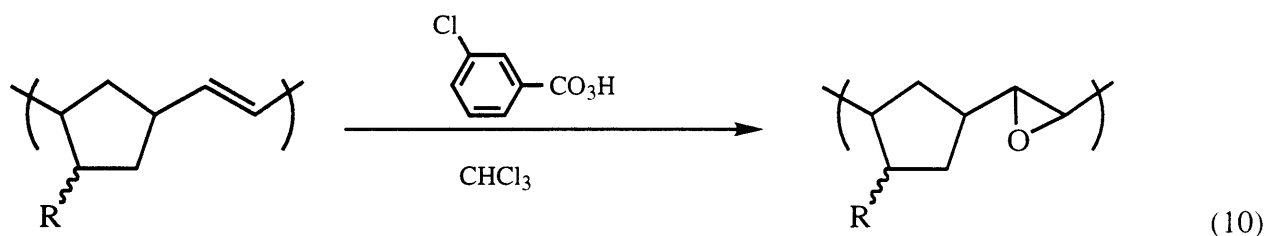
to the more sensitive polymers described above. The polynorbornenes made with NBDPA, **125**, or NBDPA', **225**, contain only ether and aromatic groups, and so are suitable for the sulfonation procedure. However, the electron-transporting NBPBD' polymer, **350**, is unsuitable because it links the *tert*-butylphenyl-*para*-biphenyloxadiazole (PBD) moiety to the norbornene via a reactive ester functionality.⁷⁴ For this reason, the monomer containing the thioether linkage, NBPBD (**4**), was designed and synthesized. The hole transporting monomer, NBHT (**5**), is unsuitable due to an ester functional group. In contrast, the monomer NBPTP (**6**), which is a potential hole-transport material as well, contains an ether linkage and so should be suitable. Sulfonation of **125**, **225**, **425**, and **650** with SO₃•dioxane under the conditions described above proceeded smoothly. Table 1.2 shows the results of the sulfonation reactions. The percent sulfonation was at least 85% in all cases. As explained above, this is a lower limit on the percent sulfonation, since the minor products in Scheme 1.5 contain olefinic protons. Little change occurred in the aromatic region of the proton NMR or in the absorption spectra, indicating that the side chain electroluminescent materials were not harmed. For polymers containing **1** or **2**, the $\lambda_{\text{max,abs}}$ remained at 400 nm. However, the emission properties of these materials changed upon sulfonation. This phenomenon will be discussed in CHAPTER 3.

A drastic change was observed in solubility of polynorbornenes before and after sulfonation. The starting materials were readily soluble in nonpolar solvents, such as toluene, chloroform, and chlorobenzene. After sulfonation, the polymers were no longer soluble in such solvents, but were quite soluble in DMSO or *N,N*-dimethylacetamide (DMA). None was readily soluble in water. However, after dissolving the polymer in 1 mL of DMSO or DMA, the solution was easily diluted with water without any polymer precipitation, even at very high water concentrations (>98% water).

The series of copolymers containing monomers **1**, **2**, **4**, and **6** was also sulfonated using this technique. The physical properties were similar to those of the sulfonated homopolymers. The luminescent properties of these sulfonated polynorbornenes and their application in assembling films for LEDs are discussed at length in CHAPTER 3.

Epoxidation of the Polynorbornene Backbone.

The epoxidation reagent *m*-chloroperoxybenzoic acid is a widely-used and commercially-available reagent for generating organic epoxides. It was found to be an excellent choice for converting the polynorbornene double bond into the corresponding epoxide (eq 10). This process (also known as the Prilezhaev reaction) is very efficient, but is also quite tolerant of functionality, not attacking aromatic rings, ethers, or esters.⁷¹ The Prilezhaev epoxidation of **14**₁₀₀ rapidly proceeded to completion, forming the epoxidized polymer, **epox-14**₁₀₀. When monitoring the reaction by proton NMR, it was found that the olefinic peak at 5.3 ppm disappeared after 5 minutes, indicating 100% conversion of starting polymer. A new broad peak was observed at 2.81 ppm, consistent with protons on an epoxide ring, and the resonance at 62.19 ppm in the carbon-13 NMR spectrum can be assigned to the epoxide ring carbons. The IR spectrum displayed the characteristic 8 μ , 11 μ , and 12 μ epoxide ring stretches at 1258, 889, and 730 cm⁻¹ respectively.^{81,82} The IR also showed a trace of the overoxidized product, a C=O stretch at 1725 cm⁻¹. However, no evidence of this was found in the carbonyl region of the carbon-13 NMR spectrum, indicating that overoxidation occurs only to a small degree.

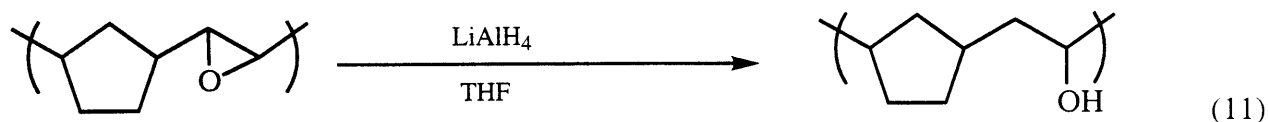


Unfortunately, further reactions with **epox-14**₁₀₀ did not readily occur. Attempts to react the material with a variety of nucleophiles, such as NaOH, NaOMe and KOCH₂CH₂NMe₂, at room temperature to 100 °C showed no change of the starting material. This was not particularly surprising because the reactivity of internal epoxides is known to be limited, especially when large groups are close to the double bond, as in this case.⁷¹ The reactivity of **epox-14**₁₀₀ was further

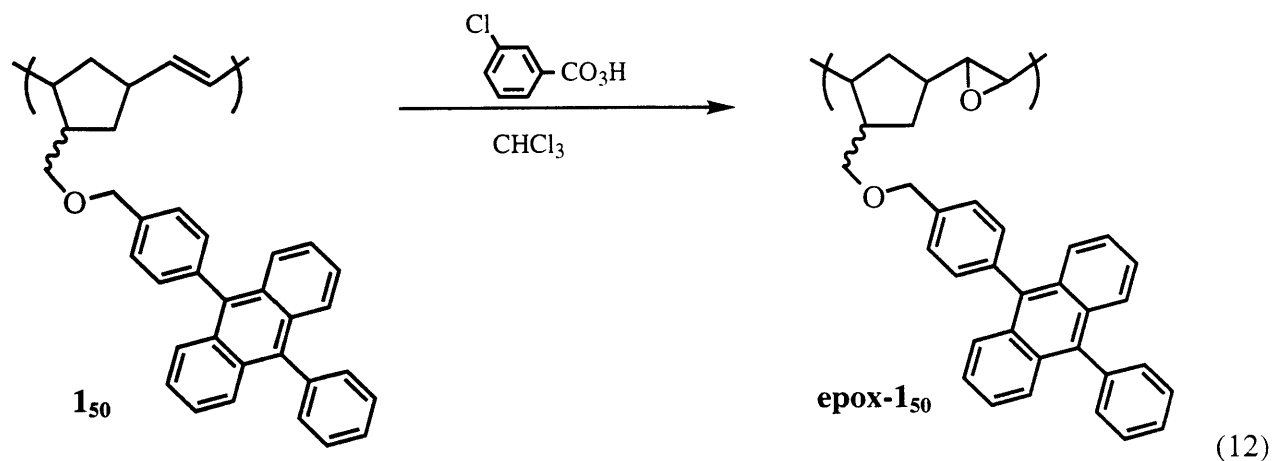
hampered by the insolubility of the material in polar solvents such as CH_3CN or DMSO, which would increase the rate of reaction.

Combining **epox-14₁₀₀** with aqueous HCl resulted in no reaction. Since **epox-14₁₀₀** was very insoluble in water (even in 5% water / 95% THF the polymer precipitated) reactions requiring hydroxyl groups from H_2O were bound to be sluggish. Combining **epox-14₁₀₀** with 2 equiv of 1 M HCl in ether, followed by addition of water, led to a dark intractable material. The proton NMR spectrum taken of a dilute sample showed mostly starting material resonances. It is possible that the HCl initiates a small degree of crosslinking in the polymer, rendering it insoluble.

One reaction that proceeds relatively cleanly with **epox-14₁₀₀** was the conversion of the epoxide ring to a monohydroxyl derivative with LiAlH_4 (eq 11). Addition of 2 equiv of LiAlH_4 in THF to **epox-14₁₀₀** gave complete conversion (based on proton NMR) to the monohydroxy, $(\text{NB}(\text{OH}))_{100}$. The chemical shifts assigned to the epoxide ring disappeared and were replaced by a peak at 4.14 ppm, typical of $-\text{CH}(\text{OH})-$. Also, the carbon-13 NMR spectrum showed a new resonance at 72.70 ppm ($-\text{C}(\text{OH})-$) and the IR spectrum showed a strong, broad OH stretch at 3448 cm^{-1} . The characteristic epoxide μ stretches were no longer apparent.



To test the generality of the epoxidation reaction the blue-light emitting polymer, **150**, was treated with the same reaction conditions described above (eq 12). The formation of **epox-150** proceeded quickly and yielded the complete conversion of the olefinic groups to epoxide rings. As expected, the DPA group was not harmed by the process. Due to the limited utility of the epoxidized polymers, no further reactions were explored.



Conclusions

It has been shown that a variety of monomers can be readily synthesized which contain both emission and charge transport functional units. Homopolymers and copolymers were polymerized with the versatile [Mo] catalyst, demonstrating once again its utility in making well-defined materials. CHAPTER 2 will explore the application of the nonpolar (i.e., unsulfonated) forms of these polynorbornenes in building films for LEDs by spin-coating.

The sulfonation procedure with $\text{SO}_3 \cdot \text{dioxane}$ allows for the ready conversion of substituted polynorbornene from a nonpolar to a polyionic material. The solubility characteristics of the two materials are vastly different. It is straightforward to prepare polynorbornenes with functional groups that are both potentially useful for applications, such as light emitting devices, and also robust enough to withstand the sulfonation conditions. Since the $\text{SO}_3 \cdot \text{dioxane}$ reagent is tolerant of aromatic rings, including heterocycles, it is possible to functionalize a wide variety of polymers in this manner.

The epoxidation reaction, although high-yielding and rapid, is disappointing from a synthetic point of view. Further reactions of all but the most limited type have not been successful, making the polymers of little use as synthetic intermediates. However, if the synthetic target is only to remove the double bonds, this procedure may provide an alternative to hydrogenation. The limited reactivity in this case would be advantageous, not interfering in subsequent application or

reaction. The primary advantages over hydrogenation would be: 1) the solubility characteristics are more favorable than the relatively insoluble hydrogenated polymer,⁶⁸ and 2) the reaction is quick and complete.

In CHAPTER 3 the polyionic nature of the sulfonated homopolymers and copolymers described above will be exploited to form films via sequential adsorption with a polycation such as poly(allylamine HCl) (PAH). This method of depositing films layer by layer provides great flexibility in both film structure and creation of high-quality (i.e., uniform and defect-free) films.

Experimental Section

Characterization. HPLC grade CH_2Cl_2 was used in gel permeation chromatography (GPC) runs and was distilled over CaH_2 prior to use. GPC was carried out using a Waters Ultrastaygel 10573: Shodex KF-802.5, 803, 804, 805, and 800P columns; a Visotek Differential Refractometer/Viscometer H-500; and a Spectroflow 757 absorbance detector on samples 0.1 - 0.3 % (w/v) in CH_2Cl_2 . Samples were first filtered through a Millex-SR 0.5 μm filter in order to remove particulates. GPC columns were calibrated versus polystyrene standards (Polymer Laboratories Ltd.) which ranged from MW = 1260 to 2.75×10^6 . Elemental analyses were performed by H. Kolbe Laboratories, Mülheim an der Ruhr, Germany. NMR data were obtained at 300 or 500 MHz and listed in parts per million downfield from tetramethylsilane. IR spectra were taken with a Perkin-Elmer FT-IR of either a cast polymer film on a NaCl plate or of powdered polymer in a KBr pellet. Absorbance spectra were taken with an Oriel Instaspec spectrophotometer. Photoluminescence spectra were taken using a spectrograph coupled to a Peltier-cooled CCD array (Oriel Instaspec IV). The system response was calibrated using a tungsten lamp. Excitation for the photoluminescence was from the multiline UV mode of an argon ion laser. Spectra were obtained at 25 °C unless otherwise noted.

Preparation of Monomers. Unless otherwise stated, all experiments were performed under a nitrogen atmosphere in a Vacuum Atmospheres drybox or using standard Schlenck techniques. The preparation of (5-norbornenyl)methyl tosylate, **3**, and **5** have been described

elsewhere.⁷⁴ All chemicals were reagent grade and were purified by standard methods. Pd(PPh₃)₄ and NiCl₂(PPh₃)₄ were purchased from Strem Chemicals. All other chemicals were purchased from Aldrich Chemical Company and used as received.

***para*-(Diethylborate)benzyl (5-Norbornenyl)methyl Ether (7).** In a nitrogen-filled drybox *n*-butyl lithium (1 mL, 2.5 M in hexanes) was added to *para*-bromobenzyl (5-norbornenyl)methyl ether (422 mg, 1.44 mmol) in 25 mL Et₂O. An additional 1 mL portion of *n*-butyl lithium (total of 5 mmol) was added after 20 min (otherwise, the reaction did not go to completion). The flask was cooled to -35 °C after 20 min and B(OEt)₃ (1.75 mL, 10.3 mmol) was added. It was necessary at this point to add THF to the mixture to better solublize the products. (However, if THF is used instead of ether during the lithiation step, yields decrease dramatically.) After stirring for 1.5 h, this solution was used directly to prepare either **1**, **2**, or **6**.

9-Bromo-10-phenylanthracene (8). Bromine (1.1 mL, 21.4 mmol) was added to a solution of 9-phenylanthracene (5.0 g, 19.7 mmol) in 60 mL methylene chloride. After 4 h, proton NMR showed complete disappearance of the starting material singlet resonance at 8.5 ppm. The mixture was quenched with aqueous sodium sulfite. The phases were separated and the organic layer washed 3 times with water. The organic layer was dried over MgSO₄ and the solvent removed *in vacuo* to give 6.43 g (98.1%) of a light yellow solid, pure by tlc and ¹H NMR. [Note: It was extremely important to use fresh Br₂ for this procedure. There was a dramatic decrease in the yield of **8** the longer a bottle of Br₂ had been exposed to air. Yields typically dropped below 70% if Br₂ was older than 6 months, necessitating the use of column chromatography to purify the material.] ¹H NMR (CDCl₃): δ 8.61 (d, 2H), 7.68-7.50 (m, 7H), 7.42-7.32 (m, 4H); TLC: rf = 0.50 (silica gel, n-hexane).

9,10-Diphenylanthracene methyl (5-norbornenylmethyl) ether [NBDPA] (1). A solution of **7** (1.44 mmol) was prepared as described above. To that mixture, **8** (480 mg, 1.44 mmol) was added and the reaction flask removed from the drybox. An aqueous solution of K₂CO₃ (50 mL, 1 M, sparged 25 min with N₂) was then added. The mixture was brought to reflux under N₂, and Pd(PPh₃)₄ (30 mg, 0.026 mmol) in 2 mL THF (prepared in the drybox) was

added via syringe. The flask was covered with Al foil and refluxed under N₂ overnight. After cooling to RT, *n*-hexane (200 mL) was added and the phases separated. The organic layer was washed with water, dried over MgSO₄, and the solvent removed *in vacuo*. The crude product was purified by column chromatography (silica gel, 3:1 hexanes:CH₂Cl₂ with 1% MeOH), yielding 330 mg (49.1% for both steps) of a white powder. ¹H NMR (CDCl₃): (endo) δ 7.75-7.30 (m, 17H, Ar), 6.17 (m, 1H, olefinic), 5.98 (m, 1H, olefinic), 4.65 (dd, 2H, O-CH₂-Ar), 3.38 (q, 1H, nor-CH₂-O), 3.23 (t, 1H, nor-CH₂-O), 3.05 (broad s, 1H), 2.83 (broad s, 1H), 2.58-2.40 (m, 1H), 1.90 (m, 1H), 1.47 (broad d, 1H), 1.30 (d, 1H), 0.57 (m, 1H); (exo) δ 7.75-7.30 (m, 17H, Ar), 6.17 (m, 1H, olefinic), 6.10 (m, 1H, olefinic), 4.65 (dd, 2H, O-CH₂-Ar), 3.70 (q, 1H, nor-CH₂-O), 3.53 (t, 1H, nor-CH₂-O), 3.05 (broad s, 1H), 2.83 (broad s, 1H), 2.58-2.44 (m, 1H), 1.90 (m, 1H), 1.47 (broad d, 1H), 1.30 (d, 1H), 1.22 (m, 1H); ¹³C{¹H} NMR (CDCl₃) δ 139.51, 138.59, 137.45, 137.27, 132.80, 131.66, 131.62, 130.27, 128.66, 127.91, 127.72, 127.27, 127.24, 127.23, 74.85, 73.24, 49.78, 44.48, 42.62, 39.31, 29.64; TLC: rf = 0.70 (silica gel, 1:3 CH₂Cl₂:*n*-hexane). Anal. Calcd. for C₃₅H₃₀O: C, 90.09; H, 6.48. Found: C, 90.25; H, 6.47.

1-Bromo-4-chloromethyl-2,6-isopropylbenzene. Concentrated HCl (5 mL) and formalin (1 mL, 37% formaldehyde in water) were added to 1-bromo-2,6-diisopropylbenzene (1.021 g, 4.234 mmol). Gaseous HCl was rapidly bubbled into the stirred mixture for 4 h. After cooling, Et₂O was added and the phases separated. The organic layer was washed with water, dried over MgSO₄, and the solvent removed *in vacuo*, yielding a yellow oil (0.998 g). ¹H NMR was identical to the starting material -- no reaction.

First Attempt: 1-Bromo-2,6-dimethyl-4-[(5-norbornenyl)methoxy]-benzene (9). Potassium hydride (399 mg, 9.95 mmol) was slowly added to 4-bromo-3,5-dimethylphenol (0.999 g, 4.97 mmol) in 50 mL THF. The mixture was stirred 40 min (until gas evolution was complete), then (5-norbornenyl)methyl tosylate (1.389 g, 4.99 mmol) was added. The reaction was stirred at RT in the drybox for 16 h. An aliquot of the reaction mixture was removed and analysis by ¹H NMR showed only starting material. The reaction flask was then

removed from the drybox and the mixture brought to reflux under N₂. After 6 h, there was still only starting material present, so a small amount of Aliquat 336 (200 mg) was added. After refluxing for several days, there was still no observed product.

Second Attempt: 1-Bromo-2,6-dimethyl-4-[(5-norbornenyl)methoxy]-benzene (9). The reagents (5-norbornenyl)methyl tosylate (2.000 g, 7.187 mmol), 4-bromo-3,5-dimethylphenol (1.449 g, 7.206 mmol), and K₂CO₃ (2.450 g, 17.73 mmol) were combined in a flask with 100 mL DMF. The mixture was warmed to 95 °C and stirred 48 h. After cooling, Et₂O was added and the phases separated. The organic layer was washed with water, dried over MgSO₄, and the solvent removed *in vacuo*, yielding a pale yellow oil (2.442 g). Purification by column chromatography (silica gel, 1:1 CH₂Cl₂:hexanes with 1% MeOH) gave 1.351 g of a clear liquid (61.2 % yield). ¹H NMR (CDCl₃): (endo) δ 6.61 (s, 2H, Ar), 6.13 (m, 1H, olefin), 5.91 (m, 1H, olefin), 3.63 (q, 1H, nor-CH₂-O), 3.46 (t, 1H, nor-CH₂-O), 2.99 (broad s, 1H), 2.83 (broad s, 1H), 2.51 (m, 1H), 2.35 (s, 6H, ArCH₃), 1.88 (m, 1H), 1.53 (m, 1H), 1.44 (m, 1H), 1.24 (m, 1H), 0.58 (m, 1H); (exo) δ 6.65 (s, 2H, Ar), 6.13 (m, 1H, olefin), 6.09 (m, 1H, olefin), 3.95 (q, 1H, nor-CH₂-O), 3.77 (t, 1H, nor-CH₂-O), 2.99 (broad s, 1H), 2.83 (broad s, 1H), 2.51 (m, 1H), 2.35 (s, 6H, ArCH₃), 1.88 (m, 1H), 1.53 (m, 1H), 1.44 (m, 1H), 1.24 (m, 1H), 0.85 (m, 1H); ¹³C{¹H} NMR (CDCl₃): δ 157.87, 139.20, 137.77, 132.58, 114.66, 71.77, 49.66, 44.11, 42.46, 38.59, 29.25, 24.26.

1-(10-Phenylanthracyl)-2,6-dimethyl-4-[(5-norbornenyl)methoxy]-benzene. A solution of **9** (591 mg, 1.92 mmol) in 25 mL Et₂O was prepared in the drybox. *n*-BuLi (1.5 mL of 2.5 M in Et₂O) was added to the solution. After 20 min stirring at RT, another portion of *n*-BuLi (1.5 mL) was added. The reaction vessel was cooled to -35 °C after 20 min and triethylborate (2.195 g, 15.03 mmol) in 100 mL THF was added. The mixture was stirred at RT for 2 h. 9-Bromo-10-phenylanthracene (642 mg, 1.927 mmol) was added and the reaction flask removed from the box. An aqueous solution of K₂CO₃ (75 mL, 1.0 M) was sparged 25 min with N₂ then added. The mixture was brought to reflux under N₂ and Pd(PPh₃)₄ (42 mg, 0.036 mmol) in 1.5 mL THF (prepared in the drybox) was added via syringe. The reaction flask was covered

with Al foil and refluxed under N₂ 16 h. After cooling to RT, Et₂O was added and the phases separated. The organic layer was washed with water, dried over MgSO₄, and the solvent removed *in vacuo*, yielding a dark sticky solid (1.720 g). Analysis by ¹H NMR and tlc (silica gel, 1:3 CH₂Cl₂:hexanes) showed a mixture of starting materials and several products. Purification by column chromatography (silica gel, 1:3 CH₂Cl₂:hexanes with 1% MeOH) failed to yield the expected product.

9-(2,4,6-triisopropylphenyl)-anthracene. 9-Bromoanthracene (1.004 g, 3.905 mmol) and NiCl₂(PPh₃)₂ (125 mg, 0.191 mmol) were combined in 100 mL Et₂O and cooled to -35 °C. 1.5 equiv of 2,4,6-triisopropylphenylmagnesium bromide (7.3 mL, 0.8 M in Et₂O) was added and the solution brought to reflux under N₂ overnight. After quenching with HCl (aq), the phases were separated. The organic layer was washed with water, dried over MgSO₄, and the solvent removed *in vacuo*, yielding a yellow-brown sludge. Analysis by ¹H NMR and tlc (silica gel, hexanes) showed a mixture of starting materials and several products. Purification by column chromatography (silica gel, hexanes with 1% MeOH) failed to yield the expected product. Similar results were obtained with dioxane as the solvent.

9-mesitylanthracene (10). Combined 9-bromoanthracene (0.998 g, 3.88 mmol) and NiCl₂(PPh₃)₂ (127 mg, 0.194 mmol) in 100 mL Et₂O and cooled to -35 °C. Added 1.5 equiv of mesitylmagnesium bromide (5.3 mL, 1.10 M in Et₂O) and stirred at RT. Over the course of several hours the solution darkened. Another 2 mL of Grignard was added after 2 h, and the solution was refluxed under N₂ overnight. The reaction was quenched with HCl (aq) and the layers were separated. The organic layer was washed with water, dried over MgSO₄, and the solvent removed *in vacuo*, yielding a yellow-brown sludge (1.399 g). Purification by column chromatography (silica gel, hexanes with 1% MeOH) gave 619 mg of a white powder (58% yield). ¹H NMR (CDCl₃): δ 8.51 (s, 1H, Ar), 8.17 (d, 2H, Ar), 7.48 (t, 2H, Ar), 7.46 (d, 2H, Ar), 7.37 (t, 2H, Ar), 7.12 (s, 2H, Ar), 2.49 (s, 3H, ArCH₃), 1.74 (s, 6H, ArCH₃); ¹³C{¹H} NMR (CDCl₃): δ 137.69, 137.23, 135.89, 134.61, 131.75, 129.89, 128.77, 128.40, 126.13, 125.72, 125.50, 125.33, 21.61, 20.34.

9-Bromo-10-mesitylanthracene (11). Into 100 mL of dry CH_2Cl_2 was placed **10** (610 mg, 2.06 mmol). Bromine (0.115 mL, 2.23 mmol) was added, and the solution stirred for 35 min. (As described in the preparation of 9-bromo-10-phenylanthracene, the reaction is much cleaner if Br_2 is used fresh from an ampule.) The mixture was quenched with 50 mL of saturated NaSO_3 (aq) solution. After another hour, additional Et_2O was added and the phases separated. The organic layer was washed with water, dried over MgSO_4 , and the solvent removed *in vacuo*, yielding 764 mg of a yellow powder (99%). The material was pure by ^1H and ^{13}C NMR and was used in the next step without further purification. ^1H NMR (CDCl_3): δ 8.61 (d, 2H, Ar), 7.59 (t, 2H, Ar), 7.49 (d, 2H, Ar), 7.34 (t, 2H, Ar), 7.08 (s, 2H, Ar), 2.47 (s, 3H, ArCH_3), 1.71 (s, 6H, ArCH_3); ^{13}C NMR [^1H] (CDCl_3): δ 137.58, 137.53, 136.68, 134.19, 130.69, 130.64, 128.47, 128.20, 127.18, 126.50, 126.00, 122.38, 21.56, 20.30.

***para*-(10-Mesitylanthracyl)benzyl (5-Norbornenyl)methyl] Ether [NBDPA'] (2).** A solution of **7** (4.741 mmol) was prepared as described above. To that mixture, **11** (1.609 g, 4.287 mmol) was added and the reaction flask removed from the drybox. An aqueous solution of K_2CO_3 (100 mL, 1.0 M, sparged 25 min with N_2) was then added. The mixture was brought to reflux under N_2 , and $\text{Pd}(\text{PPh}_3)_4$ (97 mg, 0.084 mmol) in 1.5 mL THF (prepared in the drybox) was added via syringe. The flask was covered with Al foil and the mixture refluxed under N_2 16 h. An aliquot showed mostly starting material by proton NMR, so 100 mg more Pd^0 was added to the reaction. After 3 days, Et_2O was added and the phases separated. The organic layer was washed with water, dried over MgSO_4 , and the solvent removed *in vacuo*, yielding a dark yellow solid (3.176 g). Purification by column chromatography (silica gel, 1:3 CH_2Cl_2 :hexanes with 1% MeOH) gave 1.253 g of white powder (57.5% for both steps). ^1H NMR (CDCl_3): (endo) δ 7.73 (m, 2H, Ar), 7.50 (m, 6H, Ar), 7.29 (m, 4H, Ar), 7.11 (s, 2H, Ar), 6.18 (m, 1H, olefin), 5.98 (m, 1H, olefin), 4.62 (q, 2H, ArCH_2O), 3.47 (q, 1H, nor- $\text{CH}_2\text{-O}$), 3.23 (t, 1H, nor- $\text{CH}_2\text{-O}$), 3.04 (broad s, 1H), 2.84 (broad s, 1H), 2.51 (m, 1H), 2.49 (s, 3H, ArCH_3), 1.88 (m, 1H), 1.79 (s, 6H, ArCH_3), 1.48 (m, 1H), 1.24 (m, 1H), 0.59 (m, 1H); (exo) δ 7.73 (m, 2H, Ar), 7.50 (m, 6H, Ar), 7.29 (m, 4H, Ar), 7.11 (s, 2H, Ar), 6.18 (m,

1H, olefin), 6.11 (m, 1H, olefin), 4.62 (q, 2H, ArCH₂O), 3.71 (q, 1H, nor-CH₂-O), 3.66 (t, 1H, nor-CH₂-O), 3.04 (broad s, 1H), 2.84 (broad s, 1H), 2.51 (m, 1H), 2.49 (s, 3H, ArCH₃), 1.88 (m, 1H), 1.79 (s, 6H, ArCH₃), 1.48 (m, 1H), 1.24 (m, 1H), 0.89 (m, 1H); ¹³C NMR {¹H} (CDCl₃): δ 138.18, 137.91, 137.42, 137.36, 136.75, 136.02, 135.00, 132.76, 131.74, 130.37, 129.67, 128.53, 127.92, 127.54, 126.29, 125.47, 125.21, 74.63, 73.29, 49.72, 44.42, 42.62, 39.20, 29.58, 21.66, 20.41. Anal. Calcd. for C₃₈H₃₆O: C, 89.72; H, 7.13. Found: C, 89.67; H, 7.18.

4-(5-(4-*tert*-Butylphenyl)-1,3,4-oxadiazole-2-yl)-biphenyl-4'-yl Sulfonic Acid (12). ClSO₃H (32 mL) was added dropwise to a solution of *t*-Bu-PBD (10.13 g, 28.58 mmol) in 50 mL CH₂Cl₂ at 0 °C. After addition was complete, the mixture was brought to reflux. After 4 h 100 mL of ice and water was slowly added, and the solution concentrated *in vacuo* to remove the CH₂Cl₂. The resulting white sludge was collected by filtration. Excess water was removed by adding benzene and removing the azeotrope and excess benzene *in vacuo*. This yielded 12.31 g of pure white powder (99.14%). No further purification was necessary. ¹H NMR (CDCl₃): δ 8.27 (d, 2H, Ar), 8.14 (d, 2H, Ar), 8.08 (d, 2H, Ar), 7.87 (d, 2H, Ar), 7.78 (d, 2H, Ar), 7.56 (d, 2H, Ar), 1.37 (CMe₃); ¹³C{¹H} NMR (CDCl₃): δ 165.0, 165.8, 155.6, 146.8, 143.6, 141.5, 128.3, 128.1, 127.7, 127.6, 126.8, 126.1, 125.5, 124.6, 120.9, 35.1 (CMe₃), 31.1 (CMe₃).

4-(5-(4-*tert*-Butylphenyl)-1,3,4-oxadiazole-2-yl)-biphenyl-4'-thiol (13). Anhydrous **12** (11.608 g, 26.72 mmol) was dissolved in 250 mL dry THF. A solution of PPh₃ (28.40 g, 108.3 mmol) and I₂ (3.411 mg, 13.43 mmol) in 50 mL THF was added dropwise. Triethylamine (2 mL, 19.76 mmol) was added and the solution was brought to reflux. The dark solution gradually changed into a mustard yellow-orange suspension. 1,4-Dioxane (60 mL) in water (30 mL) was added after 1 h. The solution immediately became colorless and the solid dissolved. After refluxing for an additional hour, Et₂O was added and the phases separated. The organic layer was washed with water, dried over MgSO₄, and the solvent removed *in vacuo*. There was complete conversion of **12** to **13** in the crude material. However, a significant quantity

of triphenylphosphine oxide remained, which was difficult to remove without using column chromatography. Since this material was quite light sensitive (see Results and Discussion), higher overall yields were obtained by proceeding to the next step without further purification. ^1H NMR (CDCl_3): δ 8.16 (d, 2H, Ar), 8.05 (d 2H, Ar), 7.68 (d, 2H, Ar), 7.54 (d, 2H, Ar), 7.50 (d, 2H, Ar), 7.34 (d, 2H, Ar), 3.52 (s, SH), 1.35 (s, CMe_3); $^{13}\text{C}\{^1\text{H}\}$ NMR (CDCl_3): δ 164.8, 164.3, 155.4, 143.4, 137.1, 131.5, 129.8, 127.7, 127.5, 127.3, 126.9, 126.1, 122.9, 121.2, 35.2 (CMe_3), 31.2 (CMe_3).

(5-Norbornenyl)methyl-(2-(Biphenyl)-5-(4-*tert*-butyl-phenyl)-1,3,4-oxadiazole)-4'-yl Thioether [NBPBD] (4). All of the crude from **13** (10.32 g, 26.72 mmol of product) was dissolved in 200 mL toluene. KOH powder (6.80 g, 121 mmol) and 8 drops of Aliquat 336 were added to form the potassium salt. After stirring 45 min at RT, (5-norbornenyl)methyl tosylate (6.636 g, 23.85 mmol) was added to the bright orange mixture and the reaction brought to reflux. After 48 h the reaction was cooled to RT, EtO_2 was added and the phases separated. The organic layer was washed with water, dried over MgSO_4 , and the solvents removed *in vacuo*. The crude was purified by column chromatography (silica gel, 6:1 hexane:EtOAc with 1% MeOH) to yield 2.515 g (20%) of a white powder. ^1H NMR (CDCl_3): δ 8.15 (d, 2H, Ar), 8.05 (d, 2H), 7.70 (d, 2H, Ar), 7.52 (m, 4H, Ar), 7.39 (d, 2H, Ar), 6.10 (m, 2H, olefin), 3.02 (m, 2H), 2.74 (m, 3H), 2.32 (m, 1H), 1.97 (m, 1H), 1.36 (s, 9H, *t*-Bu), 1.28 (m, 2H), 0.69 (m, 1H); $^{13}\text{C}\{^1\text{H}\}$ NMR (C_6D_6): δ 164.85, 164.43, 155.53, 143.80, 138.23, 138.14, 137.05, 132.21, 129.09, 129.02, 127.58, 127.48, 126.98, 126.25, 122.89, 121.31, 49.88, 45.66, 42.96, 38.63, 38.34, 35.28, 32.95, 31.32. Anal. Calcd for $\text{C}_{32}\text{H}_{32}\text{N}_2\text{OS}$: C, 78.01; H, 6.55; N, 5.69. Found: C, 77.94; H, 6.51; N, 5.62.

(*para*-Triphenyl)methyl (5-Norbornenylmethyl) Ether [NBPTP] (6). A solution of **7** (1.44 mmol) was prepared as described above. To that mixture, 4-bromobiphenyl (480 mg, 1.44 mmol) was added and the reaction flask removed from the drybox. An aqueous solution of K_2CO_3 (50 mL, 1.0 M, sparged 25 min with N_2) was then added. The mixture was brought to reflux under N_2 , and $\text{Pd}(\text{PPh}_3)_4$ (30 mg, 0.026 mmol) in 2 mL THF (prepared in the

drybox) was added via syringe. The flask was covered in Al foil and refluxed under N₂ overnight. After cooling to RT, *n*-hexane (200 mL) was added and the phases separated. The organic layer was washed with water, dried over MgSO₄, and the solvent removed *in vacuo*. The crude was purified by column chromatography (silica gel, 3:1 hexanes:CH₂Cl₂ with 1% MeOH) to give 330 mg (49.1%) of a white powder. ¹H NMR (CDCl₃): (endo) δ 7.75-7.58 (m, 8H, Ar), 7.50-7.32 (m, 5H, Ar), 6.10 (m, 1H, olefin), 5.90 (m, 1H, olefin), 4.53 (dd, 2H, O-CH₂-Ar), 3.25 (q, 1H, nor-CH₂-O), 3.10 (t, 1H, nor-CH₂-O), 2.98 (broad s, 1H), 2.80 (broad s, 1H), 2.50-2.35 (m, 1H), 1.84 (m, 1H), 1.43 (broad d, 1H), 1.26 (broad d, 1H), 0.57 (m, 1H); (exo) δ 7.75-7.58 (m, 8H, Ar), 7.50-7.32 (m, 5H, Ar), 6.10 (m, 1H, olefin), 6.07 (m, 1H, olefin), 4.53 (dd, 2H, O-CH₂-Ar), 3.57 (q, 1H, nor-CH₂-O), 3.42 (t, 1H, nor-CH₂-O), 2.98 (broad s, 1H), 2.80 (broad s, 1H), 2.50-2.35 (m, 1H), 1.84 (m, 1H), 1.43 (broad d, 1H, J = 8.0 Hz), 1.26 (broad d, 1H), 1.14 (m, 1H); ¹³C{¹H} NMR (CDCl₃): δ 140.96, 140.36, 140.12, 138.24, 137.47, 132.73, 129.08, 128.38, 127.77, 127.70, 127.61, 127.31, 127.25, 74.21, 73.02, 49.95, 44.18, 42.46, 39.67, 29.55.

Preparation of Polymers. All handling of catalyst and polymerization was done in a nitrogen-atmosphere drybox. CH₂Cl₂ for polymerization was dried by distillation over CaH₂. Toluene was distilled from sodium benzophenone. THF was dried by passing it through two large columns of activated alumina.⁸³ All solvents were stored over 4 Å molecular sieves prior to use in the drybox.⁸⁴ Mo(NAr)(CHCMe₂Ph)(O-*t*-Bu)₂ was prepared as outlined in the literature.³²

General Polymerization Procedure: Homopolymers. To a rapidly stirred solution of monomer (0.50 mmol) in 10 mL toluene, the catalyst Mo(NAr)(CHCMe₂Ph)(O-*t*-Bu)₂ (11 mg, 0.020 mmol) in 2 mL toluene was added all at once. The reaction mixture was stirred for 1 h, quenched with 4 drops benzaldehyde and further stirred for 15 min. Precipitation into 75 mL MeOH afforded high yield (92-99%) of polymer. *M_n* and *M_w/M_n* are given in text. NMR and IR data are given below.

(NBDPA)₂₅ (1₂₅). ¹H NMR (CDCl₃): δ 7.70-7.10 (broad, 17H, Ar), 5.50-5.30 (broad, 2H, olefin), 4.65-4.40 (broad, 2H), 3.65-3.25 (broad, 2H), 2.80-1.10 (broad, 7H);

$^{13}\text{C}\{^1\text{H}\}$ NMR (CDCl_3): δ 139.28, 138.21, 137.30, 134.77, 133.45, 131.47, 130.05, 123.68, 128.57, 127.77, 127.70, 127.62, 127.17, 127.14, 125.17, 73.05, 46.86, 44.28, 43.02, 40.12, 37.57. IR: $\nu(\text{CH}_2 \text{ bend})$ 1437 cm^{-1} , $\nu(\text{olefinic CH bend, trans})$ 939 cm^{-1} , $\nu(\text{olefinic CH bend, cis})$ 766 cm^{-1} .

(NBDPA')₂₅ (2₂₅). ^1H NMR (CDCl_3): δ 7.73 (broad, 2H, Ar), 7.50 (broad, 6H, Ar), 7.29 (broad, 4H, Ar), 7.11 (broad, 2H, Ar), 5.51 (broad, 2H, olefin), 4.47 (broad, 2H, ArCH_2O), 3.43 (broad, 1H), 3.38 (broad, 1H), 2.36 (broad s, 3H, ArCH_3), 1.95 (broad, 1H), 1.55 (broad s, 6H, ArCH_3), 1.41 (broad, 1H), 1.13 (broad, 2H), 0.81 (broad, 1H).

(NBPBD)₂₅ (4₂₅). ^1H NMR (CDCl_3): δ 8.10-7.95 (broad, 4H, Ar), 7.71-7.26 (broad, 8H), 5.50-5.25 (broad, 2H, olefin), 3.10-2.45 (broad, 4H), 2.40-1.65 (broad, 5H), 1.16 (CMe_3 , 9H). IR: $\nu(\text{CH}_2 \text{ bend})$ 1479 cm^{-1} , $\nu(\text{olefinic CH bend, trans})$ 962 cm^{-1} , $\nu(\text{olefinic CH bend, cis})$ 738 cm^{-1} .

(NBPTP)₅₀ (6₅₀). ^1H NMR (CDCl_3): δ 7.70-7.30 (broad, 13H, Ar), 5.45-5.25 (broad, 2H, olefin), 4.65-4.35 (broad, 2H), 3.50-3.20 (broad, 2H), 2.70-1.10 (broad, 7H). IR: $\nu(\text{CH}_2 \text{ bend})$ 1446 cm^{-1} , $\nu(\text{olefinic CH bend, trans})$ 968 cm^{-1} , $\nu(\text{olefinic CH bend, cis})$ 759 cm^{-1} .

(NB)₁₀₀ (14₅₀). ^1H NMR (CDCl_3): δ 5.35-5.17 (broad, 2H, olefin), 2.78 (broad, 1H), 2.43 (broad, 1H), 1.85-1.72 (broad, 2H), 1.33 (broad, 4H), 1.04 (broad 1H); ^{13}C NMR $\{^1\text{H}\}$ (CDCl_3): δ 134.24 (olefin), 133.20 (olefin), 43.67, 43.37, 41.82, 38.80, 38.66, 33.34, 33.10, 32.61, 32.46. IR: $\nu(\text{CH}_2 \text{ bend})$ 1447 cm^{-1} , $\nu(\text{olefinic CH bend, trans})$ 966 cm^{-1} , $\nu(\text{olefinic CH bend, cis})$ 740 cm^{-1} ; GPC: $M_n = 7200 \pm 300$, $M_w/M_n = 1.02 \pm 0.05$.

General Polymerization Procedure: Copolymers. A well-mixed solution of two monomers (0.50 mmol total) in 5 mL toluene was added over the course of 1 h to a solution of the catalyst, $\text{Mo}(\text{NAr})(\text{CHCMe}_2\text{Ph})(\text{O}-t\text{-Bu})_2$ (11 mg, 0.020 mmol), in 10 mL toluene. The reaction mixture was stirred for 1 h, quenched with 4 drops benzaldehyde and further stirred for 15 min. Precipitation into 75 mL MeOH afforded a high yield (88-99%) of polymer. ^1H -NMR data are given below.

[(DPA)_{50%}(PBD)_{50%}]₅₀ [(1_{50%}4_{50%})]₅₀. ¹H NMR (CDCl₃): δ 8.10-7.95 (broad, 4H, Ar), 7.70-7.10 (broad, 25H, Ar), 5.50-5.25 (broad, 4H, olefin), 4.65-4.40 (broad, 2H), 3.65-3.25 (broad, 2H), 3.10-2.45 (broad, 6H), 2.40-1.20 (broad, 10H), 1.16 (CMe₃, 9H).

[(DPA)_{10%}(PBD)_{90%}]₅₀ [(1_{10%}4_{90%})]₅₀. ¹H NMR (CDCl₃): δ Identical peaks as above, except ratio of resonances from **1** to **4** is 1:10 instead of 1:1.

[(DPA)_{2%}(PBD)_{98%}]₅₀ [(1_{2%}4_{98%})]₅₀. ¹H NMR (CDCl₃): δ 8.10-7.95 (broad, 4H, Ar), 7.71-7.26 (broad, 8H), 5.50-5.25 (broad, 2H, olefin), 3.10-2.45 (broad, 4H), 2.40-1.65 (broad, 5H), 1.16 (CMe₃, 9H). (Essentially identical to the spectrum of **4**₂₅.)

[(NBDPA)_{2%}(NBPTP)_{98%}]₅₀ [(1_{2%}6_{98%})]₅₀. ¹H NMR (CDCl₃): δ 7.70-7.30 (broad, 13H, Ar), 5.45-5.25 (broad, 2H, olefin), 4.65-4.35 (broad, 2H), 3.50-3.20 (broad, 2H), 2.70-1.10 (broad, 7H). (Essentially identical to the spectrum of **6**₅₀.) GPC: $M_n = 19200 \pm 150$, $M_w/M_n = 1.24 \pm 0.20$.

[(NBDPA')_{50%}(NBPBD)_{50%}]₅₀ [(2_{50%}4_{50%})]₅₀. ¹H NMR (CDCl₃): δ 8.05 (broad, 4H), 7.73 (broad, 2H, Ar), 7.50 (broad, 10H, Ar), 7.29 (broad, 8H, Ar), 7.11 (broad, 4H, Ar), 5.51 (broad, 2H, olefin), 4.47 (broad, 2H, ArCH₂O), 3.43 (broad, 1H), 3.38 (broad, 1H), 3.02 (broad, 1H), 2.65 (broad, 4H), 2.38 (broad s, 3H, ArCH₃), 2.22 (broad, 1H), 1.95 (broad, 5H), 1.55 (broad s, 6H, ArCH₃), 1.41 (broad, 1H), 1.31 (broad s, 9H, CCH₃), 1.13 (broad, 2H), 0.81 (broad, 2H); GPC: $M_n = 13100 \pm 200$, $M_w/M_n = 1.10 \pm 0.02$.

General Sulfonation Procedure. (NBDPA)₂₅ (1 equiv) was dissolved in several mL dry CH₂Cl₂. In a separate flask, dioxane (15 equiv) was dissolved in 30 mL CH₂Cl₂. The dioxane solution was removed from the drybox, and chilled to ice bath temperature. Under a flow of N₂, melted SO₃ (10 equiv) was added via gas tight syringe (CAUTION: VERY CORROSIVE MATERIAL) and the solution stirred for 0.5 h. Still at ice bath temp, the polymer was added slowly under N₂ flow, and the solution stirred for 4 h. Aqueous NaOH was added to quench the reaction (added until just basic by pH paper), and then all solvents were removed *in vacuo*. Extraction by DMSO (to remove insoluble Na₂SO₄ and NaOH), centrifugation, collection of the supernatant, and distillation of DMSO yielded 85-99% product as a light tan powder. Proton

NMR was similar to spectra detailed above, except that the olefinic region was depleted. IR data of sulfonated homopolymers provided below.

Sulfonated (NB)₁₀₀ (sulf-14₁₀₀). Sulfonation was 79% by ¹H NMR olefin integration (versus aliphatic region). IR: $\nu(\text{CH}_2 \text{ bend})$ 1454 cm^{-1} , $\nu(\text{SO}_2 \text{ stretch})$ 1199, 1043 cm^{-1} .

Sulfonated (NBDPA)₂₅ (sulf-1₂₅). Sulfonation was 85% by ¹H NMR olefin integration (versus aromatic region). IR: $\nu(\text{CH}_2 \text{ bend})$ 1450 cm^{-1} , $\nu(\text{SO}_2 \text{ stretch})$ 1222, 1112 cm^{-1} .

Sulfonated (NBDPA')₂₅ (sulf-2₂₅). Sulfonation was 90% by ¹H NMR olefin integration (versus aromatic region). IR: $\nu(\text{CH}_2 \text{ bend})$ 1430 cm^{-1} , $\nu(\text{SO}_2 \text{ stretch})$ 1221, 1041 cm^{-1} .

Sulfonated (NBPBD)₂₅ (sulf-4₂₅). Sulfonation was 92% by ¹H NMR olefin integration (versus aromatic region and *t*-butyl peak). IR: $\nu(\text{CH}_2 \text{ bend})$ 1483 cm^{-1} , $\nu(\text{SO}_2 \text{ stretch})$ 1189, 1041 cm^{-1} .

Sulfonated (NBPTP)₅₀ (sulf-6₅₀). Sulfonation was 89% by ¹H NMR olefin integration (versus aromatic region). IR: $\nu(\text{CH}_2 \text{ bend})$ 1425 cm^{-1} , $\nu(\text{SO}_2 \text{ stretch})$ 1137, 1055 cm^{-1} .

General Epoxidation Procedure. (NB)₁₀₀ (134 mg, 1.4 mmol by monomer) was dissolved in 10 mL CHCl₃. 2 equiv of *m*-ClC₆H₄CO₃H (0.86g of 57%) were added and the solution stirred 10 min. Precipitation from MeOH yielded 159 mg of a white powder (100%). NMR and IR data of the epoxidized polymers provided below.

Epoxidized (NB)₁₀₀ (epox-14₁₀₀). ¹H NMR (CDCl₃): δ 2.81 (broad, 1H), 2.67 (broad, 1H), 2.12 (broad, 1H), 1.95 (broad, 3H), 1.79 (broad, 2H), 1.51 (broad, 1H), 1.20 (broad, 1H); ¹³C NMR {¹H} (CDCl₃): δ 62.19 (epoxide), 61.53 (epoxide), 41.70, 38.88, 35.16, 32.66, 30.74, 28.69. IR: $\nu(\text{epoxide CH rocking})$ 1258 cm^{-1} , 8 μ ; 889 cm^{-1} , 11 μ ; 730 cm^{-1} , 12 μ ; GPC: $M_n = 6300 \pm 400$, $M_w/M_n = 1.03 \pm 0.08$.

Epoxidized (NBDPA)₅₀ (epox-1₅₀). ¹H NMR (CDCl₃): δ 7.62-7.01 (broad, 17H, Ar), 4.51 (broad, 2H), 3.42 (broad, 2H), 2.58 (broad, 2H), 2.36 (broad, 1H), 1.73 (broad, 4H), 1.19 (broad, 1H), 0.81 (broad, 1H); ¹³C NMR {¹H} (CDCl₃): δ 133.50, 131.56, 129.98, 128.52, 127.84, 127.67, 127.14, 125.22, 123.64, 73.26, 62.01 (broad, epoxide), 42.05 (broad), 33.26 (broad); IR: $\nu(\text{epoxide CH rocking})$ 1249 cm^{-1} , 8 μ ; 902 cm^{-1} , 11 μ ; 732 cm^{-1} , 12 μ .

(NB(OH))₁₀₀. A solution of **epox-14₁₀₀** (127 mg, 1.15 mmol) in 3 mL THF was cooled to -35 °C, and added to a -35 °C solution of LiAlH₄ (2.3 mmol, 2 equiv) in THF. The mixture was allowed to come to RT and stirred overnight. After quenching with 10 mL of 1 M NH₄Cl (aq) adjusted to pH 5, all solvent was removed *in vacuo*. The residue was washed with water and MeOH to remove salts. ¹H NMR (DMSO): δ 4.14 (broad, 1H, CHOH), 3.18 (broad, 2H, CHOHCH₂), 1.95 (broad, 2H), 1.73 (broad, 2H), 1.71-1.12 (broad, 4H); ¹³C NMR {¹H} (DMSO): δ 72.70 (CHOH), 46.45, 42.998, 39.20, 36.47, 32.04, 26.57. IR: ν (OH stretch) 3448 cm⁻¹; ν (C-O stretch) 1090, 1037 cm⁻¹.

CHAPTER 2

Light-Emitting Devices Constructed by Spin-Coating Polynorbornene and by Sequential Adsorption of Poly(Phenylene Vinylene)

Much of the material covered in this chapter has appeared in print:

Boyd, T. J.; Geerts, Y.; Lee, J.-K.; Fogg, D. E.; Lavoie, G. G.; Schrock, R. R.;
Rubner, M. F. *Macromolecules* **1997**, *30*, 3553.

Introduction

Making films by spin coating is the most commonly used route to build polymer LEDs. It has the advantage of being relatively quick, and good quality films with uniform thicknesses generally can be made via this technique. This chapter will explore the construction and evaluation of blue LEDs made with the spin-coated homopolymers and copolymers of norbornene monomers **1**, **3**, **5**, and **6**. The role of charge transport in efficient devices, as well as the limitations of this approach, will be discussed.

A second film-forming technique was employed in order to build multilayer devices, as depicted in the GENERAL INTRODUCTION (Figure Intro.1). As mentioned previously, it would be difficult to spin-coat two layers sequentially from organic solvents without etching the bottom layer during the application of the top layer. Professor Dr. Michael Rubner and coworkers

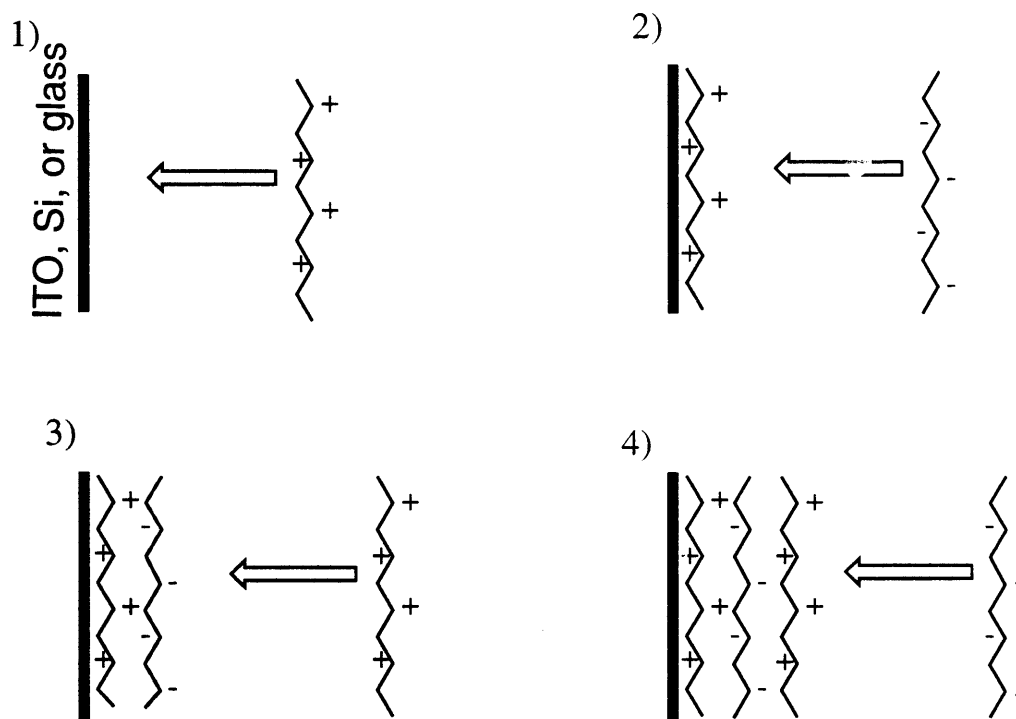
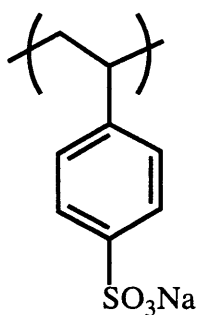


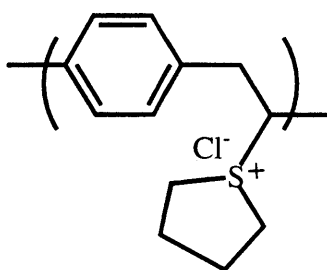
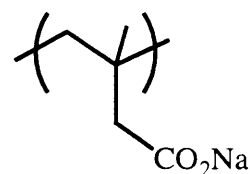
Figure 2.1. Deposition of polyelectrolytes by sequential adsorption. 1) Polycation adsorbs to substrate; 2) polyanion adsorbs to cationic substrate; 3) polycation adsorbs to anionic substrate; 4) polyanion adsorbs to cationic substrate (total of 2 bilayers).

at the Massachusetts Institute of Technology have recently developed a new sequential adsorption technique for building polymer films layer by layer (Figure 2.1).^{9,10,44,45} A substrate is dipped into an aqueous solution containing a polycation, which adsorbs onto the surface. After the excess is removed by rinsing, the substrate is dipped into a solution of negatively-charged polymer, which adsorbs onto the now cationic surface. The substrate is rinsed and the sequence is repeated until the desired number of layers has been formed. Since the layers are deposited from aqueous solution, it is an ideal complement to the organic solvent spin-coating of polynorbornene. (The polynorbornene films are severely etched by a variety of organic solvents, including THF, DMF, toluene, and acetone. They are not significantly etched by isopropanol, ethanol, methanol, or water.) A variety of charged and partially charged polymeric material has been successfully deposited by Professor Rubner and coworkers via this technique, which provides excellent control of both thickness and composition of very thin polymeric films.

The sequential adsorption technique has been used to make LEDs with a cationic derivative of poly(phenylene vinylene) (PPV). Bilayers of PPV with poly(styrenesulfonic acid) (SPS) provide effective hole injection, and bilayers of PPV with poly(methylacrylic acid) emit green light. The LEDs emit 600 nW of light with an efficiency of up to 30 nW/mA (internal quantum efficiency of 0.01%)¹⁰. The greatest efficiency is reported for a device composed of 5 bilayers of PPV/SPS and 20 bilayers of PPV/PMA.



Sulfonated polystyrene, SPS

Poly(phenylenevinylene), PPV
Precursor

Poly(methylacrylic acid, PMA

Results and Discussion

Devices with One Layer of Polynorbornene (Type A Devices).

Before device construction it was necessary to determine the spin-coating characteristics of the nonpolar polynorbornenes. Figure 2.2 shows the thicknesses resulting from systematic variation of both the solution concentration and the spin-rate for polymers of **1**. It was possible to deposit films that were uniform and relatively defect-free (as determined by profilometry, film luminescence with a hand-held UV lamp, and 400 \times microscopy). All the spin-coating was done out of chlorobenzene, which has a convenient volatility and the ability to dissolve most of the polymers discussed here.

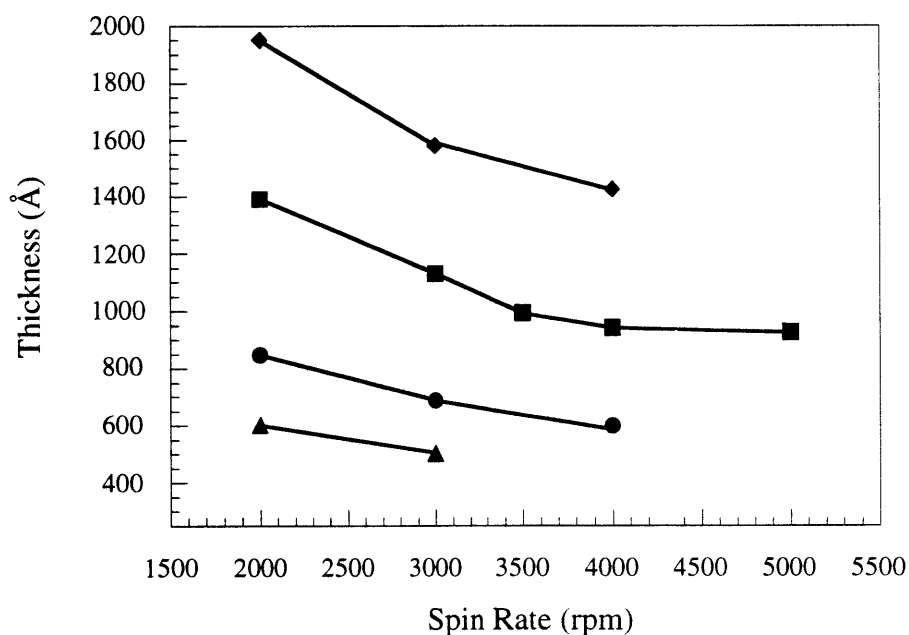


Figure 2.2. Spin-coating characteristics of **125**. Stationary glass substrate coated with chlorobenzene solution (5 drops), then spun at indicated speed. Solution concentrations (w/w) were 5% (diamonds), 3.75% (squares), 2.5% (circles), and 1.8% (triangles). Film thickness measured by profilometry.

When using a uniform spin rate, it was found that a linear relationship existed between the solution concentration and the thickness of the film being formed. This relationship provided a way to determine quickly the necessary conditions for depositing a film with a specific desired thickness. Figure 2.3 shows the calibration curves generated for homopolymer **125** and copolymer [150%350%]50.

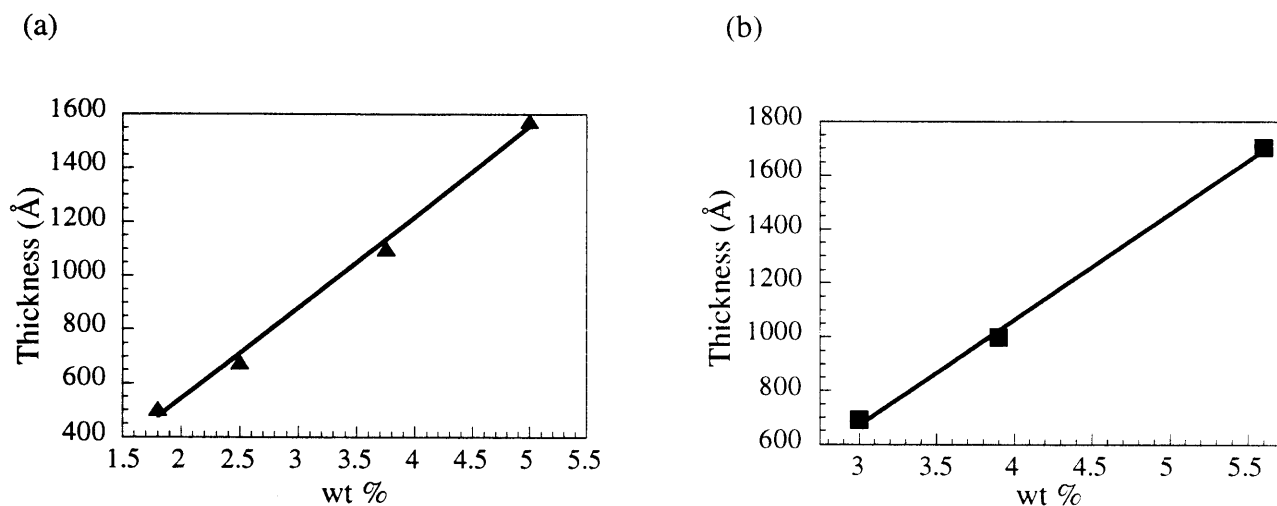


Figure 2.3. Calibration curves for spin-coating polymers (a) **125** and (b) [150%350%]50.

For the construction of devices, the polymers were spin-coated onto glass with 2 mm wide strips of Indium Tin Oxide (ITO), a transparent conducting electrode (Figure 2.4). The solutions were filtered immediately prior to use in order to remove any dust and other large particles. Also, the exposure of solution and substrate to atmospheric contamination was minimized (all spin-coating was performed under a stream of N_2 in a low-humidity glove box.) After deposition, the polymer layer was dried, first under N_2 and then under dynamic vacuum and low heat (50 °C). Aluminum strips (2 mm wide) were placed perpendicular to the ITO via thermal evaporation. The intersection of ITO anode and aluminum cathode created an individually addressable pixel. (The device in Figure 2.4b includes 2 strips of ITO + 2 strips of aluminum = 4 pixels).

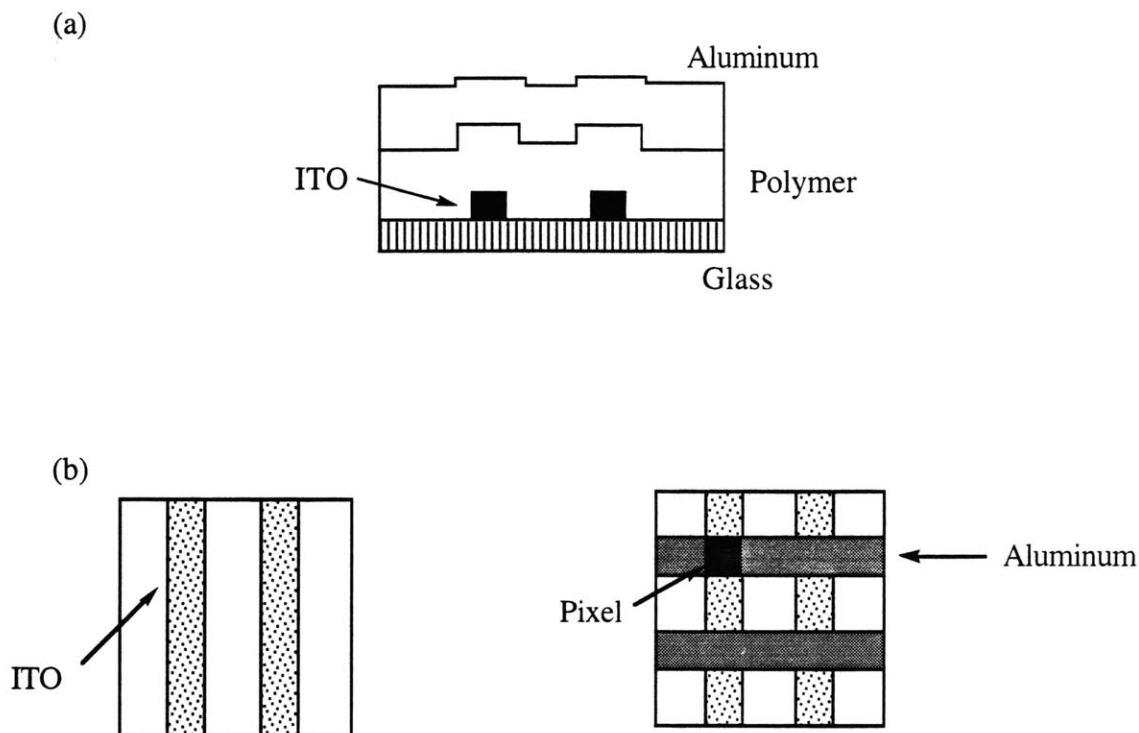


Figure 2.4. Schematic of light emitting devices. (a) Side-on view; (b) Top view, before and after deposition of aluminum (at each intersection is one pixel, four total).

Two different types of devices were constructed and evaluated in this study. Type A devices (Figure 2.5) were made by spin coating a single 600 Å layer of polynorbornene to make a device as described above. No other materials were blended into the polynorbornene layer. Table 2.1 lists the device characteristics. The *Efficiency* in Table 2.1 is the ratio of light to current and is useful as a relative comparison. The *Threshold* in Table 2.1 is the voltage at which the light rises above the baseline noise (about 0.5 nW).

The performance of individual pixels was determined by applying a steady voltage across the polymer film and measuring both the current and the light. Voltage was increased incrementally, and current and light output were recorded at each step. Figure 2.6 shows the I-V (current-voltage) and L-V (light-voltage) curves for device A-[150%350%]50. The initial current

spike (or ohmic relationship) observed in the I-V curve was typical of Type A devices, and is widely seen by other researchers in the field. The behavior is generally ascribed to poor film quality, especially defects at the polymer-electrode interface.⁸⁵ In this example, the defect was self-correcting, and by 10 V the current had dropped back to near baseline levels. More often in the case of Type A device pixels, however, the current increased until the aluminum cathode evaporated, making it difficult to obtain useful information about performance. Also, after several voltage sweeps, most pixels were no longer operating.

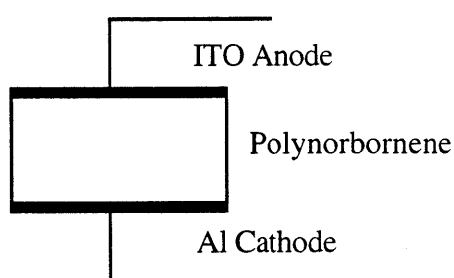


Figure 2.5. Configuration of Type A polymer EL devices. ITO/polynorbornene/Al.

Table 2.1. Performance of Type A Devices.

Polymer	Color	Output (nW)	Efficiency (nW/mA)	Threshold (V) ^a
125	blue ^b	0.5	0.03	22
[150% 350%]50	blue	31	1.7	21
[150% 550%]50	blue	26	4.3	13

^aThe voltage at which light output rises above 0.5 nW (well above baseline noise). ^b $\lambda_{\max,em} = 450$ nm.

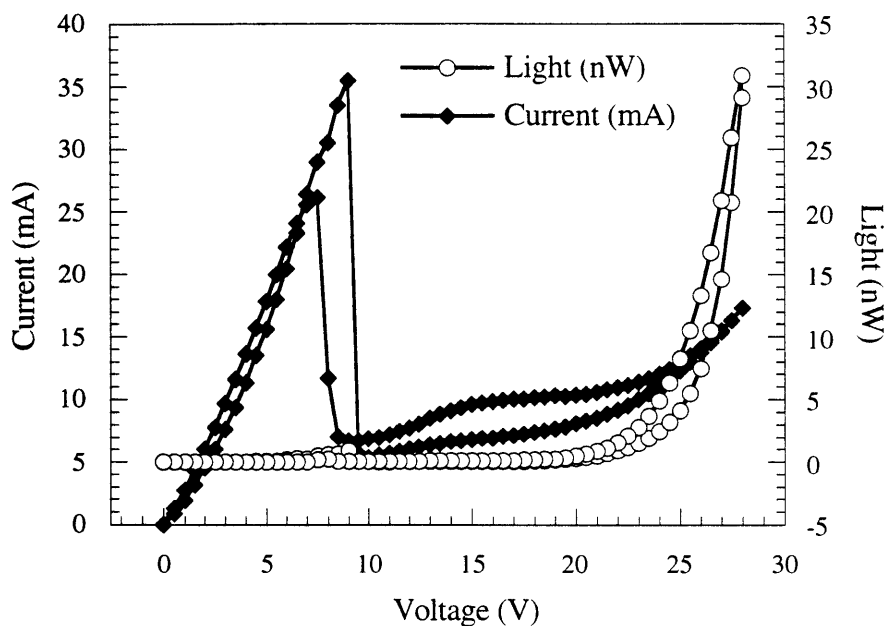


Figure 2.6. Performance of device **A-[150%350%]50**. Current-voltage (diamonds) and light-voltage (open circles) curves.

Blue light at $\lambda_{\max,em} = 450$ nm was observed for devices **A-125**, **A-[150%350%]50**, and **A-[150%550%]50**. Figure 2.7 shows the optical spectra of spin-coated films of **125**. As expected, the photoluminescence and electroluminescence share a maximum at 450 nm, and similar spectra were obtained for **[150%350%]50** and **[150%550%]50**. No peak was observed at $\lambda_{\max,em} = 425$ nm (the photoluminescent emission of **3** alone) for **A-[150%350%]50**. On the basis of the $\lambda_{\max,em}$ values, emission from **A-[150%350%]50** occurred solely from the DPA, indicating that energy transfer between the DPA and PBD pendant groups was possible. DPA has a smaller energy gap than the oxadiazole and therefore would be expected to be the sole emitter if energy transfer between PBD and DPA were efficient.

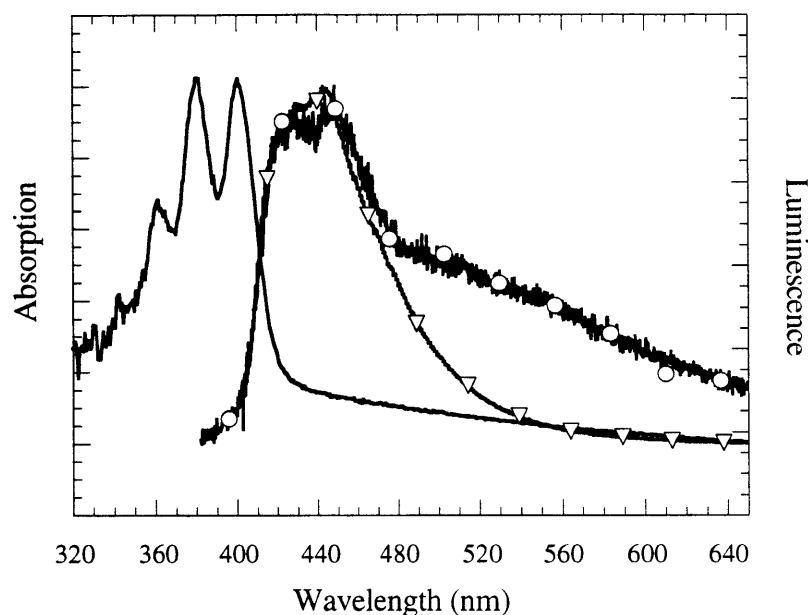


Figure 2.7. Optical spectra of **125**. Device **A-125**: film absorbance (no symbols), electroluminescence at 20 V (open circles), and photoluminescence with excitation at 360 nm (open triangles).

The overall efficiencies for Type A devices, which were measured in nW/mA (i.e., light observed/electrons injected), were low (see Table 2.1), as was the maximum light output from these devices (light from **A-125** was just barely observable to dark-adjusted eyes). Low light intensity could be ascribed in part to poor charge balance. Also, at such high electrical fields (3.3 MV/cm at 20 V for a 600 Å film) and high currents (750-1000 mA/cm²), devices may fail by polymer break-down or by evaporation of the aluminum cathode. In an effort to improve both film quality and charge balance, a two-layer device was explored.

Devices with Two-Layers, Polynorbornene with Multilayered Heterostructure (Type B Devices).

Two-layer devices of Type B were constructed by spin-coating polynorbornene onto a sequentially adsorbed multilayer structure. Figure 2.8 shows a general schematic of Type B devices. On top of the ITO anode were assembled 5 bilayers of a polycationic precursor to poly(p-phenylene vinylene) (PPV) and polyanionic poly(styrene-4-sulfonic acid) (SPS). Next, 20 bilayers of cationic PPV and poly(methylacrylic acid) (PMA) were added. After thermal conversion of the PPV (under dynamic vacuum at 210 °C for 11 h), this particular heterostructure has been reported to make stable electroluminescent devices with an emission wavelength of $\lambda_{\text{max,em}} = 530 \text{ nm}$ (green light from the PPV).¹⁰ When such a structure is used as a hole-injection layer in devices with non-polymeric emitters, significant increases in device efficiency are observed.⁸⁶ Also, the films are known to be especially uniform and defect free, so it was hoped that the frequent breakdowns discussed above for Type A devices would be alleviated.

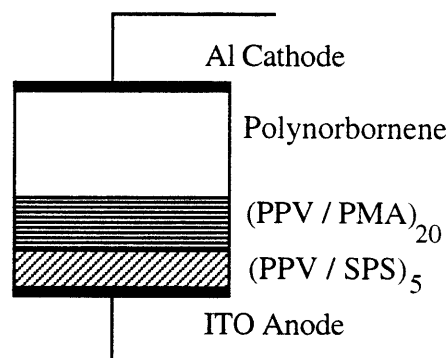


Figure 2.8. Configuration of Type B polymer EL devices. ITO/PPV-SPS(5 bilayers)/PPV-PMA(20 bilayers)/polynorbornene/Al.

Norbornene polymers were spin coated onto the PPV heterostructure platform as shown in Figure 2.8. Table 2.2 summarizes the characteristics of the Type B devices. For **B-125**, **B-**

[150% 350%]50, and **B-[150% 550%]50**, $\lambda_{\max,em}$ was the same as for the Type A devices, indicating that emission was occurring from DPA in the polynorbornene layer; no peak at $\lambda_{\max,em} = 530$ nm from the PPV was observed. Since PPV has a smaller energy gap for emission, recombination of hole and electron carriers must have been localized in the polynorbornene layer. In this case, the polynorbornene acted as a partial barrier to electron movement through the device, while the PPV-containing heterostructure transported holes more easily.

Table 2.2. Performance of Type B Devices.

Polymer	Color	Output (nW)	Efficiency (nW/mA)	Threshold (V) ^a
125	blue ^b	5.4	1.4	12
350	green ^c	42	41	12
[350% 650%]50	green ^c	13	0.8	15
[150% 350%]50	blue	675	31	8
[150% 550%]50	blue	140	48	6

^aThe voltage at which light output rises above 0.5 nW (well above baseline noise). ^b $\lambda_{\max,em} = 450$ nm. ^c $\lambda_{\max,em} = 530$ nm.

Figure 2.9a shows the electroluminescence and photoluminescence of **B-[150% 350%]50**. The broad shoulder evident in the electroluminescent spectra was apparent in all devices (both Type A and B) containing monomer **1** (see also Figure 2.7 of **A-125**). The shoulder may have arisen from degradation of the DPA (see below) into lower energy emitting products. Since the shoulder was observed for devices that do not contain PPV, emission from the heterostructure was not implicated. However, the light emitted from Type B devices was observed through the PPV and the ITO layers, so some light may have been re-absorbed by the PPV. To what extent this occurred was unknown, although no PPV emission was observed.

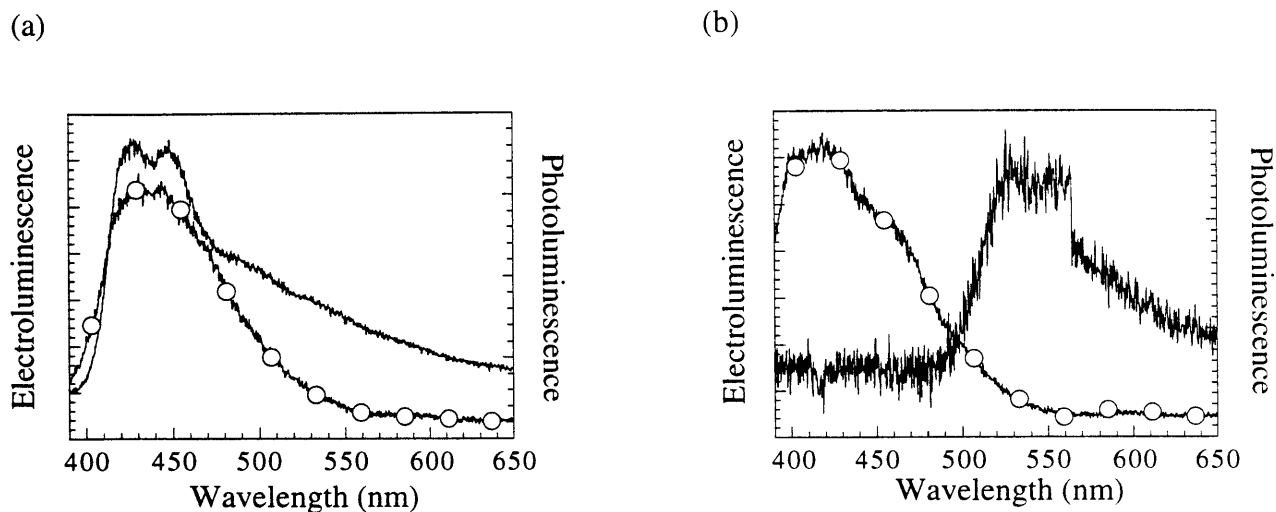


Figure 2.9. Optical spectra of polymers [150%350%]50 and 350. (a) Device B-[150%350%]50: electroluminescence at 20 V (no symbols) and photoluminescence with excitation at 360 nm (open circles); (b) Device B-350: electroluminescence at 20 V (no symbols) and photoluminescence with excitation at 330 nm (open circles).

Devices B-350 and B-[350%650%]50 both had a $\lambda_{\text{max,em}} = 530$ nm (Figure 2.9b). This electroluminescent green light was different from the emission observed in the photoluminescent spectra of 350 or [350%650%]50. Instead, it corresponded to the emission observed for the heterostructure alone; i.e., carriers recombined not in the polynorbornene layer, but in the PPV-containing layer. This effect is explained by the ability of 3 to block holes and to transport electrons through the polymer layer. APPENDIX A explores the ability of homopolymers of 3 and 4 to function solely as electron-transporting/hole-blocking layers.

In general, Type B devices operated with more consistency than Type A devices (they were less prone to failure, produced more working “pixels”, etc.). The SPS/PPV/PMA heterostructure is a particularly uniform film¹⁰ which is likely to mitigate problems resulting from small defects (such as pinholes) in the spin-coated polynorbornene layer.

All devices, Type A and B, based on monomer **1** had a short lifetime of operation (5 to 10 minutes), possibly due to decomposition of radical ions derived from DPA in the presence of traces of water or oxygen.^{22,24,47,48} Figure 2.10 shows the rapid decay of light in device **B-[150%350%]50** from blue to green-white. A more rigorous exclusion of water and oxygen in spin-coating and subsequent steps of device construction might help to alleviate this problem. If the over-oxidized or over-reduced forms of DPA (i.e., DPA^{2-} and DPA^{2+}) were being formed, then their extremely reactive nature might have led to the rapid decomposition of the emissive material.^{47,48} This situation would be more difficult to control.

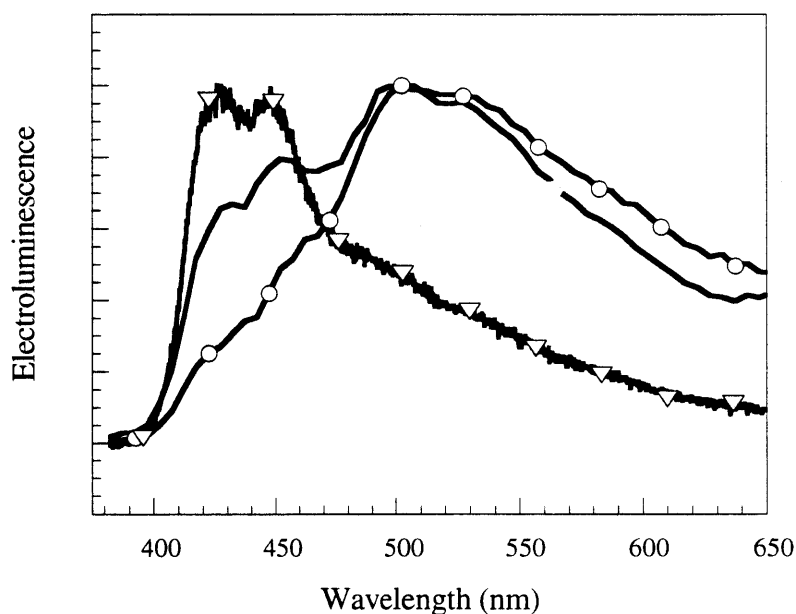


Figure 2.10. Degradation of device **B-[150%350%]50**. Electroluminescence measured during continuous operation at 20 V (all maxima are normalized to equal intensity to facilitate comparison); Time = 0 s (open triangles), 30 s (no symbols), and 60 s (open circles).

Role of Charge-Transport in Type A and B Device Performance.

Employing charge transport material, both hole-transporting and electron-transporting, in the polymer film provided significant improvements in device performance. Incorporation of the hole-transporting material, **5**, into the polynorbornene layer reduced the threshold voltage, as shown by data in Tables 2.1 and 2.2. The threshold voltage of **A-[150%550%]50** was 9 volts less than **A-125**, while that of **B-[150%550%]50** was 6 volts less than **B-125**. A device of Type B was also clearly superior to a device of Type A, even though the increased thickness (900 Å versus 600 Å) would normally be expected to *increase* the threshold. The PPV heterostructure facilitates hole transport in this case.^{10,43} The light-voltage (L-V) curves are compared in Figure 2.11. A lower threshold voltage facilitated device operation; at voltages greater than 20 V, degradation of the device increased dramatically. Often, this degradation was accompanied by evaporation of the aluminum cathode from the region above the addressed pixel.

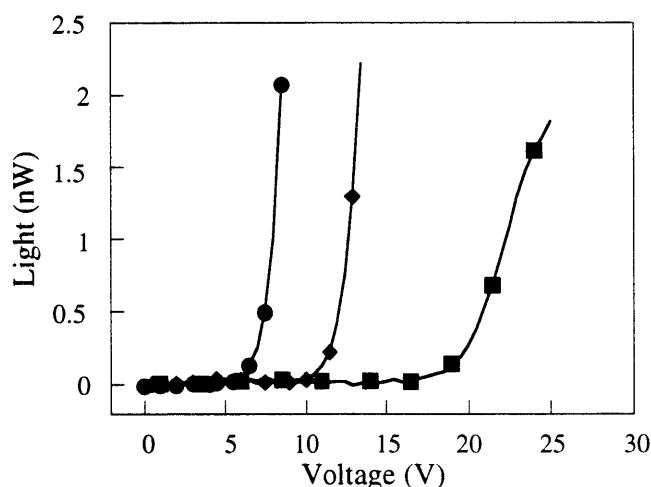


Figure 2.11. Variation in threshold voltage. Devices **B-[150%550%]50** (circles), **B-[150%350%]50** (diamonds), and **A-[150%350%]50** (squares). **B-[150%550%]50** and **B-[150%350%]50** had a 900 Å total polymer thickness; **A-[150%350%]50** had a 600 Å polymer thickness. The L-V curves of **B-[150%550%]50** and **B-[150%350%]50** are cut off at 2 nW to facilitate comparison.

As expected, an increase in efficiency upon incorporation of an electron transport material was also seen clearly in both device types.^{6,43} The relative efficiency increased dramatically from **A-125** to **A-[150%350%]50**, an improvement from 0.03 nW/mA to 1.7 nW/mA. A similar improvement, from 1.4 nW/mA to 31 nW/mA, was observed from **B-125** to **B-[150%350%]50**. This greater efficiency led directly to greater emissive output from the devices. Figure 2.12 shows the I-V and L-V curves for **B-[150%350%]50**. The highest output observed in this study was for device **B-[150%350%]50**; at 675 nW with an external quantum efficiency of EL (photons/electron), $\Phi_{\text{EL,ext}} = 3.50 \times 10^{-4} \%$.

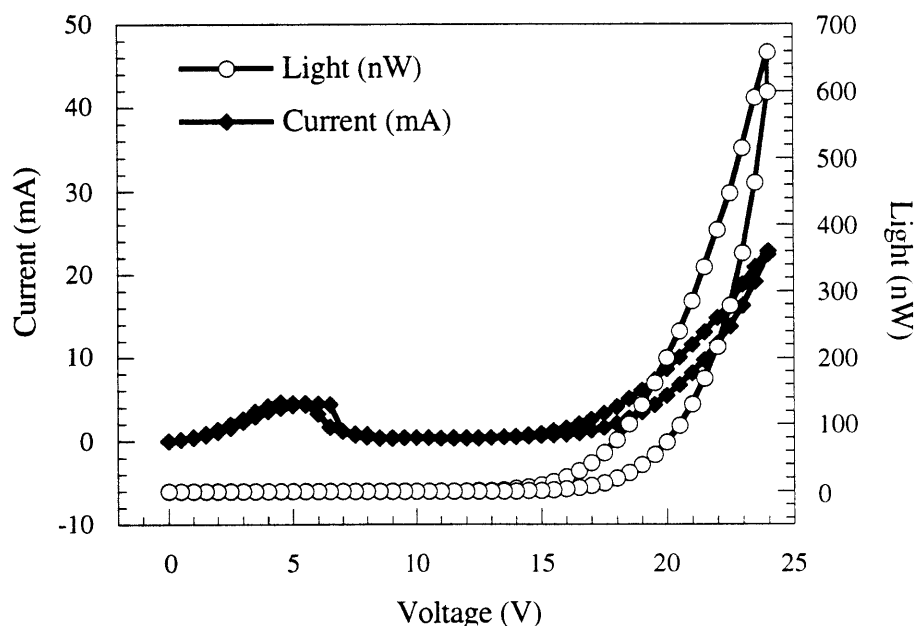


Figure 2.12. Performance of device **B-[150%350%]50**. Current-voltage (diamonds) and light-voltage (open circles) curves.

Both **B-350** and **B-[150%550%]50** had efficiencies that were comparable to that of **B-[150%350%]50**, although the light output from the devices was not as high. In the case of **B-350**, the device broke down at the high voltages necessary to produce the observed green light. As

noted above, on the basis of emission properties, electrons appeared to pass completely through the 600 Å thick polynorbornene layer before recombination in the PPV layer. (APPENDIX A discusses using a thinner layer for electron transport.) **B-[150% 550%]50** also showed a higher efficiency than **B-125**. Therefore, facilitating charge transport of either holes or electrons improved the ability of the DPA-containing polymers to produce light.

Conclusions

The incorporation of functionalized polynorbornenes into efficient, high-output LEDs has been demonstrated. A series of new blue-light emitting polymers was evaluated for efficacy in electroluminescent device application. Blue light of 450 nm was produced by diphenylanthracene-containing polymers. Hole transport structural units were found to decrease the threshold voltage. Electron transport structural units greatly increased the efficiency of LEDs, by a factor of 20 or more. A multilayer and multicomponent approach to device fabrication yielded the best performance, up to 675 nW and up to 48 nW/mA.

Experimental Section

General Procedures. Film thicknesses were measured with a Gartner Ellipsometer and a Sloan Dektak 8000 profilometer. Measurements of current and luminescence as a function of applied field were made under forward bias. A silicon photodiode (Newport Instruments, Model 1830-C) was used to measure device light output, which is measured in nW. Electroluminescence and photoluminescence spectra were taken using a spectrograph coupled to a Peltier-cooled CCD array (Oriel Instaspec IV). The system response was calibrated using a tungsten lamp. Excitation for the photoluminescence was from the multiline UV mode of an argon ion laser. Absorbance spectra were taken with an Oriel Instaspec spectrophotometer. PPV precursor was provided by Dr. Bing Hsieh of Xerox corporation. All other polymers and reagents were purchased from Aldrich Chemical Company. Solutions of polymers for sequential adsorption were prepared by dissolving an appropriate amount in 750 mL to make a 1×10^{-2} M solution. Sodium chloride was added to

SPS and PMA solutions to reach 0.1 M salt content, and then the solutions were pH adjusted with HCl and NaOH: SPS to pH 4.0 and PMA to pH 3.5. A HMS Series Programmable Slide Stainer from Carl Zeiss, Inc. was used to automatically dip the substrates in the appropriate solution.

Formation of Thin Films, Spin-Coating. Solutions of polymer in chlorobenzene ranging from 1.2-2.5% (w/w) were prepared and filtered through a 0.2 μ syringe filter. Polymer films were applied to the substrate by placing 5 drops of solution onto the substrate and then spinning it rapidly, using a Headway Research, Inc. Photo-Resist Spinner spin coater. An appropriate thickness, generally about 600 Å, was obtainable by methodically varying both the spin rate (around 2000-5000 rpm) and the polymer concentration. A typical set of conditions for **125**: 5 drops; 1.8% (w/w) in chlorobenzene; 2000 rpm; yields uniform film, 602 \pm 50 Å.

Light-Emitting Device Fabrication. Devices of Type A. Commercially patterned Indium Tin Oxide (2 mm wide strips, spaced 2 mm apart) on a 2 cm \times 2 cm piece of glass was prepared by a previously reported cleaning/sonication procedure.¹⁰ Exposure of cleaned substrate to atmosphere was minimized. In a low humidity N₂-filled glove box, polynorbornene (600 Å) was spin coated from chlorobenzene onto the cleaned ITO. After deposition, the polymer layer was dried, first under N₂ and then under dynamic vacuum and low heat (50 °C). Three 2000 Å thick aluminum strips, 2 mm wide and spaced 2 mm apart, were laid perpendicular to the ITO by thermal evaporation at 1×10^{-6} Torr. Connection to the electrodes was made with gold wire, generating 12 individually addressed "pixels" where the electrodes crossed.

Devices of Type B. A heterostructure of 5 bilayers of poly(p-phenylene vinylene) and poly(styrene-4-sulfonate) and 20 bilayers of poly(p-phenylene vinylene) and poly(methacrylic acid) (300 Å total thickness) was sequentially adsorbed from aqueous solution onto cleaned ITO using a previously reported procedure.¹⁰ Polynorbornene (600 Å) and the aluminum cathode were deposited as above.

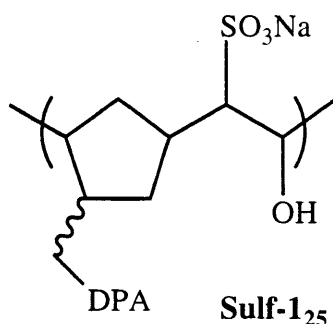
CHAPTER 3

Light-Emitting Devices Constructed by Sequential Adsorption of Sulfonated Polynorbornene and the Effect of Excimer Formation on Emission and Device Output

Introduction

This chapter will explore the making of films and devices by sequential adsorption of sulfonated polynorbornenes (see Figure 2.1). CHAPTER 2 showed that significant improvements in device performance were realized when a sequentially adsorbed film of PPV was used in conjunction with spin-coated polynorbornene. These improvements included an increase in output, a decrease in the threshold voltage, and more reliable device operation. Therefore, we became interested in investigating whether an all-polynorbornene film constructed in the same layer-by-layer fashion would show similar benefits. Using this approach would not only enhance design flexibility, but also reduce dependence on the supply of PPV.

The characteristics of the water-soluble sulfonated polynorbornenes described in CHAPTER 1 will be explored here more fully. These polyanions contain highly-charged backbones and nonpolar side groups, a structure which leads to vastly different luminescent behavior than that observed in the nonpolar polymer forms. The polymer **sulf-1₂₅**, containing the DPA structural unit, displays self-quenching behavior indicative of the presence of excimers both in water and in films. A series of copolymers containing monomers **1**, **2** and **4** (see Figure Intro.2 on page 19) will be described that probes the extent to which these excimers can be limited and controlled. A variety of strategies to control excimers will be employed, including: 1) diluting the polymer solution, 2) diluting the DPA-containing monomer in the polymer, and 3) introducing a bulkier environment about the planar aromatic group. The efficacy of each of these strategies will be explored, especially in the context of device performance.



One of the greatest advantages of the sequential adsorption technique is the ability to create complex film structures containing layers that transport either holes or electrons (such as in Figure Intro.1). This type of construction will be demonstrated for the sulfonated polynorbornenes. Homopolymers and copolymers containing hole- or electron- transport groups will be prepared and assembled in different regions of a film containing an emitting group. A definite improvement in device performance is observed with the layered design, although the excimer problems encountered with **sulf-125** and copolymers of **1** and **4** or **6** make this approach less effective.

Results and Discussion

Layer-by-Layer Deposition of Ultra-Thin Films by Sequential Adsorption.

The layer-by-layer deposition of the sulfonated polynorbornenes synthesized in CHAPTER 1 was accomplished using techniques that have been reported elsewhere.^{9,10,13,87} In this case, it was found that **sulf-125** did not immediately deposit onto a cleaned glass slide or silicon wafer when adsorbed sequentially with poly(allylamine HCl) (PAH). This behavior has been observed previously for highly sulfonated systems, such as those reported by Dr. Jeffrey Baur of the Massachusetts Institute of Technology.^{13,87} However, after first sequentially adsorbing 5 bilayers of PAH with poly(methylacrylic acid) (PMA) to prepare the glass or silicon substrate, it was possible to sequentially adsorb polymers containing **1**, **2**, **4**, and **6**. Table 3.1 lists the thickness of each PAH/polynorbornene bilayer.

Figure 3.1 shows the linear deposition of **sulf-125** with PAH, measured by ellipsometry. Films prepared by this method appeared to be quite uniform, both visually and as measured by profilometry and ellipsometry. As expected for highly-charged sulfonates, the thickness per bilayer (with PAH) was relatively thin in these cases: 8-13 Å.⁹ Addition of 0.1 M NaCl to the polynorbornene and PAH dipping solutions increased the thickness to 20-40 Å/bilayer. The added sodium ions effectively shielded the highly-charged sulfonate groups from each other and allowed the polymer to adopt a more loopy, less linear configuration. For **sulf-650** no deposition occurred unless 0.1 M NaCl was added to both dipping solutions.

Table 3.1. Deposition of Sulfonated Polynorbornenes^a

Polymer	Thickness/Bilayer (Å) ^b
no salt:	
sulf-1₂₅	10
sulf-2₂₅	8
sulf-4₂₅	13
(150% 450%)₅₀	8
(110% 490%)₅₀	10
(12% 498%)₅₀	13
(12% 698%)₅₀	8
(250% 450%)₅₀	11
with salt: ^c	
sulf-1₂₅	20
sulf-4₂₅	151
sulf-6₅₀	23
(150% 450%)₅₀	38
(12% 498%)₅₀	40
(250% 450%)₅₀	42

^a Deposition of polymer alternating with PAH, onto a silicon wafer prepared with 5 bilayers of PAH/PMA. ^bDetermined by ellipsometry. ^cBoth dipping solutions contain 0.1 M NaCl.

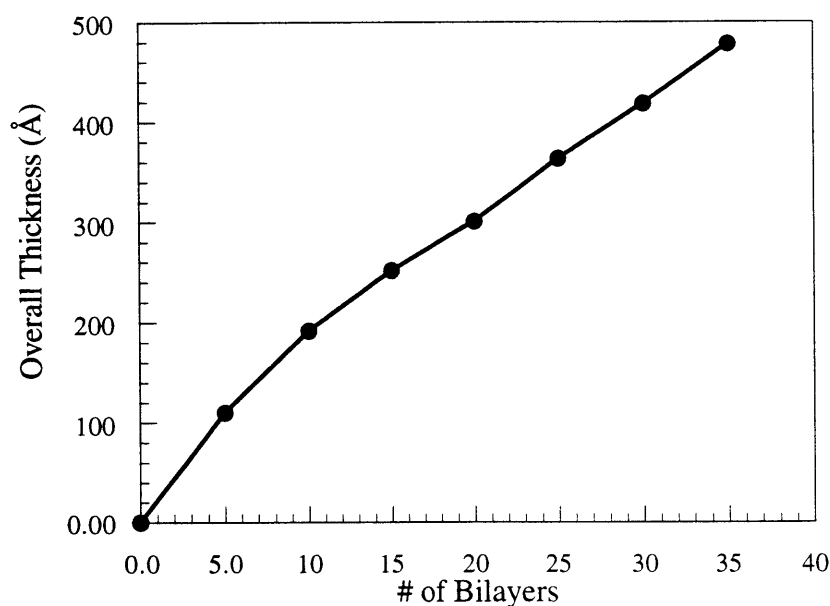


Figure 3.1. Sequential adsorption of **sulf-125** and poly(allylamine HCl). Ellipsometry measurements on a silicon wafer.

Films of the sulfonated copolymers described in CHAPTER 1 were also prepared in this manner. The deposition characteristics listed in Table 3.1 show that these materials were very similar to the homopolymers. In both the copolymers and homopolymers, a transition region existed in the film where the thickness of the PAH/PMA prep layer influenced the PAH/polynorbornene layer (see Figure 3.1). Generally, after the first 5 bilayers of polynorbornene were deposited on the prep layer, the thickness per bilayer assumed a more constant value.

As mentioned in the GENERAL INTRODUCTION, one of the goals of this project was to produce multilayered films with separate hole- and electron-transporting regions. By sequentially building layers containing different homopolymers and copolymers, it was possible to create a variety of film structures, the device properties of which will be discussed in the following sections. Figure 3.2 illustrates thickness as a function of the number of bilayers during device

construction. Again, notice the irregularity in the transition between the three layers. Unfortunately, this irregularity made it difficult to predict precisely the thickness of each layer without first making a test film, and then carefully monitoring the deposition by ellipsometry. The results were found to be consistent from one film-building run to another, however, so it was possible to replicate the previously obtained film structure quickly once conditions were determined.

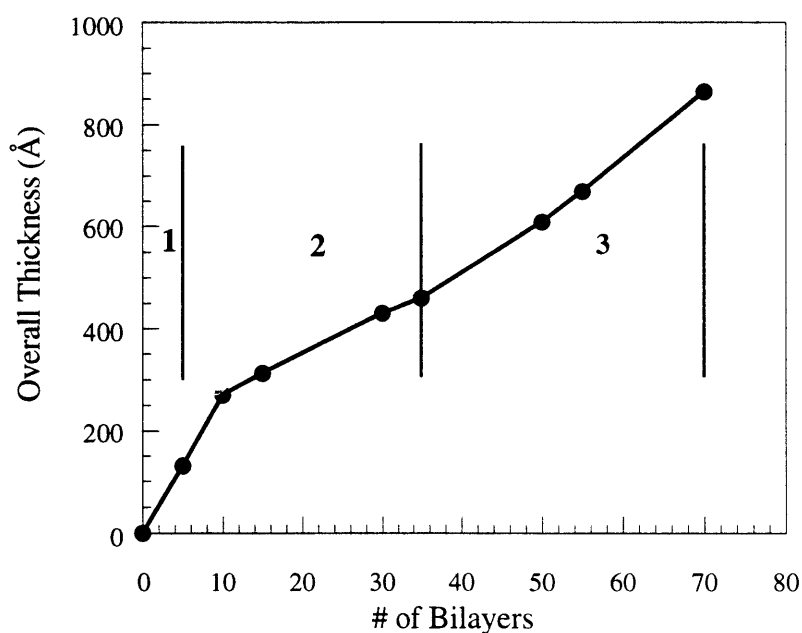


Figure 3.2. Sequential adsorption of poly(allylamine HCl) (PAH) with 1) poly(methylacrylic acid) (PMA), 5 bilayers; 2) **sulf-(12% 698%)50**, 30 bilayers; 3) **sulf-(12% 498%)50**, 35 bilayers. Ellipsometry measurements on a silicon wafer.

Excimer Formation with DPA-Containing Polymers.

The photoluminescent emission of 1×10^{-3} M solution of **sulf-125** in DMSO or DMAc was the same as that observed for **125** in nonpolar solvents: intense blue light at 450 nm ($\lambda_{ex}=360$ nm).^{46,74} However, the photoluminescence of **sulf-125** at a similar concentration in

predominantly water (95% or greater) was broader, red shifted to 600 nm, and emitted with a much lower intensity (see Figure 3.3). This effect was unexpected, since the nonpolar form did not exhibit this behavior. However, considerable precedent exists for anthracene-like molecular structures, including diphenylanthracene, to form excimers, or excited-state dimers.^{21,88-94} These excimers generally are of lower energy, and frequently have much lower quantum yield of emission. It has also been shown that they are a short range phenomenon, facilitated by π stacking on the order of several Ångströms. Apparently, in water, unlike in DMSO, the nonpolar DPA structural units tended to form close interactions, and therefore favored excimer formation and emission over mono chromophore emission.

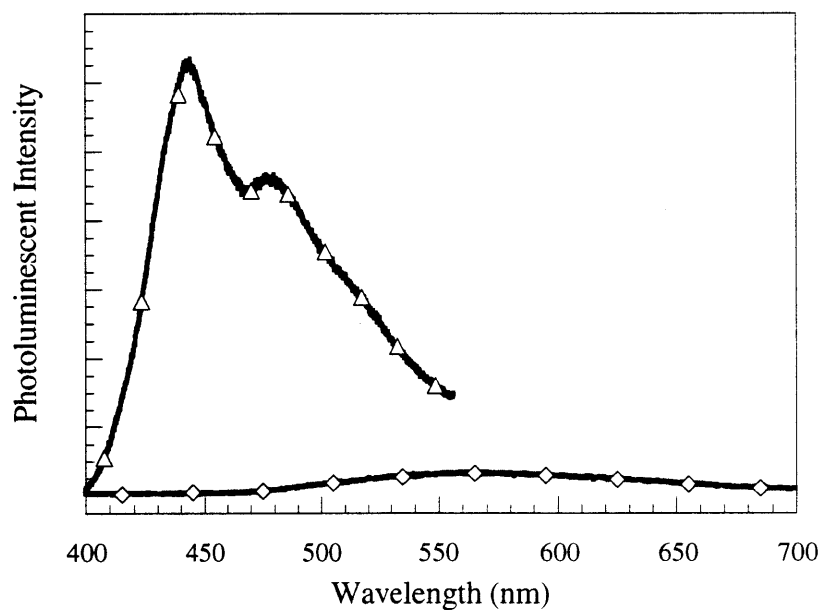


Figure 3.3. Solution photoluminescence of **sulf-125** in DMSO (Δ) and water (\diamond) at a concentration of 1×10^{-3} M.

Figure 3.4 shows the effect of dilution with water on the emission from **sulf-125**. Decreased concentration yielded a gradual shift to the higher-energy and more intense mono chromophore spectrum. Dilution decreased the likelihood of inter- and intra- chain interactions;

therefore, the number of excimer sites was also reduced. However, sequentially adsorbed films prepared from solutions with different concentrations of **sulf-125** did not show any variation in emission. Even when the solution of **sulf-125** used was at high dilution (1×10^{-4} M or less), the photoluminescent emission from the films was quite weak and red-shifted. This lack of dependence upon solution concentration makes sense when one considers that at the substrate surface *the polymer concentration is always high*. In order to control the emission process, therefore, the composition of the polymer itself must be controlled. Previous work with the perylene chromophore in Langmuir-Blodgett films provides a precedent for this approach.⁸⁸

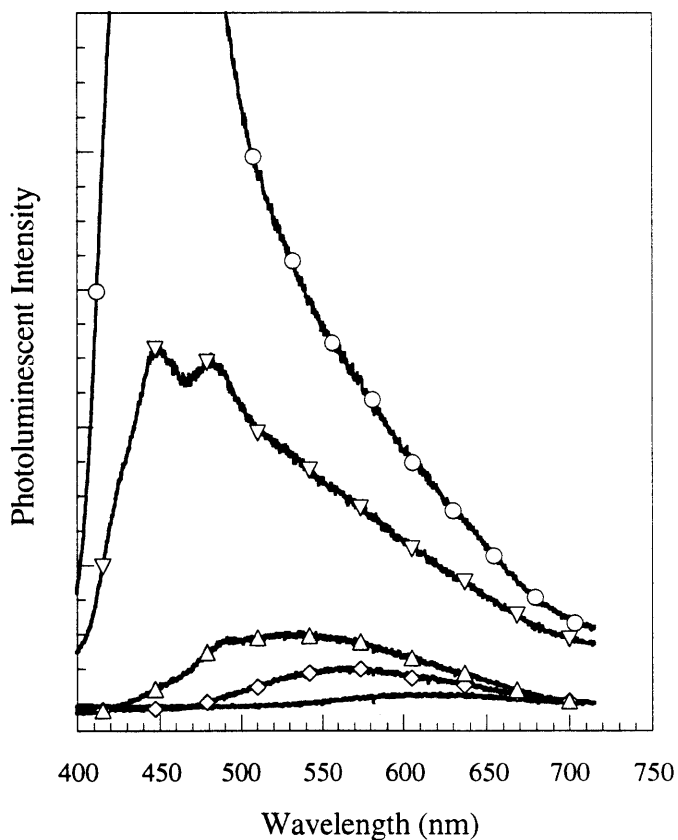


Figure 3.4. Solution photoluminescence of **sulf-125** in water. Concentration of polymer: no symbols, 7×10^{-3} M; \diamond , 2×10^{-3} M; Δ , 9×10^{-4} M; ∇ , 5×10^{-4} M; \circ , 2×10^{-4} M. As the concentration of **sulf-125** decreases, the emission increases.

When a series of *chemically* diluted DPA-containing copolymers, **sulf-(1_x%4-100-x%)50** (where the dilutant was the PBD-containing monomer, **4**), was sequentially adsorbed in equal thicknesses onto a prepared substrate, there was a dramatic shift back to the expected emission from the mono chromophore (Figure 3.5). As the percent of **1** in the copolymer decreased from 100% to 2%, the intensity of emission increased by a factor of 30. This effect was similar to that reported in the literature for chemical dilution, and provided further evidence for the existence of excimers. The solution emission at 1×10^{-3} M of this series mirrored this trend. As mentioned above, at high dilution, solutions of all of the polymers were brightly luminescent at 450 nm.

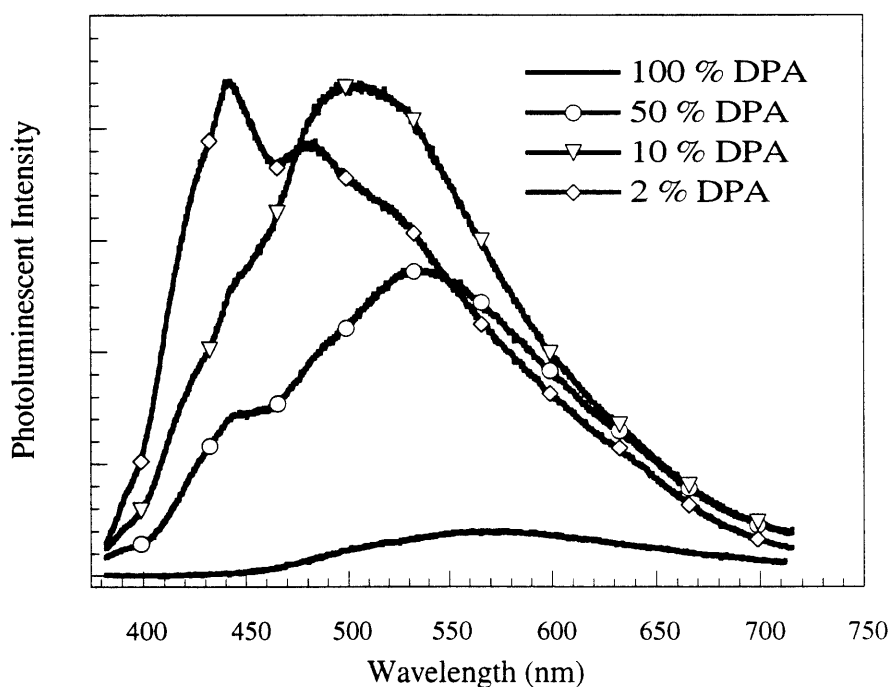


Figure 3.5. Photoluminescence of films of **sulf-(1_x%4-100-x%)50**. Film emission increases with decreasing % of DPA (**1**) in the copolymer. All films were 600 Å thick.

This behavior contrasted starkly with that observed for the spin-coated films discussed in CHAPTER 2. The spin-coated films were highly blue luminescent for both the DPA

homopolymer and the 50% copolymer. In Figure 3.6 below, the wide difference between the photoluminescence at equal thicknesses of spin-coated films of **125** and sequentially adsorbed films of **sulf-125** is shown. Additionally, the intensity of emission for the spin-coated film was over 15 times greater than that of the sequentially adsorbed film.

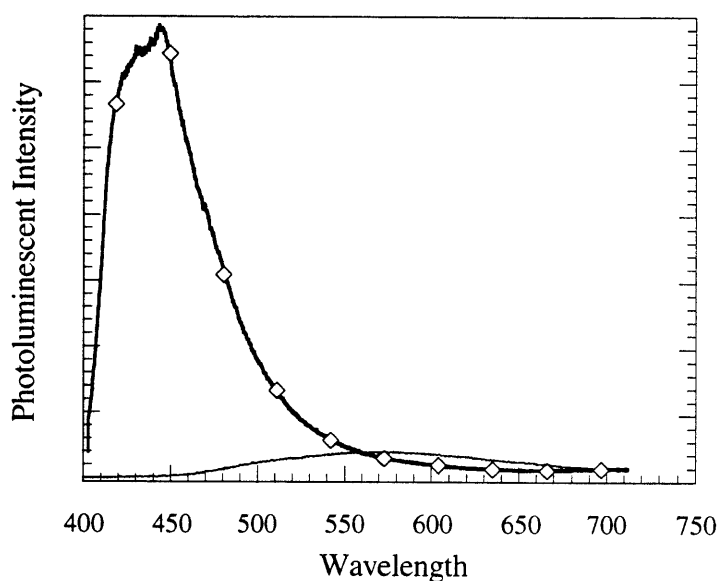
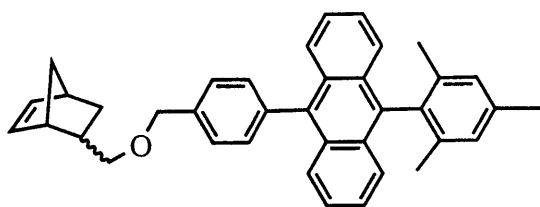


Figure 3.6. Photoluminescence of spin-coated and sequentially adsorbed films. Spin-coated film of polymer **125**, \diamond ; sequentially adsorbed film of polymers PAH and **sulf-125**, no symbols. Both films were 600 Å thick.

Another method whereby excimer formation potentially could be controlled is by increasing the sterics about the anthracene structural unit.^{89,95} Since a short distance between two anthracenes is necessary for excimer formation, an increase in the sterics above and below the ring plane should increase the emission and cause a blue-shift in relation to the parent polymer. The synthesis of a monomer, **2**, with one of the phenyl rings replaced by a mesityl ring was described in CHAPTER 1. The methyl groups projected above and below the anthracene plane, helping to prevent excimer formation.



NBDPA' (2)

This approach was found to be successful: the modified DPA polymers, **sulf-225** and **sulf-(250%450%)50** were highly luminescent in aqueous solution. Figure 3.7 depicts the photoluminescence of the polymers at a concentration of 2×10^{-3} M. The new **sulf-225** was more luminescent at this concentration than any of the previously prepared copolymers containing **1** and **4**. Note especially the difference between **sulf-225** and the original DPA polymer **sulf-125**: the wide difference in magnitude and degree of red-shifting again indicated the success of this strategy of excimer exclusion by steric blocking. However, the copolymer, **sulf-(250%450%)50**, was even more luminescent than **sulf-225**, indicating that some degree of self-quenching behavior remains at this concentration.

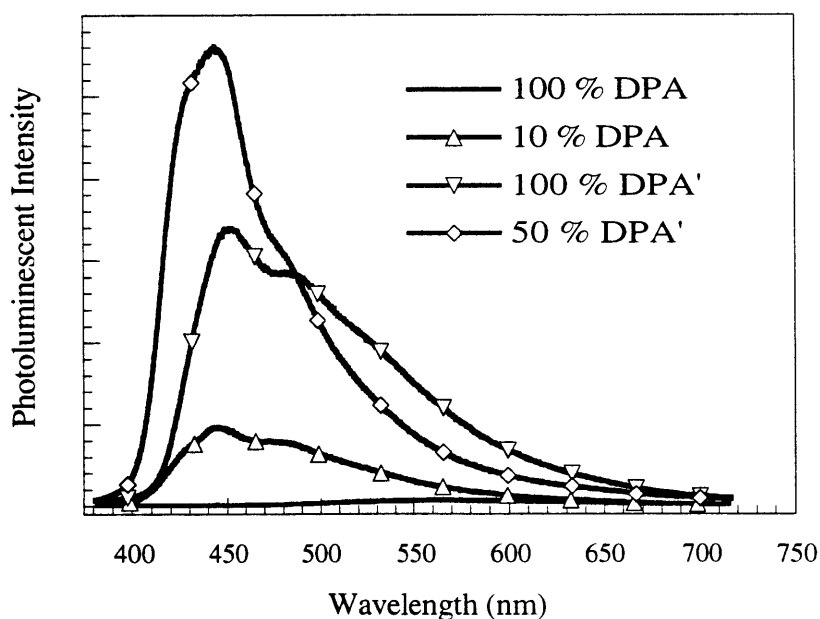


Figure 3.7. Solution photoluminescence of 2×10^{-3} M **sulf-(1_x%4100-x%)50** and **sulf-(2_x%4100-x%)50** in water.

Films were readily formed by sequential adsorption of **sulf-225** and **sulf-(250%450%)50** with PAH on glass or silicon prepared with 5 bilayers of PAH/PMA. The films appeared uniform and emitted uniformly under UV lamp excitation. The photoluminescent intensity of **sulf-225** films was much greater than that of **sulf-125** (see Figure 3.8). However, the spectrum was still red-shifted from 450 nm, indicating that excimers were still present. The film with **sulf-(250%450%)50** was more intensely photoluminescent overall and showed a more intense 450 nm emission band than the **sulf-225** film. Visually, under UV lamp excitation, the films with **sulf-225** appeared green-white, and the films with **sulf-(250%450%)50** appeared blue-white.

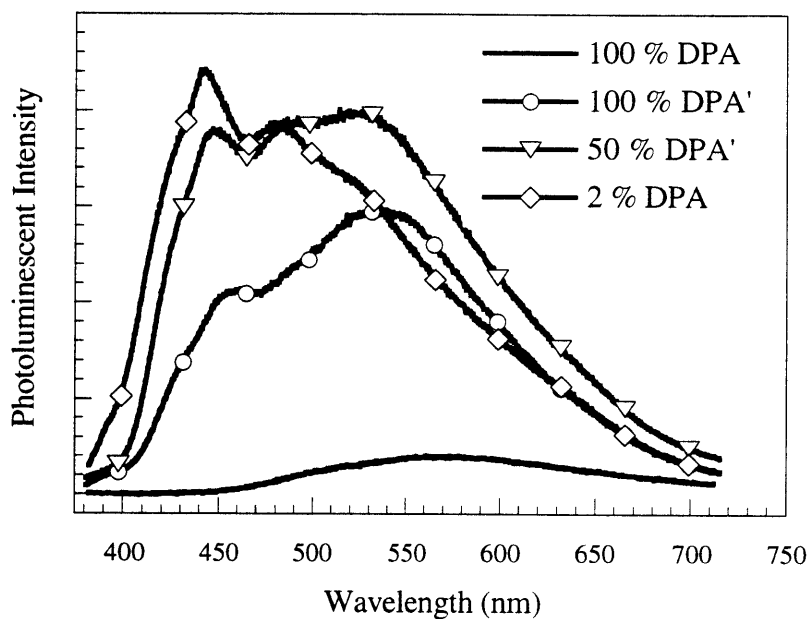


Figure 3.8. Photoluminescence of films of **sulf-(1_x%4100-x%)50** and **sulf-(2_x%4100-x%)50**.

Single-Layer Light-Emitting Devices.

Single-layer devices were constructed by building films of **sulf-(1_x%4100-x%)50** or **sulf-(2_x%4100-x%)50** onto an indium tin oxide (ITO) anode, and then placing a 2000 Å thick

aluminum cathode on top via thermal evaporation (Figure 3.9a). This procedure is described in more detail in CHAPTER 2. The device behavior is summarized in Table 3.2.

Interestingly, even with its low-intensity photoluminescent emission (see Figure 3.6), the single-layer device made with sequentially-adsorbed films of **sulf-1₂₅** showed greater output and efficiency than the device made by spin-coating **1₂₅** (see CHAPTER 2, Table 2.1). In the spin-coated device, a maximum of 0.5 nW light was obtained with an efficiency of 0.03 nW/mA, but the film itself was brightly blue photoluminescent. For **sulf-1₂₅**, even though the film was only weakly luminescent, the output and efficiency were *greater* : 6 nW and 0.1 nW/mA . In this case

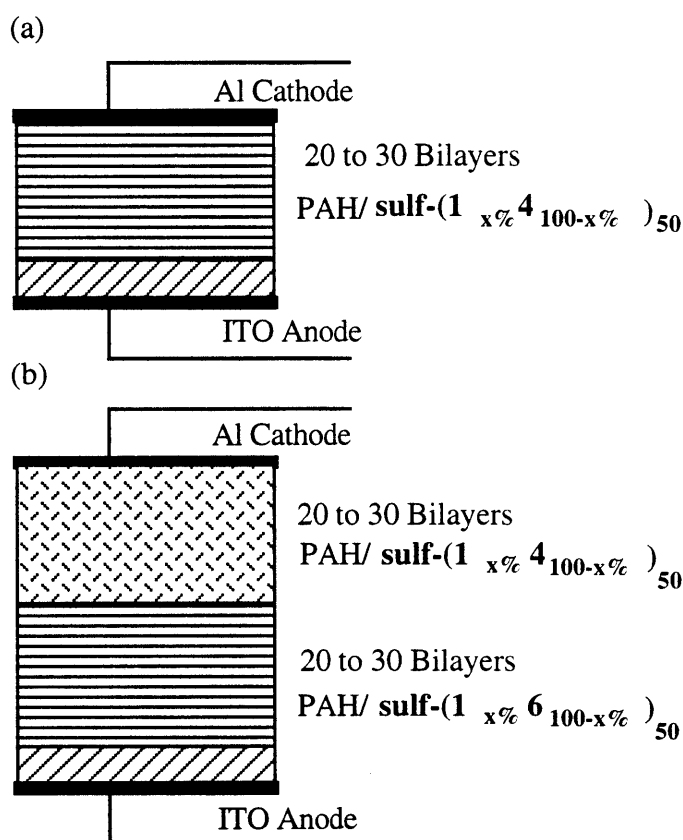


Figure 3.9. Configuration of polymer EL devices. (a) Single layer, ITO/PAH-PMA (5 bilayers)/PAH-**sulf-(1_{x%} 4_{100-x%})₅₀** (20 to 30 bilayers)/Al; (b) dual layer, ITO/PAH-PMA (5 bilayers)/PAH-**sulf-(1_{x%} 6_{100-x%})₅₀**/PAH-**sulf-(1_{x%} 4_{100-x%})₅₀** (20 to 30 bilayers)/Al.

the improvement in film quality more than made up for the vast difference in luminescence. Figure 3.10 shows the I-V and L-V curves for this device. Notice that this scan shows no evidence of the "spike" or ohmic behavior observed in all spin-coated devices. This phenomenon was observed far less frequently in devices with films made by sequential adsorption than in those with spin-coated films. Also, both the percentage of operating pixels and the overall stability of these new devices were greater. The threshold voltage was considerably lower than in the spin-coated device, which helped to explain some of the added device stability.

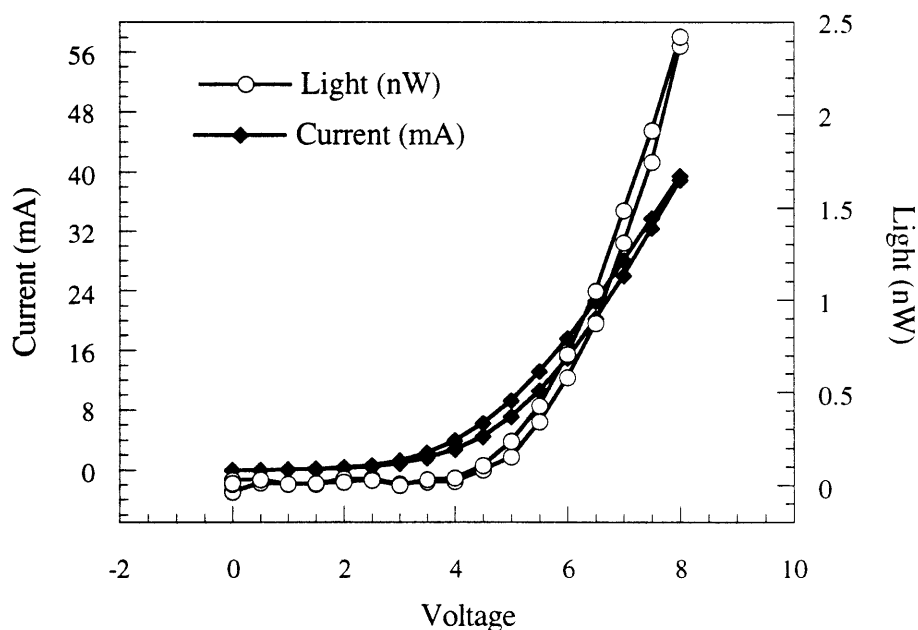


Figure 3.10. Performance of device ITO/PAH-PMA(5 bilayers)/PAH-sulf-125 (35 bilayers)/Al. Current-voltage (diamonds) and light-voltage (open circles) curves.

The performance of devices prepared with the rest of the **sulf-(1_{x%}4_{100-x%})₅₀** series is summarized in Table 3.2. Even though the photoluminescent emission of the film was greatest for **sulf-(1_{2%}4_{98%})₅₀** (see Figure 3.5), it actually displayed the worst device performance, 0.5 nW of light and 0.01 nW/mA. As the % of monomer 1 in the copolymer decreased, the devices

exhibited a loss of output and efficiency. This decrease indicated a charge balance problem caused by the increased dilution with the electron carrier (or hole blocker), **4**. As the % **1** decreased (and % **4** increased), the electron flow increasingly dominated and precluded recombination with holes to form the emissive DPA species. This explanation was supported by the high current density that was displayed in all devices (typically 400-800 mA/cm²), including those with very little output. Monomer **1**, highly diluted with the hole-transporting monomer **6**, also displayed a decrease in performance when compared to the homopolymer: down to 2 nW and 0.06 nW/mA efficiency. For all devices the threshold was 10 volts or lower, which was lower than any single-layer device made with spin-coated polymers containing the monomer **1** (see CHAPTER 2, Table 2.1).

Table 3.2. Performance of Single-Layer Devices with NBDPA (**1**) and NBDPA' (**2**)

Polymer ^a	Thickness (Å)	Output (nW)	Current (mA/cm ²)	Efficiency (nW/mA)	Threshold ^b (V)
Devices with DPA (1)					
sulf-125	250	5	830	0.1	6
sulf-(150% 450%)50	400	5	420	0.2	10
sulf-(110% 490%)50	400	1	830	0.02	9
sulf-(12% 498%)50	400	0.5	830	0.01	9
sulf(12% 698%)50	350	2	640	0.06	8.5
Devices with DPA' (2)					
sulf-225	400	21	920	0.3	13
sulf-(250% 450%)50	400	0.8	130	0.1	16

^a All films were made by sequential adsorption of polymer (1×10^{-4} M) with PAH (1×10^{-2} M) onto a prepared ITO substrate (prepared with 5 bilayers of PAH/PMA). Additional thickness of prepared layer: 100 Å. ^bThe voltage at which light output rises above 0.5 nW (well above baseline noise).

Devices made by assembling the bulkier DPA monomer, **2**, performed better than any of those containing **1**. The best result for single-layer devices was 21 nW and 0.3 nW/mA, obtained for **sulf-225**, which was comparable to the best spin-coated single-layer devices (see Table 2.1). The two devices with **2** had higher threshold voltages than those with **1**, especially the device containing **sulf-(250% 450%)50**. Also, devices with this 50% copolymer performed far worse than those with the homopolymer, which was unusual: devices made with 50% copolymers of **1** and an electron-transporting monomer (**3** or **4**) performed better than those with the homopolymer. It is possible that the very bulkiness of **2** which helps prevent excimer formation, makes the transfer of charge more difficult. This would also explain the higher threshold voltages needed to inject charge and produce light.

Dual-Layer Light-Emitting Devices

To address the charge balance problem described in the previous section, dual-layer structures were assembled which contained a hole-transporting (electron blocking) layer of sulfonated copolymers of **1** and **6**. Figure 3.9b shows the composition of these devices, constructed in a similar fashion as the single-layer devices, with 250-350 Å of **sulf-650** or **sulf-(12% 698%)50** with PAH onto which 400 Å of **sulf-(12% 498%)50** or **sulf-(2_x% 4100-x%)50** with PAH was deposited. The total film thickness was about 800 Å (including the PAH/PMA prep layer). Table 3.3 summarizes the behavior of these devices.

The use of a separate hole-transport layer improved the device performance in most cases. For the films containing **sulf-(12% 498%)50**, either a homopolymer of **6** or a copolymer of **1** and **6** (predominantly **6**) improved the performance compared to the single layer **sulf-(12% 498%)50** device (7 nW versus 0.5 nW and 0.3 nW/mA versus 0.01 nW/mA). The threshold voltages were similar to those seen for the single-layer devices, even though the films were almost twice as thick. This indicated that the barrier to hole injection was lowered by the PTP layer. This improvement in performance, greater than 10-fold, was similar to that obtained by employing the PPV multilayer heterostructure as a hole-transporting/electron-blocking layer (described in CHAPTER 2).

Dual-layer devices made with homopolymers and copolymers of **2** showed little increase in output and efficiency compared to the single-layer devices. In dual-layer devices of **sulf-225** and in both single- and dual-layer devices of **sulf-(250%450%)50** the threshold voltage was very high, making device operation difficult. Although the dual-layer device with **sulf-225** had a somewhat better efficiency than the single-layer, the higher threshold voltages made it more difficult to get greater light output without burning out the device. Therefore, the single-layer of sequentially adsorbed **sulf-225** remained the all-norbornene device with the greatest output: 21 nW of light and 0.3 nW/mA efficiency.

Table 3.3. Performance of Dual-Layer Devices with NBDPA (1) and NBDPA' (2)

Polymer ^a	Thickness (Å)	Output (nW)	Current (mA/cm ²)	Efficiency (nW/mA)	Threshold ^b (V)
Devices with DPA (1)					
sulf-650 &	350				
sulf-(12%498%)50	400	7	380	0.3	7.5
sulf-(12%698%)50 &	330				
sulf-(12%498%)50	300	4.5	960	0.1	11.5
Devices with DPA' (2)					
sulf-650 &	250				
sulf-225	400	3.2	330	0.5	18
sulf-650 &	250				
sulf-(250%450%)50	410	0.8	330	0.04	17

^a All films for devices were made by sequential adsorption of polymer (1×10^{-4} M) with PAH (1×10^{-2} M) onto a prepared ITO substrate (prepared with 5 bilayers of PAH/PMA). Additional thickness of prepared layer: 100 Å. ^bThe voltage at which light output rises above 0.5 nW (well above baseline noise).

Conclusions

The sulfonation of the polynorbornene backbone (described in CHAPTER 1) provided a technique whereby a whole class of polymers with application for light-emitting devices became suitable for making films via sequential adsorption. Films were readily prepared with these new sulfonated polynorbornenes. Incorporation of hole and electron transporting monomers provided a means both to control charge flow and to prevent excimer formation by DPA structural units. Excimer formation was also controlled by increasing the bulkiness of the groups flanking the anthracene core. Dual-layer devices with separate hole and electron transport layers increased the output from polymers containing **1** by a factor of 10. The greatest electroluminescent emission was from a single-layer film of the "bulky DPA" polymer, **225**: 21 nW of blue-white light with an efficiency (photons/electron) of $3.3 \times 10^{-6} \%$.

Experimental Section

General Procedures. Film thicknesses were measured with a Gartner Ellipsometer and a Sloan Dektak 8000 profilometer. Measurements of current and luminescence as a function of applied field were made under forward bias. A silicon photodiode (Newport Instruments, Model 1830-C) was used to measure device light output, which is measured in nW. Absorbance spectra were taken with an Oriel Instapec spectrophotometer. Electroluminescence and photoluminescence spectra were taken using a spectrograph coupled to a Peltier-cooled CCD array (Oriel Instaspec IV). The system response was calibrated using a tungsten lamp. Excitation for the photoluminescence was from the multiline UV mode of an argon ion laser.

Formation of Thin Films, Layer-by-Layer Adsorption. Silicon slides were cleaned by etching in a chromic acid bath overnight and rinsing with MilliQ water immediately prior to dipping. Glass slides were cleaned as described in the literature and sonicated prior to use.¹⁰ Both glass and silicon substrates were prepared by depositing 5 bilayers (100 Å) of poly(allylamine HCl)/poly(methylacrylic acid) using 1×10^{-2} M aqueous solutions at pH 3.5 of each polymer. It was then possible to begin deposition of single or dual-layer films. Solutions of

sulfonated polynorbornene were prepared by first dissolving an appropriate quantity of material into 1 mL of dimethylacetamide. This solution was then diluted to the desired concentration for dipping, typically 1×10^{-4} M. All solutions were adjusted to pH 3.5 with dilute HCl, and then filtered through a 0.5μ syringe filter. No salt was added for homo- and co-polymers of **1** and **2**. It was necessary to add 0.1 M NaCl to the polymer solutions for homo- and co-polymers containing **6**. A HMS Series Programmable Slide Stainer from Carl Zeiss, Inc. was used to automatically dip the substrates in the appropriate solution. Thicknesses were measured by ellipsometry and verified by profilometry. See Table 3.1 for bilayer thickness data.

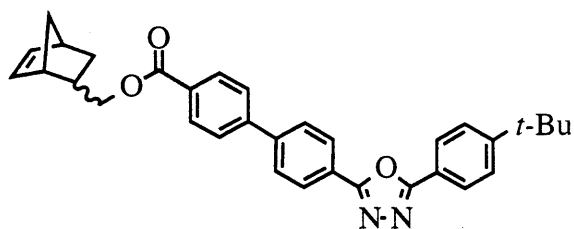
Light-Emitting Device Fabrication. Commercially patterned indium tin oxide (ITO) (two 3 mm wide strips, spaced 4 mm apart) on a 1 in \times 1 in piece of glass was prepared by a previously reported cleaning/sonication procedure.¹⁰ The ITO was prepared with 5 bilayers (100 Å) of poly(allylamine HCl)/poly(methylacrylic acid) using 1×10^{-2} M aqueous solutions of each polymer. Films of sulfonated polynorbornenes were deposited from 1×10^{-4} M aqueous solutions alternating with 1×10^{-2} M poly(allylamine HCl). All solutions were adjusted to pH 3.5 with dilute HCl before dipping. In a single-layer device, 400 Å of additional material was sequentially adsorbed. For dual-layer devices, 300 Å of one polynorbornene and 400 Å of a second polynorbornene were adsorbed. No salt was added for homo- and co-polymers of **1** and **2**. It was necessary to add 0.1 M NaCl to the polymer solutions for homo- and co-polymers containing **6**. Four 2000 Å thick aluminum strips, 2 mm wide and spaced 2 mm apart, were laid perpendicular to the ITO by thermal evaporation at 1×10^{-6} Torr. Connection to the electrodes was made with gold wire, generating 8 individually addressed "pixels" where the electrodes crossed.

APPENDIX A

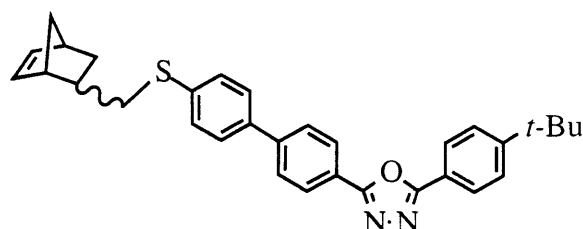
Enhancement of Device Efficiency Employing Polynorbornene with the
Oxadiazole Structural Unit for Electron Transport

Introduction

The oxadiazole unit is widely used as an electron-transporting or hole-blocking material.^{2,3,96} Several research groups, including ours, have shown that the tendency of *t*-butylphenyl-*para*-biphenyloxadiazole (PBD) to crystallize can be overcome by incorporating it into a polymer such as polynorbornene.^{18,51,74,97,98} The preparation of polymers of **3** and **4** is described in detail in CHAPTER 1. In a copolymer with diphenylanthracene, **3** was shown in CHAPTER 2 to greatly enhance emission: devices were up 60 times more efficient with **3** present. This appendix describes how PBD polymers can also be used in a separate layer for electron transport when non-polynorbornene based materials are used for emission.

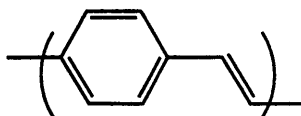


NBPBD' (3)

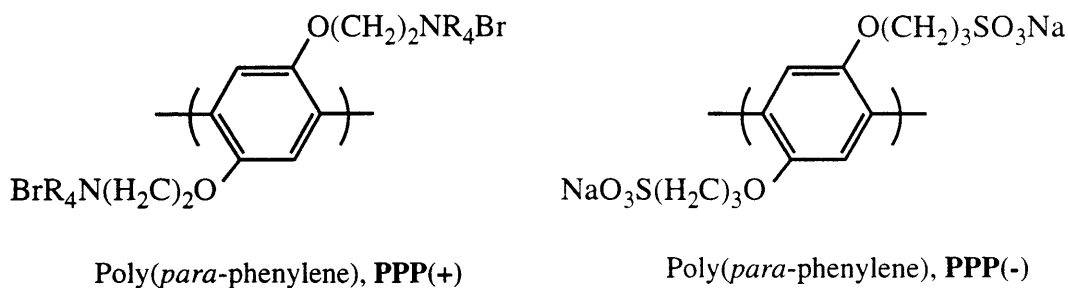


NBPBD (4)

Whereas a variety of polymeric materials for sequential adsorption are known to be good at transporting holes and blocking electrons, *none* are proven to be good electron transporters.^{45,86} Since many devices, such as those based on poly(phenylene vinylene) (PPV) and poly(*para*-phenylene) (PPP), are believed to be primarily hole-driven in nature, great enhancements in efficiency are expected by blocking the flow of holes and separating the emission layer from the defect-laden electrode surface.^{6,43}



Poly(phenylenevinylene), **PPV**



Results and Discussion

Electron-Transport/Hole-Block Nature of PBD.

Figure A.1 gives some insight into why *t*-butylphenyl-*para*-biphenyloxadiazone (PBD) is successful: PBD behaves as a one-way street for charge carriers by allowing electrons, but not holes to pass (i.e., it is reducible but not oxidizable). When PBD is used as a separate layer in a film which accepts holes readily, such as poly(phenylene vinylene) (PPV), excess charge builds up at the polymer-polymer interface. This effect is highly desirable to ensure efficient charge recombination and isolate the excited-state species away from the defect-laden electrodes.⁴³

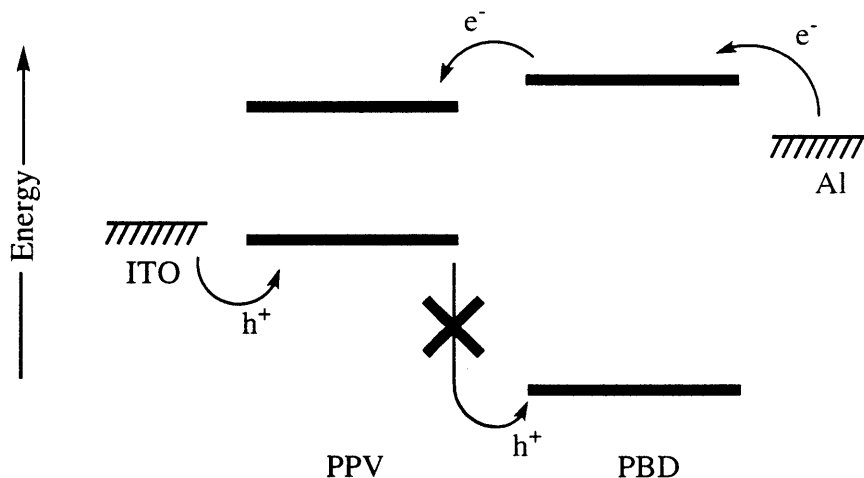


Figure A.1. Electron-transporting/hole-blocking mechanism for *t*-butylphenyl-*para*-biphenyloxadiazone (PBD) with poly(phenylene vinylene) (PPV).

Preparation of PBD Layers.

The polymer **350** was spin-coated in a separate layer from chlorobenzene onto previously prepared PPV heterostructures.^{10,44} The PPV layer did not etch in the presence of nonpolar solvents such as chlorobenzene. The lower limit of thickness for this type of spin-coating was about 600 Å, which may be thicker than is optimum for this application.^{6,39,98}

Sulf-425 was readily assembled by sequential adsorption with poly(allylamine HCl) (PAH), both with and without 0.1 M NaCl added (addition of salt made the bilayers over 10 times thicker, see Table 3.1). This kind of PBD layer was readily deposited on both PPV/poly(acrylic acid) (PAA), as well as on poly(*para*-phenylene) [PPP(+)] and PPP(-)]. (CHAPTER 2 and 3 contain a more thorough treatment of the sequential adsorption process.) In order to deposit enough PBD onto the PPP(+)/PPP(-) surface, it was necessary to add salt to the dipping solution. Figure A.2 shows the linear deposition of **sulf-425** (with 0.1 M NaCl added) on 5 bilayers PPP(+)/PPP(-). Overall thicknesses were measured at various intervals by ellipsometry on a

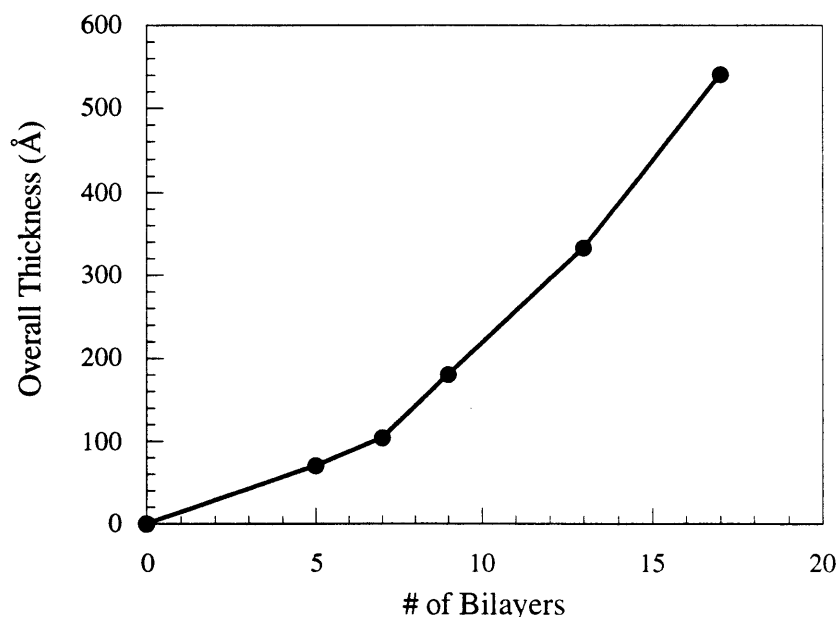


Figure A.2. Sequential adsorption of **sulf-425** and poly(allylamine HCl) on 5 bilayers of PPP(+)/PPP(-). Ellipsometry measurements on a silicon wafer.

silicon wafer. The average thickness / bilayer was 40 Å.

Devices with Spin-Coated PBD on PPV Heterostructures.

A modest improvement in efficiency was observed when the multilayer PPV heterostructure (described in CHAPTER 2) was coated with a spin-coated layer of PBD (see Table A.1). However, the threshold voltage increased significantly, and no improvement in the maximum output was obtained. The I-V and L-V curves for this device are depicted in Figure A.3. The light observed was 530 nm, the same wavelength expected from PPV (PBD emits at 395 nm). The electroluminescent spectrum of this device is shown in CHAPTER 2, Figure 2.9b. If thinner layers were made possible, then a more ideal thickness could be obtained, increasing the efficiency and output while not unduly increasing the threshold.

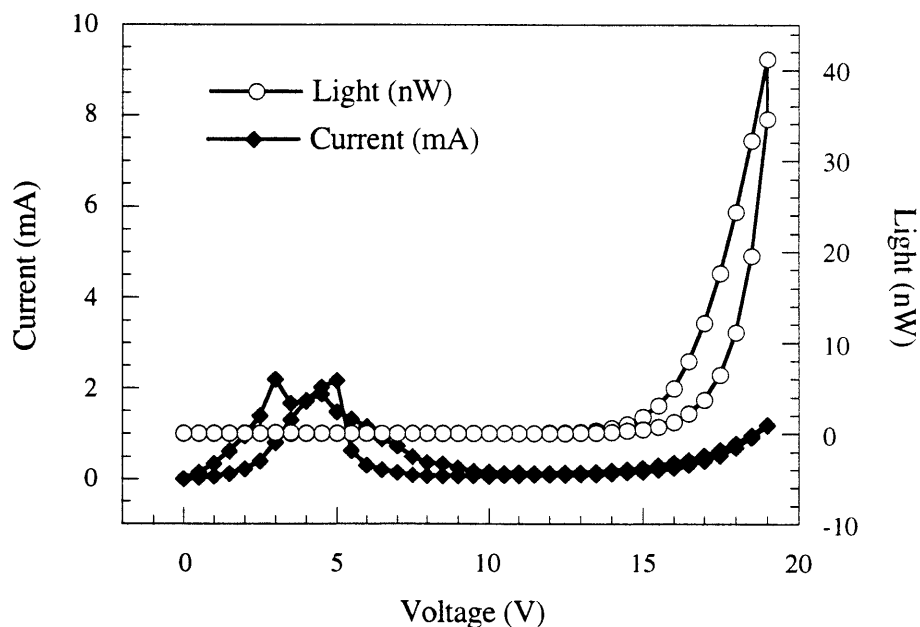


Figure A.3. Performance of device ITO/PPV-SPS (5 bilayers)/PPV-PMA(20 bilayers)/PBD (570 Å)/Al. Current-voltage (diamonds) and light-voltage (open circles) curves. PPV heterostructure: 5 bilayers PPV/SPS; 20 bilayers PPV/PMA.

Table A.1. Dual-Layer Device Performance: PPV/PMA//PPV/SPS with Spin-Coated PBD

PPV Device	Thickness (Å) ^a	Output (nW)	Efficiency (nW/mA)	Threshold (V) ^b
PPV Only	300	200	10	3
PPV w/ PBD	300 + 570	55	41	12

^aMeasured by ellipsometry on a silicon monitor slide. ^bThe voltage at which light output rises above 0.5 nW (well above baseline noise).

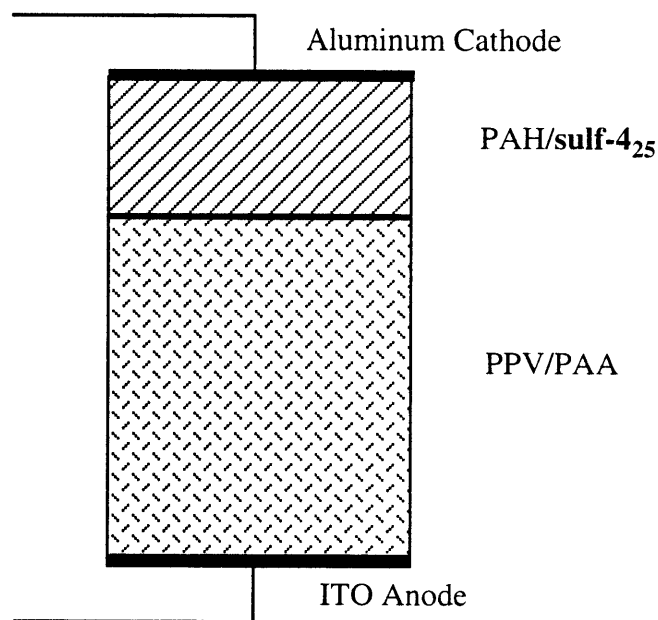
Devices with Sequentially Adsorbed PBD on PPV/PAA.

The sequential adsorption technique allows for relatively easy variation of ultra-thin film thickness. A film of sequentially adsorbed PPV/PAA was prepared, and a layer of PAH/**sulf-425** was deposited upon it. It was possible to deposit films of PAH/PBD as thin as 50 Å (one bilayer) far more easily than with spin-coating. Figure A.4 below is a schematic of a two-layer device of PAH/PBD assembled on PAA/PPV. Table A.2 summarizes the results obtained from a series of layers with increasing thicknesses. The efficiency of a two-layer device was up to 15 times better than a device with PPV alone. The output from the control (i.e., PPV without PBD) was much lower than the maximum observed previously by Mr. Michael Durstock in Professor Dr. Michael Rubner's laboratory at the Massachusetts Institute of Technology. PPV is a notoriously difficult material with which to acquire reproducible results. However, if the 8000 nW of light from PPV alone that was observed by Durstock becomes attainable once again, an improvement by a factor of 15 would make the efficiency and light output the highest ever for an aluminum cathode and PPV.

Table A.2. Dual-Layer Device Performance: PPV/PAA with PAH/PBD

PPV Device	Thickness (Å) ^a	Output (nW)	Efficiency (nW/mA)	Threshold (V) ^b
PPV Only	500	20	1.1	10
PPV w/ PBD	500 + 50	12	2.4	11
PPV w/ PBD	500 + 150	20	15	13

^aMeasured by ellipsometry on a silicon monitor slide. ^bThe voltage at which light output rises above 0.5 nW (well above baseline noise).

**Figure A.4.** Sequentially adsorbed two-layer device with PBD and PPV.

Devices with Sequentially Adsorbed PBD on PPP(+)/PPP(-).

Two water-soluble variations of PPP were prepared in small quantities by Professor Dr. John Reynolds and coworkers at the University of Florida.^{13,99} These blue-light-emitting materials have been found to produce as much as 95 nW in devices, but the quality of material

slowly deteriorates upon standing. Due to the limited supply, the solutions employed in this study were relatively old; PPP(+)/PPP(-) in these results emitted only 1-3 nW. However, by comparison to a PPP(+)/PPP(-) control, it was found that a layer of PBD for electron transport again greatly improved output and efficiency of the devices.

Table A.3 shows the performance of two-layer devices with a PPP(+)/PPP(-) bottom layer and a PAH/**sulf-425** top layer. Both of the control samples reached only several nW of light. Devices with a PBD layer displayed from 10 to 30 times the efficiency, and boosted the maximum light output by the same factor. In the thicker PPP(+)/PPP(-) device, the PBD layer also reduced the threshold voltage, which indicated that it alleviated the barrier to charge injection (most probably electron injection: PPP more readily accepts positive charge).

Table A.3. Dual-Layer Device Performance: PPP(+)/PPP(-) with PAH/PBD

# PPP Bilayers	Thickness (Å) ^a	Output (nW)	Efficiency (nW/mA)	Threshold (V) ^b
15	210	2	0.1	10
15	210 + 60	26	3.5	8
30	420	2.3	0.8	21
30	420 + 100	66	14	14

^aMeasured by ellipsometry on a silicon monitor slide. ^bThe voltage at which light output rises above 0.5 nW (well above baseline noise).

As mentioned above, when the PPP is performing well, it shows native efficiencies and outputs 10 to 40 times better than listed in Table A.3.¹³ If the same boost by PBD as seen in Table A.3 could be realized in freshly prepared polymer, outputs would then be in the hundreds or thousands of nanowatts, with high efficiencies as well. Further variation of PBD layer thickness would also be interesting at that point.

Conclusions

Both spin-coated **350** and sequentially-adsorbed **sulf-425** onto PPV (green light emitter) or PPP (blue light emitter) were shown to greatly increase both the output and efficiency of devices. Generally, the improvement was by a factor of 15 or 30. In some cases, the threshold voltage was also reduced. There is potential for future work in this area: investigation of other materials for light emission and optimization of the PBD layer thickness to achieve maximum output and efficiencies.

Experimental Section

General Procedures. Film thicknesses were measured with a Gartner Ellipsometer and a Sloan Dektak 8000 profilometer. Measurements of current and luminescence as a function of applied field were made under forward bias. A silicon photodiode (Newport Instruments, Model 1830-C) was used to measure device light output, which is measured in nW. Electroluminescence and photoluminescence spectra were taken using a spectrograph coupled to a Peltier-cooled CCD array (Oriel Instaspec IV). The system response was calibrated using a tungsten lamp. Excitation for the photoluminescence was from the multiline UV mode of an argon ion laser.

Formation of Thin Films, Spin-Coating. Solutions of polymer in chlorobenzene ranging from 1.2-2.5% (w/w) were prepared and filtered through a 0.2 μ syringe filter. Polymer films were applied to the substrate by placing 5 drops of solution onto the substrate and then spinning it rapidly, using a Headway Research, Inc. Photo-Resist Spinner spin coater. An appropriate thickness, generally about 600 Å, was obtainable by methodically varying both the spin rate (around 2000-5000 rpm) and the polymer concentration. A typical set of conditions for **350**: 5 drops; 3.4% (w/w) in chlorobenzene; 5000 rpm; yields uniform film, 570 ± 50 Å.

Formation of Thin Films, Sequential Adsorption. Silicon slides were prepared by etching in a chromic acid bath overnight and rinsing with MilliQ water immediately prior to dipping. Glass slides were prepared as described in the literature and sonicated prior to use.¹⁰

The emitting PPV or PPP layers were prepared as previously described. The solutions of sulfonated polynorbornene were prepared by first dissolving an appropriate quantity of material into 1 mL of *N,N*-dimethylacetamide. The solutions were then diluted to the desired concentration for dipping, typically 1×10^{-4} M. All solutions were adjusted to pH 3.5 with dilute HCl, and then filtered through a 0.5 μ syringe filter. A HMS Series Programmable Slide Stainer from Carl Zeiss, Inc. was used to automatically dip the substrates in the appropriate solution. Thicknesses were measured by ellipsometry and verified by profilometry. To deposit onto PPP(+)/PPP(-) films, it was necessary to add 0.1 M NaCl to the solution of **sulf-425**.

Light-Emitting Device Fabrication. Commercially patterned indium tin oxide (ITO) (two 3 mm wide strips, spaced 4 mm apart) on a 1 in \times 1 in piece of glass was prepared by a previously described cleaning/sonication procedure.¹⁰ Films were prepared as described above, with 200-500 Å of emitting layer on the bottom and 50-150 Å of electron-transport layer on top. Four 2000 Å thick aluminum strips, 2 mm wide and spaced 2 mm apart, were laid perpendicular to the ITO by thermal evaporation at 1×10^{-6} Torr. Connection to the electrodes was made with gold wire, generating 8 individually addressed "pixels" where the electrodes crossed.

APPENDIX B

Binaphtholate Complexes of Molybdenum that Catalyze Ring Opening Metathesis Polymerization (ROMP) to Form Stereoregular Polynorbornadienes

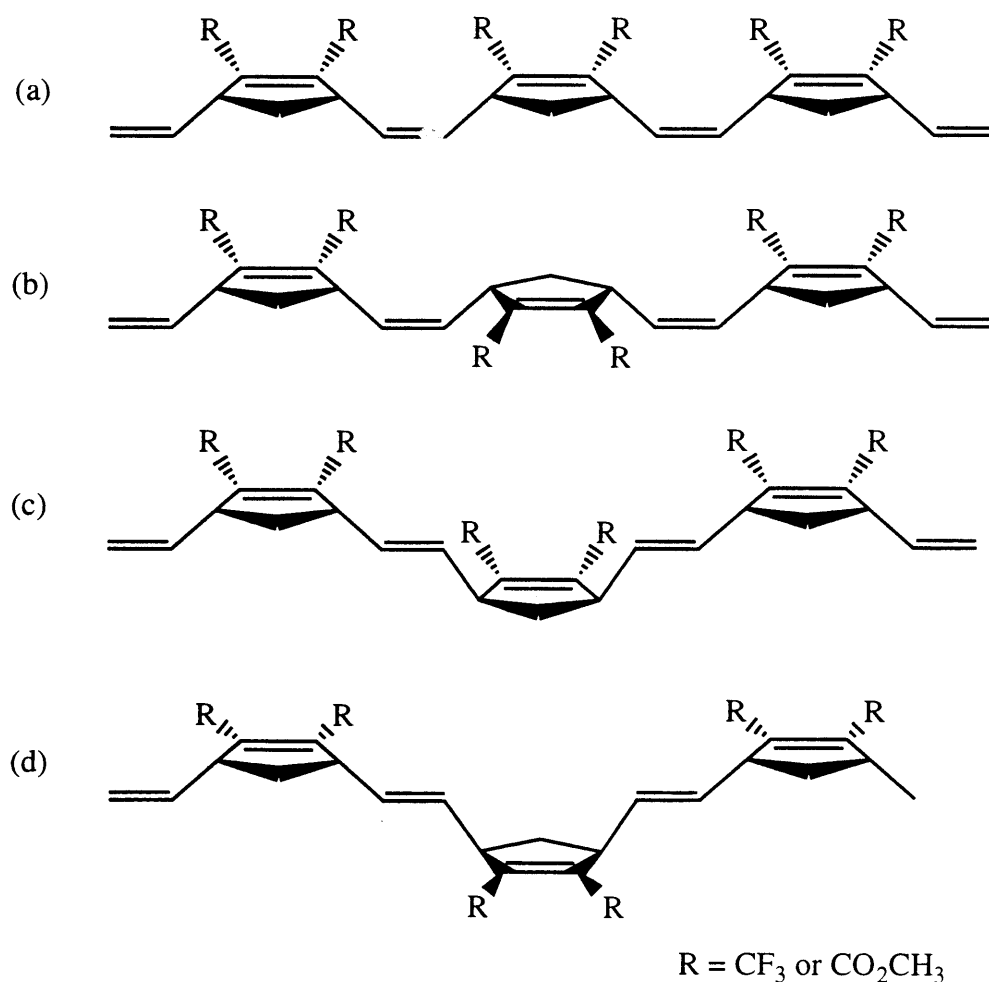
Much of the material covered in this appendix has appeared in print:

Totland, K. M.; Boyd, T. J.; Lavoie, G. G.; Davis, W. M.; Schrock, R. R.
Macromolecules **1996**, *29*, 6114.

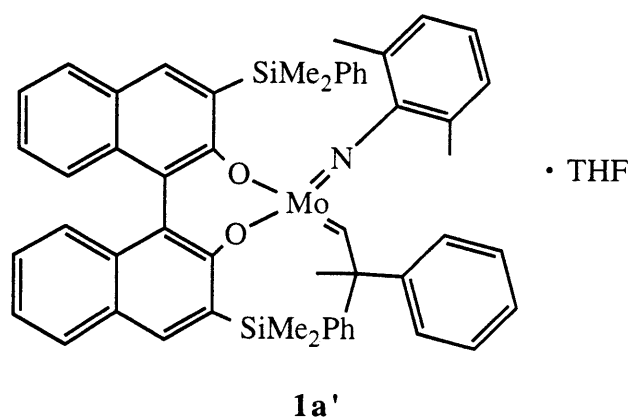
Introduction

The primary goal of this project is to design and synthesize ring-opening metathesis polymerization (ROMP) initiators which make poly(norbornadienes) with highly regular geometries. In addition to containing a chiral ligand, these initiators should ideally be thermally stable and relatively crystalline. Scheme B.1 depicts four possible regular structures of polynorbornadiene. It has been possible to prepare some, but not all, of these structures selectively by choosing appropriate ligands around a molybdenum center.^{76,100-102} The selectivity is believed to be determined by the geometry of the catalyst at the growing end of the polymer chain, and so it is reasonable to expect that modification of the initiator's ligand environment should alter the resulting polymer geometry.

Scheme B.1. Four Regular Geometries of 2,3-Disubstituted Polynorbornadienes



Previous work showed that $\text{Mo}(\text{CHCMe}_2\text{Ph})(\text{NAr}')[(\pm)\text{-BINO}(\text{SiMe}_2\text{Ph})_2](\text{THF})$ (**1a'**) ($\text{NAr}' = 2,6\text{-dimethylphenylimido}$), produced highly regular poly(bistrifluoromethyl-norbornadiene) (poly(bisCF₃NBD)) and poly(dicarbomethoxynorbornadiene) (poly(DCMNBD)). By proton and carbon-13 NMR it was shown that the polymers were 99% cis and, for poly(DCMNBD), 99% isotactic.^{101,102} (This configuration is the structure "a" in Scheme B.1 above.) However, this **1a'** was not thermally stable and attempts to get crystals suitable for X-ray analysis were unsuccessful.



In an effort to overcome these difficulties, binaphtholate ligands were synthesized with groups other than -SiMe₂Ph substituted at the 3,3' positions. A phenyl-substituted ligand was prepared by Dr. Karen Totland and used to make $\text{Mo}(\text{CHCMe}_2\text{Ph})(\text{NAr}')[(\pm)\text{-BINO}(\text{Ph})_2](\text{THF})$, **2a'**. ($\text{NAr}' = 2,6\text{-dimethylphenylimido}$). This compound was found to be stable at room temperature in solution for a week, and an X-ray crystal structure was successfully obtained from it.¹⁰³

This appendix describes the preparation of two additional binaphtholate ligands, with 2-methylphenyl or 2,6-dimethylphenyl groups at the 3,3' position. Four ROMP initiators were made with these new ligands, each binaphtholate combined with either NAr' or NAr ($\text{NAr} = 2,6\text{-diisopropylphenylimido}$) on the molybdenum neophylidene. The effects of the bulkiness of the ligands around the molybdenum on the cis/isotactic nature of the polymers will be discussed.

Results and Discussion

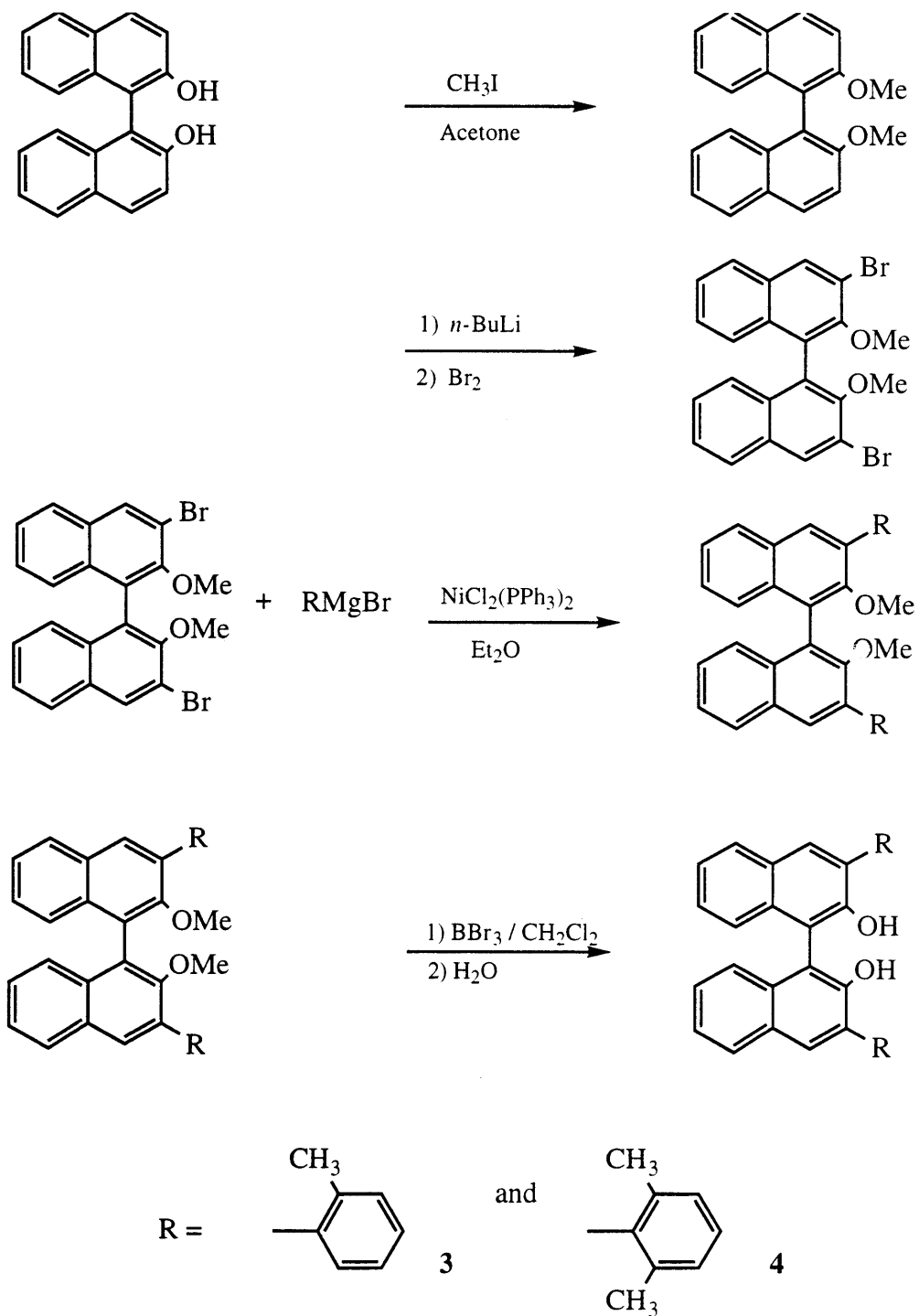
General Procedure for Preparation of 3,3' Substituted Binaphtholate Ligands.

The synthesis of (\pm)-3,3'-bis(2-methylphenyl)-2,2'-dihydroxy-1,1'-dinaphthyl (**3**) and (\pm)-3,3'-Bis(2,6-dimethylphenyl)-2,2'-dihydroxy-1,1'-dinaphthyl (**4**) is outlined in Scheme B.2 below. The procedure closely followed that developed to prepare **2**.^{73,103,104} The last two steps of the reaction sequence for **3** and **4** were carried out in 40-45% overall yield on a gram scale. This Grignard coupling sequence has been used more recently to develop ligands for asymmetric ring closing metathesis of 6-membered rings.¹⁰⁵

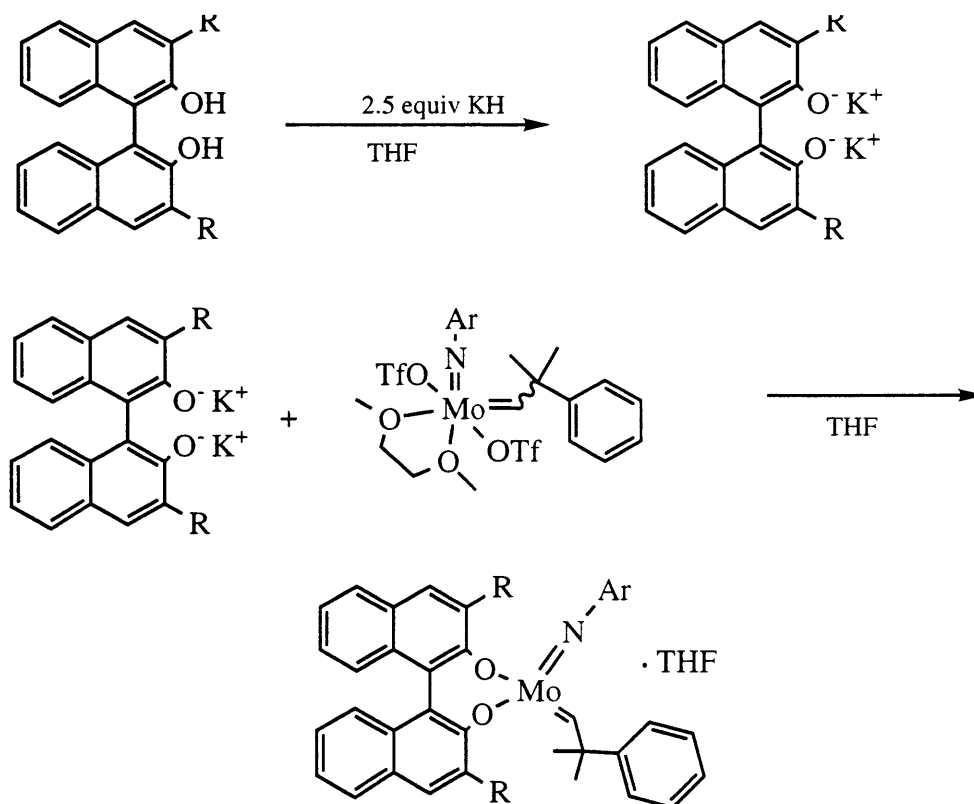
General Procedure for Initiator Synthesis.

The synthesis of initiators containing the ligands **3** and **4** was accomplished using the procedure outlined in Scheme B.3. Initiators with both 2,6-dimethylphenylimido (indicated with an **a'**) as well as 2,6-diisopropylphenylimido ligands (indicated with an **a**) were prepared with each type of binaphtholate. Best results were obtained by preparing the potassium salt of the binaphtholate ligand *in situ* and immediately reacting it with the molybdenum bistriflate.

All of the initiators prepared in this manner were thermally stable (no change in the proton NMR spectra after several days at room temperature in solution). Purification was performed readily by recrystallization; all the compounds formed star-shaped yellow crystals upon standing in Et₂O. Yields for the two-step sequence ranged from 30-65%. THF remained attached following workup, and attempts to remove the THF in a THF-toluene mixture *in vacuo* led to decomposition. However, the THF adduct did not hinder the catalytic abilities of these materials: it was possible to use all four of these initiators to polymerize norbornadienes.

Scheme B.2. Synthesis of Binaphtholate Ligands: Substitution at 3,3'.

Scheme B.3. Synthesis of Initiators for ROMP.



R = 2-methylphenyl, Ar = 2,6-diisopropylphenylimido (**3a**)

R = 2-methylphenyl, Ar = 2,6-dimethylphenylimido (**3a'**)

R = 2,6-dimethylphenyl, Ar = 2,6-diisopropylphenylimido (**4a**)

R = 2,6-dimethylphenyl, Ar = 2,6-dimethylphenylimido (**4a'**)

Synthesis of Highly-Cis, Highly-Isotactic Polynorbornadienes.

Polymers made from the monomers bisCF₃NBD and DCMNBD were prepared with each initiator (see Table B.1). The polymers were obtained in high yield and with narrow polydispersities as expected for a "living" polymerization. Dramatic effects on the cis content of the resulting polymers were observed when the initiator's steric environment was varied. Changing the arylimido from 2,6-dimethylphenyl to 2,6-diisopropylphenyl (i.e., **3a'** to **3a** and **4a'** to **4a**) produced catalysts with a greater tendency to make stereoregular polymer. Also, as the bulkiness of the binaphtholate increased from **3a'** to **4a'**, a similar increase was observed. All polymers that were >90% cis were determined to be >95% isotactic by carbon-13 NMR.¹⁰¹

Table B.1. Characterization of Poly(bisCF₃NBD) and Poly(DCMNBD)

initiator ^a	monomer	yield	M_n^b	M_w / M_n^b	cis (%)
3a'	bisCF ₃ NBD	94	-	-	93 ^c
3a'	DCMNBD	65	20230	1.41	83
3a	bisCF ₃ NBD	95	-	-	99 ^c
3a	DCMNBD	99	17450	1.07	98 ^d
4a'	bisCF ₃ NBD	95	-	-	99 ^c
4a'	DCMNBD	99	17310	1.18	91 ^d
4a	bisCF ₃ NBD	99	-	-	98 ^c
4a	DCMNBD	85	11930	1.08	99 ^d

^aPolymerizations carried out in THF, calc. MW's were **3a'** 12700, **3a** 10600, **4a'** 10600, **4a** 11700. ^bDetermined by GPC in CH₂Cl₂ using a light scattering detector coupled to a differential refractometer (highly cis/isotactic poly[bisCF₃NBD] is insoluble in solvents commonly used for GPC analysis). ^cIsotactic by ¹³C{¹H} NMR (acetone-d₆): δ 38.38 ^dIsotactic by carbon-13 NMR (CDCl₃): δ 38.5.¹⁰¹

Conclusions

Highly regular polynorbornadienes with >95% cis and >95% isotactic geometry have been obtained by ligand variation about a molybdenum neophylidene initiator. Increases in the bulkiness of both an arylimido ligand and a binaphtholate ligand caused an increase in the cis content of the polymers formed. All polymers with a cis content greater than 90% were also >95% isotactic (structure a in Scheme B.1).

Experimental Section

General Procedures. All handling of catalyst and polymerization was done in a nitrogen-atmosphere drybox. THF and Et₂O were distilled from sodium benzophenone. All solvents were stored over 4 Å molecular sieves prior to use in the drybox. All chemicals used were reagent grade and were purified by standard methods. BBr₃ (1 M in CH₂Cl₂), 2-methylphenylmagnesium bromide (1 M in THF) and NiCl₂(PPh₃)₂ were purchased from Aldrich and used as received. 2,6-Dimethylphenylmagnesium bromide⁵, bis(CF₃)NBD,¹⁰⁶ (±)-3,3'-dibromo-2,2'-dimethoxy-1,1'-dinaphthyl,¹⁰⁷ Mo(CHCMe₂Ph)(NAr')(OTf)₂(DME),¹⁰⁸ Mo(CHCMe₂Ph)(NAr)(OTf)₂(DME),⁷ and DCMNBD¹⁰⁹ were prepared by literature methods.

(±)-3,3'-Bis(2-methylphenyl)-2,2'-dimethoxy-1,1'-dinaphthyl. 2-Methylphenylmagnesium bromide (18.0 mL, 1 M in THF) was added dropwise over the course of 20 min to a stirred solution of (±)-3,3'-dibromo-2,2'-dimethoxy-1,1'-dinaphthyl (3.004 g, 6.362 mmol) and NiCl₂(PPh₃)₂ (0.244g, 0.373 mmol) in Et₂O (50 mL). After refluxing for 24 h., aqueous HCl (300 mL, 1 N) was added. The mixture was extracted with CHCl₃ (4 × 250 mL), dried over MgSO₄, and the solvent removed *in vacuo*, leaving a yellow foam. By ¹H NMR (CDCl₃) the compound was 90% pure: methoxy group resonance of starting material at δ 3.5 (s, 6H) was not apparent; two minor methoxy resonances were observed at δ 3.17 and 3.23, probably from monosubstituted compound, and a major resonance was observed at δ 3.15 (s, 6H). All of the foam was used in the next step without further purification.

(±)-3,3'-Bis(2-methylphenyl)-2,2'-dihydroxy-1,1'-dinaphthyl [**H₂-(±)-BINO(2-methylphenyl)₂**] (**3**). BBr₃ (35.0 mL, 1 M in CH₂Cl₂) was added dropwise via syringe to a stirred solution of (±)-3,3'-bis(2-methylphenyl)-2,2'-dimethoxy-1,1'-dinaphthyl (5.73 mmol from previous step) in CH₂Cl₂ (250 mL) at 0 °C. When the addition was complete the ice bath was removed. After stirring 1 h, the reaction was complete by ¹H NMR: disappearance of the methoxy CH₃ protons at δ 3.15 ppm was observed. The BBr₃ was quenched with H₂O (100 mL) at 0 °C. The mixture was extracted with CH₂Cl₂ (3 × 100 mL), dried over MgSO₄, and solvent removed *in vacuo*, leaving a yellow-brown oil. Column chromatography (silica gel, toluene) gave 1.181 g (2-step yield 39.8%) of white powder. ¹H NMR (CDCl₃): δ 7.86 (d, 2, ArH), 7.82 (s, 2, ArH), 7.38-7.22 (m, 14, ArH), 5.07 (br, 2, OH), 2.23 (br, 6, ArMe). ¹³C {¹H} NMR (CDCl₃): δ 150.40, 137.46, 137.13, 133.46, 131.29, 131.08, 130.50, 130.32, 129.43, 128.56, 128.50, 127.34, 126.23, 124.57, 124.38, 112.59, 92.11 (ArMe).

Dipotassium (±)-3,3'-bis(2-methylphenyl)-1,1'-dinaphthyl-2,2'-diolate [**K₂-(±)-BINO(2-methylphenyl)₂**]. KH (42 mg, 1.1 mmol) was added to a stirred solution of [**H₂-(±)-BINO(2-methylphenyl)₂**] (0.182 g, 0.390 mmol) in THF (15 mL). Initially, gas evolved from the stirred mixture. After 5 h the mixture had become bright yellow. Some yellow precipitate was observed, but mostly the product stayed in solution. This THF mixture was used directly in the next step.

Mo(CHCMe₂Ph)(NAr')[(±)-BINO(2-methylphenyl)₂](THF) (**3a'**). Mo(CHCMe₂Ph)(NAr')(OTf)₂(DME) (0.190 g, 0.258 mmol) was added to a stirred THF mixture of [**K₂-(±)-BINO(2-methylphenyl)₂**] (0.390 mmol) prepared as described above. After stirring at room temperature for 15 min, the solvent was removed *in vacuo* and the dark residue extracted with 2 mL toluene. The dark solution was filtered through a pad of Celite and the filtrate concentrated to 0.5 mL. Addition of 5 mL Et₂O and cooling to -40 °C gave 0.096 g (42%) of bright yellow-orange crystals. ¹H NMR (C₆D₆, 0.35:1 syn/anti ratio): δ 13.62 (s, CHCMe₂Ph, anti), 12.51 (br, CHCMe₂Ph, syn), 7.75, 7.72, 7.71, 7.69, 7.66, 7.63, 7.60, 7.42, 7.41, 7.38, 7.35, 7.32, 7.22, 7.18, 7.16, 7.13, 7.125, 7.11, 7.10, 7.07, 7.04, 7.01, 7.00, 6.98, 6.96, 6.94,

6.92, 6.89, 6.83, 6.81, 6.78, 6.72, 6.66, 6.39, 2.98 (br, THF), 2.5-1.4 (m, ArMe & CHCMe₂Ph, syn & anti), 0.82 (br, THF); ¹³C{¹H} NMR (C₆D₆): δ 314.981 (cHCMe₂Ph, ¹J_{CH} = 149 Hz, anti; syn not observed), 160.24, 158.13, 151.24, 142.97, 140.43, 138.76, 138.54, 137.09, 136.51, 135.35, 134.99, 72.18 (OCH₂CH₂), 52.14, 34.20, 33.38, 31.44, 29.54, 28.08, 25.22, 20.74, 20.13, 19.04.

Mo(CHCMe₂Ph)(NAr)[(±)-BINO(2-methylphenyl)₂](THF) (3a).

Mo(CHCMe₂Ph)(NAr)(OTf)₂(DME) (0.170 g, 0.215 mmol) was added to a stirred THF mixture of [K₂-(±)-BINO(2-methylphenyl)₂] (0.214 mmol) prepared as described above. After stirring at room temperature for 15 min., the solvent was removed *in vacuo* and the dark residue extracted with 2 mL toluene. The dark solution was filtered through a pad of Celite and the filtrate concentrated to 0.5 mL. Addition of 5 mL Et₂O and cooling to -40 °C gave 0.092 g (44%) of bright yellow-orange crystals. ¹H NMR (C₆D₆, 0.092:1 syn/anti ratio): δ 13.74 (s, CHCMe₂Ph, anti), 11.30 (br, CHCMe₂Ph, syn), 7.78, 7.76, 7.74, 7.17, 7.69, 7.67, 7.42 (d, 1 H, ArH), 7.30 (d, 1H, ArH), 7.18, 7.165, 7.16, 7.155, 7.12, 7.09, 7.08, 7.07, 7.04, 7.03, 6.99, 6.96, 6.94, 6.91, 6.89, 6.86, 6.83, 6.81, 6.66, 2.97 (br, THF), 2.48 (m, NArCHMe₂), 2.43 (s, BINOMe), 2.31 (s, BINOMe), 0.93 (br, NArCHMe₂), 0.82 (br, THF); ¹³C{¹H} NMR (C₆D₆): δ 315.80 (cHCMe₂Ph, ¹J_{CH} = 145 Hz, anti), 284.29 (cHCMe₂Ph, syn), 162.33, 160.55, 155.15, 151.34, 145.28, 143.47, 140.82, 139.15, 138.20, 136.06, 135.71, 135.57, 135.20, 133.83, 133.44, 131.26, 130.98, 130.81, 130.65, 130.43, 130.26, 129.90, 129.76, 129.44, 129.24, 128.80, 128.18, 127.85, 127.72, 127.47, 127.35, 127.18, 126.66, 126.52, 126.38, 126.31, 126.12, 126.05, 125.85, 125.46, 124.73, 123.45, 123.26, 122.53, 119.89, 73.73 (OCH₂CH₂), 66.24, 52.37, 29.72, 29.45, 28.21, 25.41, 24.42, 23.84, 23.77, 22.96, 20.82, 20.41, 15.91.

(±)-3,3'-Bis(2,6-dimethylphenyl)-2,2'-dimethoxy-1,1'-dinaphthyl. 2,6-Dimethylphenylmagnesium chloride (20.0 mL, 0.66 M in Et₂O) was added dropwise over the course of 60 minutes to a stirred solution of (±)-3,3'-dibromo-2,2'-dimethoxy-1,1'-dinaphthyl (2.198g, 4.655 mmol) and NiCl₂(PPh₃)₂ (0.166 g, 0.254 mmol) in Et₂O (50 mL). After

refluxing for 24 h, an additional amount of Grignard reagent (10 mL) was added. Refluxing continued for another 4 h, then aqueous HCl (200 mL, 1 N) was added. The mixture was extracted with CHCl₃ (3 × 200 mL), dried over MgSO₄, and the solvent removed *in vacuo*, leaving a yellow foam. By ¹H NMR (CDCl₃) the compound was 90% pure (¹H NMR methoxy group resonance of starting material at δ 3.5 (s, 6H) was not apparent; two minor methoxy resonances were observed at δ 3.01 and 3.79, probably from monosubstituted compound, and a major resonance was observed at δ 3.08 (s, 6H)). All of the foam was used in the next step, without further purification.

(±)-3,3'-Bis(2,6-dimethylphenyl)-2,2'-dihydroxy-1,1'-dinaphthyl [H₂-(±)-BINO(2,6-dimethylphenyl)₂] (4). BBr₃ (28.5 mL, 1 M in CH₂Cl₂) was added dropwise through an addition funnel to a stirred solution of (+/-)-3,3'-bis(2,6-dimethylphenyl)-2,2'-dimethoxy-1,1'-dinaphthyl (4.190 mmol from previous step) in CH₂Cl₂ (150 mL) at 0 °C. When the addition was complete, the ice bath was removed. After stirring 1 h, the reaction was complete by ¹H NMR (CDCl₃): complete disappearance of the methoxy CH₃ protons at δ 3.06. The BBr₃ was quenched with H₂O (100 mL) at 0 °C. The mixture was extracted with CH₂Cl₂ (3 × 100 mL), dried over MgSO₄, and solvent removed *in vacuo*, leaving a yellow-brown oil. Recrystallization from CH₂Cl₂ and pentane gave 1.057 g (2-step yield 45.9%) of white powder. ¹H NMR (CDCl₃): δ 7.87 (d, 2, ArH), 7.47 (s, 2, ArH), 7.38-7.15 (12, m, ArH), 4.96 (s, 2, OH), 2.17 (s, 6, ArMe), 2.09 (s, 6, ArMe); ¹³C{¹H} NMR (CDCl₃): δ 150.09, 137.50, 137.43, 136.17, 133.63, 130.73, 129.66, 128.52, 128.35, 127.89, 127.81, 127.15, 124.71, 124.17, 113.14, 20.88 (ArMe), 20.78 (ArMe).

Dipotassium (±)-3,3'-bis(2,6-dimethylphenyl)-1,1'-dinaphthyl-2,2'-diolate [K₂-(±)-BINO(2,6-dimethylphenyl)₂]. KH (26 mg, 0.66 mmol) was added to a stirred solution of [H₂-(±)-BINO(2,6-dimethylphenyl)₂] (0.125 g, 0.253 mmol) in THF (10 mL). Initially, gas evolved from the stirred mixture. After 1 h gas evolution had stopped and a bright yellow precipitate had formed. This THF mixture was used directly in the next step.

Mo(CHCMe₂Ph)(NAr')[(±)-BINO(2,6-dimethylphenyl)₂](THF) (4a').

Mo(CHCMe₂Ph)(NAr')(OTf)₂(DME) (0.190 g, 0.258 mmol) was added to a stirred THF mixture of [K₂-(±)-BINO(2-methylphenyl)₂] (0.253 mmol) prepared as described above. After stirring at room temperature for 15 min, the solvent was removed and the dark residue extracted with 2 mL toluene. The dark solution was filtered through a pad of Celite and the solvent removed *in vacuo*. Addition of 5 mL Et₂O and cooling to -40 °C gave 0.067 g (27%) of bright yellow-orange crystals. ¹H NMR (C₆D₆, 1:0.25 syn/anti ratio): δ 13.74 (s, CHCMe₂Ph, anti), 11.74 (s, CHCMe₂Ph, syn), 7.77-7.52 (m, 4H, ArH, syn and anti), 7.33-7.27 (m, 2H, ArH), 7.24-6.68 (m, 13, ArH), 6.6 (s, 3, ArH), 3.03 (br, THF), 2.59 (BINOArMe, anti), 2.55 (BINOArMe, syn), 2.51 (BINOArMe, anti), 2.48 (BINOArMe, syn), 2.32 (BINOArMe, anti), 2.09 (BINOArMe, syn), 1.90 (NArMe, syn and anti), 1.70 (BINOArMe, syn), 1.64 (BINOArMe, anti), 1.59 (CHCMe₂Ph, anti), 1.56 (CHCMe₂Ph, anti), 1.35 (CHCMe₂Ph, syn), 1.33 (CHCMe₂Ph, syn), 0.921 (br, THF); ¹³C{¹H} NMR (C₆D₆): δ 315.15 (CHCMe₂Ph, ¹J_{CH} = 141 Hz, anti), 291.28, (CHCMe₂Ph, syn), 158.48, 156.24, 150.69, 139.22, 139.09, 139.02, 138.90, 138.77, 137.10, 136.90, 136.70, 136.31, 135.82, 135.41, 133.97, 133.60, 133.08, 132.93, 132.52, 132.00, 131.19, 130.58, 130.12, 129.88, 129.81, 129.73, 128.97, 128.86, 128.57, 128.30, 128.26, 128.19, 127.95, 127.85, 127.68, 127.60, 127.55, 127.36, 127.11, 126.93, 126.83, 126.77, 126.60, 126.51, 126.45, 126.31, 126.21, 126.05, 124.37, 124.18, 123.38, 123.21, 123.14, 72.36 (OCH₂CH₂), 54.06, 51.77, 32.99, 31.06, 29.52, 28.46, 25.53, 22.79, 22.31, 21.73, 21.53, 21.46, 21.43, 21.32, 21.28, 21.16, 20.16, 19.42.

Mo(CHCMe₂Ph)(NAr)[(±)-BINO(2,6-dimethylphenyl)₂](THF) (4a).

Mo(CHCMe₂Ph)(NAr')(OTf)₂(DME) (0.118 g, 0.149 mmol) was added to a stirred THF mixture of [K₂-(±)-BINO(2-methylphenyl)₂] (0.15 mmol) described above. After stirring at room temperature for 15 min, the solvent was removed and the dark residue extracted with 2 mL toluene. The dark solution was filtered through Celite and the solvent removed *in vacuo*. Addition of 5 mL Et₂O and cooling to -40 °C gave 0.092 g (64%) of large star-shaped yellow crystals. ¹H NMR (C₆D₆, 0.35:1 syn/anti ratio): δ 13.86 (CHCMe₂Ph, anti), 11.87 (CHCMe₂Ph, syn), 7.68-6.80

(m, 24 ArH), 3.36 (br, 2, NArCHMe₂), 3.11 (br, THF), 2.51-0.63 (m, 30, ArMe, NArCHMe₂ & CHCMe₂Ph, syn & anti), 1.99 (br, THF); ¹³C{¹H} NMR (C₆D₆): δ 315.94 (CHCMe₂Ph, anti), 290.55 (CHCMe₃Ph, syn), 163.61, 161.12, 155.25, 151.61, 150.88, 142.00, 139.63, 139.35, 138.93, 138.86, 138.81, 136.97, 136.42, 136.05, 135.99, 135.87, 133.32, 132.82, 132.54, 132.26, 131.04, 130.71, 130.51, 130.43, 129.71, 129.31, 129.06, 128.94, 128.59, 128.56, 128.26, 127.87, 127.77, 127.68, 127.30, 127.20, 127.10, 126.83, 126.78, 126.63, 126.59, 126.49, 126.27, 126.07, 124.52, 124.21, 123.53, 123.39, 123.26, 73.08, 54.61, 51.89, 34.84, 33.30, 30.68, 30.11, 29.85, 29.27, 28.73, 25.54, 24.76, 23.52, 23.12, 22.60, 22.33, 21.67, 21.46, 21.19, 21.11, 14.67.

Mo(CHCMe₂Ph)(NAr)[(±)-BINO(2,6-dimethylphenyl)₂](py) was prepared by recrystallization of Mo(CHCMe₂Ph)(NAr)[(±)-BINO(2,6-dimethylphenyl)₂](THF) in the presence of pyridine. Calcd for C₆₃H₆₂N₂O₂Mo: C, 77.60; H, 6.41; N, 2.87. Found: C, 77.93; H, 6.46; N, 2.55.

General Polymerization Procedure. Dicarbomethoxynorbornadiene (110 mg, 0.5 mmol) in 2 mL THF was added all at once to a rapidly stirred solution of **4a'** (10 mg, 0.01 mmol) in 10 mL THF. The reaction mixture was stirred for 5 h, quenched with 3 drops benzaldehyde and further stirred for 1 h. Precipitation into 75 mL MeOH afforded a high yield (>95%) of polymer. *M_n* and *M_w/M_n* are given in text. Tacticity and cis double bond content also discussed in the text.

REFERENCES

- (1) Holton, W. C. in "Solid State Technology"; 1997; p 163.
- (2) Segura, J. L. *Acta. Polym.* **1998**, *49*, 319.
- (3) Sheats, J. R.; Antoniadis, H.; Hueschen, M.; Leonard, W.; Miller, J.; Moon, R.; Roitman, D.; Stocking, A. *Science* **1996**, *273*, 884.
- (4) Burroughes, J. H.; Bradley, D. D. C.; Brown, A. R.; Marks, R. N.; Mackay, K.; Friend, R. H.; Burns, P. L.; Holmes, A. B. *Nature* **1990**, *347*, 539.
- (5) Greenham, N. C.; Moratti, S. C.; Bradley, D. D. C.; Friend, R. H.; Holmes, A. B. *Nature* **1993**, *365*, 628.
- (6) Brown, A. R.; Bradley, D. D. C.; Burroughes, J. H.; Friend, R. H.; Greenham, N. C.; Burn, P. L.; Holmes, A. B.; Kraft, A. *Appl. Phys. Lett.* **1992**, *61*, 2793.
- (7) Burn, P. L.; Kraft, A.; Baigent, D. R.; Bradely, D. D. C.; Brown, A. R.; Field, R. H.; Gymer, R. W.; Holmes, A. B.; Jackson, R. W. *J. Am. Chem. Soc.* **1993**, *115*, 10117.
- (8) Hesemann, P.; Vestweber, H.; Pommerehne, J.; Mahrt, R. H.; Greiner, A. *Adv. Mater.* **1995**, *7*, 388.
- (9) Ferreira, M.; Rubner, M. F. *Macromolecules* **1995**, *28*, 7107.
- (10) Fou, A. C.; Onitsuka, O.; Ferreira, M.; Hsieh, B. R.; Rubner, M. F. *J. Appl. Phys.* **1996**, *79*, 7501.
- (11) Grem, G.; Leditzky, G.; Ullrich, B.; Leising, G. *Adv. Mater.* **1992**, *4*, 36.
- (12) Andersson, M. R.; Berggren, M.; Inganäs, O.; Gustafsson, G.; Gustafsson-Carlberg, J. C.; Selse, D.; Hjertberg, T.; Wennerstrom, O. *Macromolecules* **1995**, *28*, 7525.
- (13) Baur, J. W.; Kim, S.; Balanda, P. B.; Reynolds, J. R.; Rubner, M. F. *Adv. Mater.* **1998**, *10*, 1452.
- (14) Hilberer, A.; Brouwer, H.-J.; Scheer, B.-J. v. d.; Wildeman, J.; Hadziioannou, G. *Macromolecules* **1995**, *28*, 4525.
- (15) Kreyenschmidt, M.; Klaerner, G.; Fuhrer, T.; Ashenurst, J.; Karg, S.; Chen, W. D.; Lee, V. Y.; Scott, J. C.; Miller, R. D. *Macromolecules* **1998**, *31*, 1099.
- (16) Pei, Q.; Yang, Y. *J. Am. Chem. Soc.* **1996**, *118*, 7416.

- (17) Yang, Y. in "MRS Bulletin"; 1997; p 31.
- (18) Morgado, J.; Cacialli, F.; Gruner, J.; Greenham, N. C.; Friend, R. H. *J. Appl. Phys.* **1999**, *85*, 1784.
- (19) Lee, J.-K.; Schrock, R. R.; Baigent, D. R.; Friend, R. H. *Macromolecules* **1995**, *28*, 1966.
- (20) Yang, Z.; Skolik, I.; Karasz, F. E. *Macromolecules* **1993**, *26*, 1188.
- (21) Bisberg, J.; Cumming, W. J.; Gaudiana, R. A.; Hutchinson, K. D.; Ingwall, R. T.; Kolb, E. S.; Mehta, P. G.; Minns, R. A.; Petersen, C. P. *Macromolecules* **1995**, *28*, 386.
- (22) Keszthelyi, C. P.; Bard, A. J. *J. Electrochem. Soc.* **1973**, *120*, 241.
- (23) Heller, C. A.; Henry, R. A.; McLaughlin, B. A.; Bliss, D. E. *J. Chem. Eng. Data* **1974**, *19*, 1974.
- (24) Collinson, M. M.; Wightman, R. M. *Science* **1995**, *268*, 1883.
- (25) Chandross, E.; Sonntag, F. *J. Am. Chem. Soc.* **1964**, *86*, 3179.
- (26) Gill, S. K. *Aldrichimica Act* **1983**, *16*, 59.
- (27) Wightman, R. M.; Curtis, C. L.; Flowers, P. A.; Maus, R. G.; McDonald, E. R. *J. Phys. Chem. B* **1998**, *102*, 9991.
- (28) Abagli, D.; Bazan, G.; Wrighton, M. S.; Schrock, R. R. *J. Am. Chem. Soc.* **1992**, *114*, 4150.
- (29) Schrock, R. R. *Acc. Chem. Res.* **1990**, *23*, 158.
- (30) Schrock, R. R.; Murdzek, J. S.; Bazan, G. C.; Robbins, J.; DiMare, M.; O'Regan, M. J. *Am. Chem. Soc.* **1990**, *112*, 3875.
- (31) Schrock, R. R. in "Ring-Opening Polymerization"; D. J. Brunelle, Ed.; Hanser: Munich, 1993; pp 129.
- (32) Schrock, R. R.; Murdzek, J. S.; Bazan, G. C.; Robbins, J.; DiMare, M.; O'Regan, M. J. *Am. Chem. Soc.* **1990**, *112*, 3875.
- (33) Oskam, J. H.; Fox, H. H.; Yap, K. B.; McConville, D. H.; O'Dell, R.; Lichtenstein, B. J.; Schrock, R. R. *J. Organomet. Chem.* **1993**, *459*, 185.

- (34) Bazan, G. C.; Khosravi, E.; Schrock, R. R.; Feast, W. J.; Gibson, V. C.; O'Regan, M. B.; Thomas, J. K.; Davis, W. M. *J. Am. Chem. Soc.* **1990**, *112*, 8378.
- (35) Wagaman, M. W.; Grubbs, R. H. *Macromolecules* **1997**, *30*, 3978.
- (36) Fogg, D. E.; Radzilowski, L. H.; Blanski, R.; Schrock, R. R.; Thomas, E. L. *Macromolecules* **1997**, *30*, 417.
- (37) Fogg, D. E.; Radzilowski, L. H.; Dabbousi, B. O.; Schrock, R. R.; Thomas, E. L.; Bawendi, M. G. *Macromolecules* **1997**, *30*, 8433.
- (38) Adachi, C.; Tsutsui, T.; Saito, S. *Appl. Phys. Lett.* **1990**, *56*, 799.
- (39) Adachi, C.; Tsutsui, T.; Saito, S. *Appl. Phys. Lett.* **1989**, *55*, 1489.
- (40) Adachi, C.; Tokito, S.; Tsutsui, T.; Saito, S. *Japanese Journal of Applied Physics* **1988**, *27*, L269.
- (41) Kido, J.; Kimura, M.; Nagai, K. *Science* **1995**, *267*, 1332.
- (42) Posch, P.; Fink, R.; Thelakkat, M.; Schmidt, H.-W. *Acta Polym.* **1998**, *49*, 487.
- (43) Parker, I. D. *J. Appl. Phys.* **1994**, *75*, 1656.
- (44) Onitsuka, O.; Fou, A. C.; Ferreira, M.; Hsieh, B. R.; Rubner, M. F. *J. Appl. Phys.* **1996**, *80*, 4067.
- (45) Judge, M. in "New Scientist"; 1997; p 40.
- (46) Berlman, I. B. *Handbook of Fluorescence Spectra of Aromatic Molecules*; Academic Press: New York, 1965
- (47) Hammerich, O.; Parker, V. D. *J. Am. Chem. Soc.* **1973**, *96*, 4289.
- (48) Jensen, B. S.; Parker, V. D. *J. C. S. Chem. Comm.* **1974**, 367.
- (49) Marcoux, L. S.; Fritsch, J. M.; Adams, R. N. *J. Am. Chem. Soc.* **1967**, *89*, 5766.
- (50) Hamada, Y.; Adachi, C.; Tsutsui, T.; Saito, S. *Jpn. J. Appl. Phys* **1992**, *31*, 1812.
- (51) Huang, W.; Yu, W.-L.; Meng, H.; Pei, J.; Li, S. F. Y. *Chem. Mater.* **1998**, *10*, 3340.
- (52) Kim, D.-J.; Kim, S.-H.; Zyung, T.; Kim, J.-J.; Cho, I.; Choi, S. K. *Macromolecules* **1996**, *29*, 3657.

- (53) Stolka, M.; Pai, D. M.; Renfer, D. S.; Yanus, J. F. *J. of Poly. Sci.: Poly. Chem. Ed.* **1983**, *21*, 969.
- (54) Emoto, K.; Alstine, J. M. V.; Harris, J. M. *Langmuir* **1998**, *14*, 2722.
- (55) Jiang, W.; Irgum, K. *Anal. Chem.* **1999**, *71*, 333.
- (56) Marechal, E. in "Comprehensive Polymer Science"; G. C. Eastmond, A. Ledwith, S. Russo and P. Sigwalt, Ed.; Pergamon Press: New York, 1989; Vol. 6.
- (57) El-Shoubary, Y.; Speizer, N.; Seth, S.; Savoia, H. *Environ. Prog.* **1998**, *17*, 209.
- (58) Glater, J.; Hong, S.-K.; Elimelech, M. *Desalination* **1994**, *95*, 325.
- (59) Kabsch-Korbutowicz, M.; Pozniak, G.; Trochimczuk, W.; Winnicki, T. *Separ. Sci. Tech.* **1994**, *29*, 2345.
- (60) Guo, Q.; Pintauro, P. N.; Tang, H.; O'Connor, S. *J. Membr. Sci.* **1999**, *154*, 175.
- (61) Chowdhury, G.; Matsuura, T.; Sourirajan, S. *J. Appl. Polym. Sci.* **1994**, *51*, 1071.
- (62) Hamada, T.; Taya, M.; Tone, S. *J. Chem. Eng. Jpn.* **1998**, *31*, 125.
- (63) Pozniak, G.; Bryjak, M.; Trochimczuk, W. *Angew. Makromol. Chem.* **1995**, *233*, 23.
- (64) Shahinpoor, M.; Bar-Cohen, Y.; Simpson, J. O.; Smith, J. *Smart Mater. Struc.* **1998**, *7*, R15.
- (65) Ratner, B. D. in "Comprehensive Polymer Science"; S. L. Aggarwal, Ed.; Pergamon Press: New York, 1989; Vol. 7.
- (66) Planche, J. P.; Revillon, A.; Guyot, A. *J. Polym. Sci. Chem. Ed.* **1988**, *26*, 429.
- (67) Planche, J. P.; Revillon, A.; Guyot, A. *J. Polym. Sci. Chem. Ed.* **1990**, *28*, 1377.
- (68) Sohn, B. H.; Gratt, J. A.; Lee, J.-K.; Cohen, R. E. *J. Appl. Polym. Sci.* **1995**, *58*, 1041.
- (69) Ivin, K. J.; Kenwright, A. M.; Hofmeister, G. E.; McConville, D. H.; Schrock, R. R.; Amir-Ebrahimi, V.; Carbill, A. G.; Hamilton, J. G.; Rooney, J. J. *Macromol. Chem. Phys.* **1998**, *199*, 547.
- (70) Egboh, S. H. O. *Eur. Polym. J.* **1988**, *24*, 1005.
- (71) March, J. *Advanced Organic Chemistry*; John Wiley & Sons: New York, 1992

- (72) *Friedel-Crafts and Related Reactions*; Olah, G. A., Ed.; John Wiley and Sons, Ltd: New York, 1964; Vol. 2, p 660.
- (73) Tamao, K.; Sumitani, K.; Kiso, Y.; Zembayashi, M.; Fujioka, A.; Kodama, S.; Nakajima, I.; Minato, A.; Kumada, M. *Bull. Chem. Soc. Jpn.* **1976**, *49*, 1958.
- (74) Boyd, T. J.; Geerts, Y.; Lee, J.-K.; Fogg, D. E.; Lavoie, G. G.; Schrock, R. R.; Rubner, M. F. *Macromolecules* **1997**, *30*, 3553.
- (75) Schrock, R. R.; Lee, J.-K.; O'Dell, R.; Oskam, J. H. *Macromolecules* **1995**, *28*, 5933.
- (76) Oskam, J. H.; Schrock, R. R. *J. Am. Chem. Soc.* **1993**, *115*, 11831.
- (77) Gilbert, E. E. *Sulfonation and Related Reactions*; Interscience Publishers: New York, 1965
- (78) Bordwell, F. G.; Rondestvedt, C. S. *J. Am. Chem. Soc.* **1948**, *70*, 2429.
- (79) Bordwell, F. G.; Osborne, C. E. *J. Am. Chem. Soc.* **1959**, *81*, 1995.
- (80) Sutter, C. M.; Evans, P. B.; Kiefer, J. M. *J. Am. Chem. Soc.* **1938**, *60*, 538.
- (81) Silverstein, R. M.; Bassler, G. C.; Morrill, T. C. *Spectrometric Identification of Organic Compounds*; John Wiley & Sons, Inc.: New York, 1991
- (82) Szymanski, H. A. *Interpreted Infrared Spectra*; Plenum Press: New York, 1967
- (83) Pangborn, A. B.; Giardello, M. A.; Grubbs, R. H.; Rosen, R. K.; Timmers, F. J. *Organometallics* **1996**, *15*, 1518.
- (84) Burfield, D.; Lee, K.-H.; Smithers, R. H. *J. Org. Chem.* **1977**, *42*, 3060.
- (85) Ettetdgui, E.; Razafitrimo, H.; Park, K. T.; Gao, Y.; Hsieh, B. R. *Surf. Interface Anal.* **1995**, *23*, 89.
- (86) Lee, J.-K.; Yoo, D. S.; Handy, E. S.; Rubner, M. F. *Appl. Phys. Lett.* **1996**, *69*, 1686.
- (87) Baur, J. W. Thesis, Massachusetts Institute of Technology, 1997.
- (88) Mahrt, J.; Willig, F.; Storck, W.; Weiss, D.; Kietzmann, R.; Schwarzburg, K.; Tufts, B.; Trosken, B. *J. Phys. Chem.* **1994**, *98*, 1888.
- (89) Fox, M. A.; Britt, P. F. *Macromolecules* **1990**, *23*, 4533.
- (90) Mattes, S. L.; Farid, S. *Science* **1984**, *226*, 917.
- (91) Fox, M. A.; Jones, W. E.; Watkins, D. M. in "C&EN"; 1993; pp 38-48.

- (92) Fox, M. A.; Thompson, H. W. *Macromolecules* **1997**, *30*, 7391.
- (93) Kiserow, D. J.; Itoh, Y.; Webber, S. E. *Macromolecules* **1997**, *30*, 2934.
- (94) Webber, S. E. *Chem. Rev.* **1990**, *90*, 1469.
- (95) Watkins, D. M.; Fox, M. A. *Macromolecules* **1995**, *28*, 4939.
- (96) Tsutsui, T. in "MRS Bulletin"; 1997; p 39.
- (97) Greczmiel, M.; Stroehriegl, P.; Meier, M.; Brutting, W. *Macromolecules* **1997**, *30*, 6042.
- (98) Pei, Q.; Yang, Y. *Chem. Mater.* **1995**, *7*, 1568.
- (99) Kim, S.; Jackiw, J.; Robinson, E.; Schanze, K. S.; Reynolds, J. R.; Baur, J.; Rubner, M. F.; Boils, D. *Macromolecules* **1998**, *31*, 964.
- (100) Bazan, G. C.; Khosravi, E.; Schrock, R. R.; Feast, W. J.; Gibson, V. C.; O'Regan, M. B.; Thomas, J. K.; Davis, W. M. *J. Am. Chem. Soc.* **1990**, *112*, 8378.
- (101) O'Dell, R.; McConville, D. H.; Hofmeister, G. E.; Schrock, R. R. *J. Am. Chem. Soc.* **1994**, *116*, 3414.
- (102) McConville, D. H.; Wolf, J. R.; Schrock, R. R. *J. Am. Chem. Soc.* **1993**, *115*, 4413.
- (103) Totland, K. M.; Boyd, T. J.; Lavoie, G. G.; Davis, W. M.; Schrock, R. R. *Macromolecules* **1996**, *29*, 6114.
- (104) Lingenfelter, D. S.; Helgeson, R. C.; Cram, D. J. *J. Org. Chem.* **1981**, *46*, 393.
- (105) Zhu, S. S.; Cefalo, D. R.; Jamieson, J. Y.; Hoveyda, A. H.; Schrock, R. R. *in preparation*.
- (106) Yue, J.; Cohen, R. E. *Supramolecular Science* **1994**, *1*, 117.
- (107) Lee, J.-K. Ph.D. Thesis, Massachusetts Institute of Technology, 1995.
- (108) Tang, C. W.; VanSlyke, S. A.; Chen, C. H. *J. Appl. Phys.* **1989**, *65*, 3610.
- (109) Gustofsson, G.; Y.Cao; Treacy, G. M.; Klavetter, F.; Colaneri, N.; Heeger, A. J. *Nature* **1992**, *357*, 477.

Acknowledgements

Here we are: the end! (Or perhaps for you, reader: the beginning!) There are so many people who had a hand in getting me successfully to this point. First, I would like to thank my advisor, Professor Richard Schrock. He has allowed me a great deal of freedom in pursuing a project that is pretty far afield from what folks normally do in his lab. This has taken a lot of patience and trust on his part, for which I am very grateful.

I had the good fortune to have a series of great people walk through my little part of the lab in 6-430. Dr. Nadia Zanetti was very patient with me when I first started; I learned later how difficult it is for Nadia to be that patient about *anything*. I will always be grateful for her friendship, and even for her tendency to be blunt about what bothers her. My next postdoc was Dr. Michael Aizenburg, from whom I learned a lot of fascinating things about what life was like in the former Soviet Union. Michael sometimes came across at first as very serious, but he was an inveterate joke-teller, which helped keep spirits up on days when experiments were failing. I (briefly) had an actual U.S. citizen in my lab - Sarah Aeilts. Enjoy the rest of your time, Sarah! My last box-mate was Dr. Arturo Casado (poh-pough!), singer-extraordinaire. Thank you for giving me a very good excuse to leave the lab and start writing!

There have been so many others that have gone through the Schrock lab since I began: Joel, Rusty, Klaus, Céline, Yann, Michelle, Miguel, Gino, Michael, Robert, John, Kotohiro, Jin-Kyu, Diana, Jesse, Eric, David, Parisa, Connie, Dan, Karen, Steve, George, Alex, Scott, Shifang, Deryn, Laura, Sherry, Rüdiger, Peter, Tim, Florian, Frank, Sasha, Jonathan, Anne, Brigitte, Myra, Shirley, John, Jennifer, Denyce, Ivan, Oliver, and Gretchen. Good luck to you all! Thanks for shop-talk, idle chatter, rounds at the Muddy, arguments about international politics, etc., and in general, keeping me sane. Extra thanks go to Sherry Zhu and John Alexander, who kindly proofread this thesis.

Since my project is very interdisciplinary, I relied heavily upon Professor Michael Rubner and his group in the Materials Science and Engineering Department at MIT. Professor Rubner helped focus my work, and I am grateful for his insight and unabashed enthusiasm. I would also like to thank everyone in his research group, especially Dr. Mary-Silvia Ferreira who got me started in the LED business.

I would like to thank my family for encouragement and for providing a lot of scientist role-models. Both my father and mother have been a source of steadfast support, no matter where I was wandering - I'm only narrowly not a clarinetist! I would like to thank my cats, Sasha and Nathan, who kept me company while I was writing at home (and kept me alert by stalking the Macintosh Computer <Reset> key). And finally, I would like to thank my wife, Kathryn, to whom this thesis is dedicated. Kathryn celebrated with me when experiments went completely right, commiserated with me when experiments were complete and utter failures, and always had patience, knowing that victories follow failures follow victories. Thank you.